The Islamic University of Gaza
Faculty of Graduate Studies
Department of Electrical Engineering

Comparison for Maximum Power Point Tracing Algorithms for Photovoltaic System in Purpose of Developing an Efficient System

Prepared by

Khalid Hamooda Matter

Supervisor
Prof. Dr. Hala J. El-Khozondar

A Thesis Submitted to the Faculty of Engineering in Partial Fulfillment of the Requirements for the Degree of Master of Science in Electrical Engineering

The Islamic University of Gaza, Palestine

June. 27, 2014

Abstract

Renewable energy is a priority in this day and age, in light of the crisis that has plagued the whole world which drives some people to get energy in ways sound and unsound. From this point, the interest in renewable energy and expand from it is the way to people's happiness and convergence between countries.

In this study, we dealt with a range of methods used to get the maximum power and we make simple compared with each other to determine the merits of each method and location for the other way. So it's easy for the researcher to choose the best way for practical applications in accordance with the limitations and the possibilities available to him

We have detailed study for all the factors affecting the properties of the cell and the impact of the change on the resulting energy, factors have been split between internal Such as the impact of change in resistors and external such as the impact of the change in temperature and radiation and shade.

In the end, we have implemented a simple practice demonstrates the use of one of the maximum power point tracking (*MPPT*) methods to get the maximum power. This method called Incremental Conductance Algorithm. The control is simulated using MATLAB software.

ملخص البحث

تعتبر الطاقة المتجددة اولوية هذا العصر في ظل الازمة التي يعاني منها العالم باسره وهو ما يدفع البعض للحصول علي الطاقة بالطرق السليمة وغير السليمة من هذا المنطلق كان الاهتمام بالطاقة المتجددة والتوسع فيها سبيل لسعادة الناس والتقريب بين الدول.

في هذه الدراسة تناولنا مجموعة من الطرق المستخدمة للحصول علي الطاقة القصوى بشكل مختصر ومن تم قمنا بالمقارنة فيما بينها لتحديد مميزات كل طريقة وموقعها بالنسبة للطريقة الأخرى بحيث يسهل علي الباحث اختيار الطريقة الافضل للتطبيقات العملية وفق المحددات والامكانيات المتوفرة لديه .

تم قمنا بدراسة مفصلة لمعرفة جميع العوامل المؤثرة في خصائص الخلية وتأثير التغير فيها علي الطاقة الناتجة وقد انقسمت العوامل ما بين داخلية كتأثير التغير في المقاومات وأخري خارجية كتأثير التغير في درجة الحرارة والاشعاع والظل .

وفي النهاية قمنا بتطبيق عملي بسيط يوضح استخدام احدي الطرق للحصول علي الطاقة القصوى وهي طريقة Incremental Conductance Algorithm.

Dedication

To my parents

Brothers

Sisters

Wife Ola

Daughter Seham

Son Mohammad

Friends

Acknowledgment

At the beginning, I thank ALLAH for enabling me to complete this work . I have taken efforts in this research which really would have been impossible without the indebted support and help of many individuals. I would like to extend my sincere thanks to all of them.

I would like to starting by expressing my deepest gratitude to my professional assistance, thesis supervisor Prof. Dr Hala J. EL-Khozondar for her guidance support, and constant supervision.

I also would like to extend my thanks to my thesis committee members Dr. Rifa J. EL-Khozondar, Dr. Fady E. El-nahal and Prof. Teuvo Suntio.

Many thanks go to my parents for their co-operation, prayers and encouragement all my life helping me going forward especially in completion of this research. Words will not be enough to thank my wife and children for their support.

Also, I would like to thank my friend Ahmed Badawi for his continuous encouragement.

LIST OF FIGURES

LIST OF TABLES

ABBREVIATIONS

Maximum Power Point Tracking	MPPT
Photovoltaic	PV
Greenhouse Gas	GHG
Clean Development Mechanism	CDM
Municipal Solid Waste	MSW
Silicon	Si
Direct Current	DC
Fill Factor	FF
Copper Indium Gallium Selenide	CIGS
Duty Ratio	D
Perturb and Observe	P&O
Incremental Conductance	IC
Parasitic Capacitance	Cp
Fuzzy logic Controller	FLC
Negative Big	NB
Negative Small	NS
Zero	ZE
Positive Small	PS
Positive Big	PB
Error	E
Center of Gravity	COG
Ripple Correlation Control	RCC
Reference Maximum Power	RMP
One-Cycle Control	OCC
Best Fixed Voltage	BFV

Linear Reoriented Coordinates Method	LRCM
PV Output Senseless	POS
Sloped Air-Gap	SAG
Continuous Current Mode	CCM
Variable Step-Size Incremental Resistance	INR
Modified Perturb and Observe	MP&O
Estimate, Perturb and Perturb	EPP
Quadratic Interpolation	QI
Particle Swarm Optimization	PSO
Pulse Width Modulation	PWM
Stimulated Annealing	SA
Artificial Neural Network	ANN
Total Harmonic Distortion	THD
Extremum Seeking Control Method	ESC
Polynomial Curve Fitting	PCF
Differentiation Method	DM
Power Conditioning System	PCS

Table of Contents

CHAPTER 1 INTRODUCTION

This chapter gives us general information about the concept of energy starting with the motivation in Section 1.1. Section 1.2 gives a brief history of energy. Benefits of clean energy initiatives are explained in Section 1.3. Section 1.4 is dedicated to clean development mechanism. Sources of renewable energy are listed in Section 1.5. While Section 1.6 presents the renewable energy in the Palestinian Territory. The main future plans to increase using photovoltaic (*PV*) cell are summarized in Section 1.7.

1.1 Motivation

"Renewable energy is derived from natural processes that are replenished constantly. In its various forms, it derives directly from the sun, or from heat generated deep within the earth. Included in the definition is electricity and heat generated from solar, wind, ocean, hydropower, biomass, geothermal resources, and biofuels and hydrogen derived from renewable resources"[1].

Pollution resulting from the use of conventional energy leads to environmental health hazards and economic threats; therefore, the use of alternative energy will reduce these effects and reduce the global energy crisis. It also supports global stability and prevent conflicts that have erupted for control of conventional energy sources. Recently using renewable energy technology increased globally and developed rapidly where it plays an important role in clean application especially in electric power generation. By using solar energy, we can get electric energy directly by using photovoltaic module then using maximum power point tracker (*MPPT*) to maximize the photovoltaic output power.

1.2 History of Solar Energy

Human was keen to exploit the natural resources which God harness them for him. Sun is one of the most important resources which have been exploited. Back to the fifth century *BC*, Greeks exploited the sun for heating purposes. The effect of photovoltaic cells discovered by Becquerelin 1839 while experimenting with an electrolytic cell but not developed as a power source until 1954 by Chapin et al. (Bell Laboratory scientists)[2]. They invented the first *PV* cell which capable of converting enough of the sun's energy into power to run every day electrical equipment. The practical applications

of *PV* system refer to 1973 when the first company established to manufacture terrestrial *PV* cells in the *U.S.* It was launched as a fully owned subsidiary of Exxon the first introduced to supply power to remote locations (telecommunications, coast guard etc.). It was intended in the long run to compete with conventional power sources. However, the boom in the field of solar energy observed significantly in recent years, especially after 2000. There are rule to promote challenges facing solar energy such as a Renewable Energy Law in 2005 which designed to promote the development and utilization of renewable energy, and safeguard energy security which amended in 2009 to require electricity grid companies to buy all the electricity produced by renewable energy generators[2].

The annual production of cells grew tenfold from about 50MW in 1990 to more than 500MW by 2003. This growth continues due to the advantages of solar energy as standalone and grid-linked opportunities, reliability, ease of use, lack of noise and emissions, and reducing cost per unit energy produced[3].

1.3 Multiple Benefits of Clean Energy Initiatives

There are many advantages resulting from the use of clean energy distributed on fields of environmental, economic and health. The clean energy has benefits include diversity, security, improved quality of life, environment and human health. It also improves economic gains through avoiding medical costs, higher disposable incomes, and more jobs[4].

1.3.1 Economic Impacts

Technological advances in the field of renewable energy has become clear in recent years. We note that while the prices of traditional energy sources constantly rise, the costs of Renewable energy decline steadily so the advantages of investment in renewable energy has become increasingly clear, even in areas that traditionally supports fossil fuels. The main reasons that make renewable energy technologies offer an economic advantage are labor intensive, so they generally create more jobs invested than conventional electricity generation technologies, from high-tech manufacturing of photovoltaic components to maintenance jobs at wind power. They also use primarily indigenous resources, so most of the energy dollars can be kept, where the individuals, companies, or communities can reduce their utility bills. For example, schools can cut

costs by using wind and electric cooperatives can provide cheaper electricity to members with photovoltaic[5][6][10].

1.3.2 Health and Environment Impacts

All energy sources have some impact on our environment and health which varies between long-term and short-term effects. Fossil fuels are more harmful than renewable energy sources. Thus, we need to improve access to low-emission, renewable, and modern energy technologies both at home and at community. They can benefit from long term sustainability. Notably, the inefficient combustion of fossil fuels and biomass for energy purposes is the major cause of climate change. Air pollution, often due to inefficient modes of energy production, distribution, and consumption, is a large and growing cause of environmental health risks[7], so it is advisable to increase reliance on renewable energy sources, and support clean energy initiatives. This appears through better air quality which enhances local quality of life. Healthier people reduces strain on the health system, using fewer sick days also lower carbon dioxide emissions in the near term may have a large impact on our ability to meet long term climate goals since greenhouse gas (*GHGs*) accumulate and can remain in the atmosphere for decades, affecting our global climate system and human health for the long term[4][8][9].

1.4 Clean Development Mechanism

The clean development mechanism (*CDM*) is one of the flexible mechanisms under the Kyoto Protocol. It provides for industrialized countries to invest in emission reducing plants in developing countries also it enables develop countries to meet their emission reduction commitments in a flexible and cost effective manner and assists developing countries in meeting their sustainable development objectives.

To reach the targets, Kyoto Protocol allowed three flexibility mechanisms: (i) joint implementation, (ii) clean development mechanism and (iii) international emissions trading. Among these three mechanisms, *CDM* plants would achieve their sustainable development objectives. Such plants would also lead to indirect benefits in the developing country like income generation, employment generation, improvement in local air quality, and enhancement of quality of life[11].

1.5 Sources of Renewable Energy

The main sources and components used in renewable energy systems included solar, wind, hydropower, biomass, and geothermal resources. In this section a brief is given for each type of these sources.

1.5.1 Biomass and Biofuels

Bioenergy term sometimes used to cover biomass and biofuels together[3]. Bioenergy resources are widely available worldwide and have the largest share of all renewable energy sources. Biomass resource was the first energy source harnessed by humans[13]. It comes in many forms. Traditionally, wood, crop residues and animal waste have been used for heating or cooking, but today biomass is also used in many other ways. Municipal solid waste (*MSW*) can be used for heat or electricity. Landfill gases can be used for heat, electricity or fuels. Biological conversion of *MSW* using anaerobic digestion can produce electricity, heat or fuel gas. Wood and wood wastes can be used to produce electricity, heat for industrial purposes or domestic space heating.

Recently, the interest in producing liquid fuels from grain and dedicated energy crops are increasing. They are only renewable source of liquid transportation fuels, which can be in the form of ethanol or biodiesel[1]. Moreover, the carbon in biomass is obtained from CO_2 in the atmosphere via photosynthesis, and not from fossil sources. When biomass is burnt or digested, the emitted CO_2 is recycled into the atmosphere without adding to atmospheric CO_2 concentration over the lifetime of the biomass growth[3].

1.5.2 Wind Power

The extraction of power from the wind with modern turbines and energy conversion systems is an established industry. Machines are manufactured with a capacity from tens of watts to several megawatts, and diameters of about 1m to more than 100 m[3].

The power output increases rapidly with an increase in available wind velocity. Small wind speed difference makes a very big difference because the energy contained in the wind increases with the cube of the wind speed. A maximum of about 59 % of the energy can be extracted (Betz number). For this reason, good wind sites are important[16]. We must take into account the wind does not blow equally or evenly everywhere on earth. Over open sea or flat stretches of land the wind is stronger than over towns or woods[14]. Modern turbines have already greatly reduced noise pollution, which is less than traffic noise[18], efficiencies and availabilities have improved and wind farm concept has

become popular in addition to that, wind turbines have become larger, combine with solar[15].

1.5.3 Hydropower

The term hydropower is usually restricted to the generation of shaft power from falling water. The power is then used for direct mechanical purposes or, more frequently, for generating electricity. Other sources of water power are waves and tides[3]. But Hydroelectric technology is the most mature form of renewable energy and extremely reliable, but it requires very high initial investments, with low maintenance cost. Its design life is more than a century. Natural and pumped storage dams are suitable for peak electricity demand. Hydropower is cheap if calculated in the conventional manner[16]. Worldwide, about 45 000 large dams have been built for electricity generation, flood protection, water storage, agricultural irrigation, navigable waterways and recreation. As a result of economies of scale, approximately 97 % of hydroelectric plants have a capacity in excess of 10 MW[16]. The main disadvantages of hydro-power are associated with effects other than the generating equipment, particularly for large systems. These include possible adverse environmental impact, effect on fish, silting of dams, corrosion of turbines in certain water conditions, social impact of displacement of people from the reservoir site, loss of potentially productive land (often balanced by the benefits of irrigation on other land) and relatively large capital costs compared with those of fossil power stations[3].

1.5.4 Geothermal

Geothermal activity in the earth's crust derives from the hot core of the earth[12]. Where the inner core of the earth reaches a maximum temperature of about 4000°C. Heat passes out through the solid submarine and land surface mostly by conduction and occasionally by active convective currents of molten magma or heated water[3].

Examples of geothermal energy are the natural geysers and hot water sources employed for power generation and space heating or using deep hot dry rock as heat exchangers by pumping water through the natural rock fissures to produce steam for power generation[12].

1.5.5 Photovoltaic

Solar energy can be used in a number of ways. For electricity generation the most common process is through solar photovoltaic where *PV* panels convert sunlight directly into *DC* electricity. *PV* panels, having no moving parts, require little maintenance, are highly reliable, long lived where the semiconductor materials are encapsulated and sealed hermetically making it lasts for a longer period of more than 25 year. In addition, *PV* panels are highly modular. Also it is easy to assemble *PV* panels into an array that can meet any given sized load. With suitable electronics, *PV* systems can be grid-connected or stand-alone, where they can also be used for water pumping or other mechanical work. *PV* arrays do not emit vibrations, noises and pollutants during their operation. This means they can be integrated into new and existing buildings, which then become energy exporters instead of consumers. All above advantages make this modern technology increasingly attractive. Despite this, the main disadvantage of *PV* is its high capital cost[16][18][19].

1.6 Renewable Energy in the Palestinian Territory

The Palestinian territories are facing critical situation concerning the achievement of sustainable development. Several problems have contributed to the continuous deterioration of the political, economic, social and environmental conditions and hindered development initiatives. The lack of a Palestinian infrastructure for close to four decades has impeded any realistic progress on the energy front. Scarcity of conventional energy resources and the limited renewable resources has created unrealistic price control, energy shortage and future energy crisis. The national and comprehensive energy policy is still not clear due to the continuous Israeli occupation, weak and fragmented institutional framework and the incomplete framework of the Palestinian State. Renewable energy market is strongly affected by the political stability in the region, economic situation of the people, rising demand on energy and availability of the indigenous resources. The environment of political risk and uncertainty has inhibited investors from making large scale energy or industrial investments. In spite of all these challenges, Palestine has gone forward to utilize its natural resources for rehabilitation and construction[20], such as the exploitation of solar energy and other forms of renewable energy. Biomass which is the use of agricultural waste for heating and cooking is common in rural areas. In addition to that, there are a few wind energy projects underway, including one at the hospital in Hebron. Other technologies are already in use,

including thermal energy which is a form of kinetic energy producing heat, photovoltaic energy and geothermal energy and the most common type of renewable energy used in Gaza, is the use of solar energy for water heating. According to the survey on household energy by the Palestinian Central Bureau of Statistics, over 60% of households use solar water heaters[21].

1.7 Renewable Energy in the Future

In the ongoing efforts of the countries of the world, many countries have developed future policies to take advantage of alternative energy and participation in the treatment of the implications of conventional energy. Many countries set a timetable and specific proportions for 2020. For example, European Union countries committed to increase its reliance on renewable energy to reach 20% of the total energy consumption. Ambition does not stop at that but it extends to the 2030 year to ensure that the *EU* is on track to meet longer term climate objectives. In addition to that, energy Roadmap has developed for 2050. Roadmaps suggested findings, by 2030 *GHG* emissions would need to be reduced by 40% in the *EU* to be on track to reach a *GHG* reduction between 80-95% by 2050, consistent with the internationally agreed target to limit atmospheric warming to below 2°C[22]. An overview of the estimates scenarios of the expected increase in the world's dependence on alternative energy and its impact on reduced emissions is shown in Fig. 1**[**17**].**

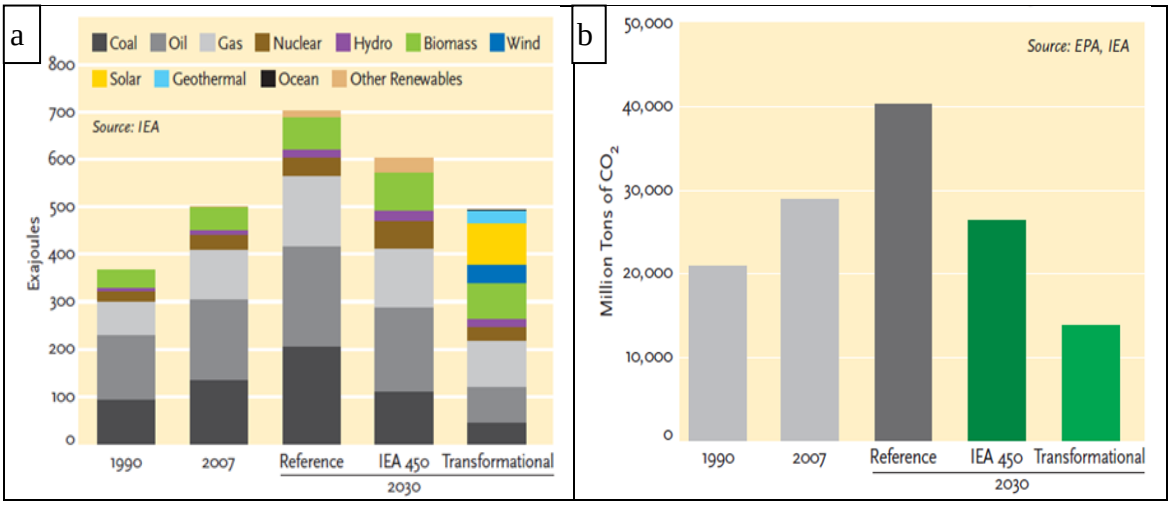

Fig. 1: a) Global primary energy demand,1990,2007,and three scenarios for 2030
b) Global energy- related demand CO_2 emission ,1990,2007,and three scenarios for 2030

At the local level, the Palestinian Authority announced that it will increase reliance on renewable energy to reach 5% of the energy consumed in 2020. Israel is seeking to increase its production in the same period of up to 10%. Knowing it's topping the world's dependence on solar energy where it is up to 3%[23].

CHAPTER 2 PHOTOVOLTAIC CELLS

In this chapter, photovoltaic cells will be introduced. The operation principle is summarized in Section 2.1. While Section 2.2 explain equivalent circuit of a solar cell. basic concepts of Solar *PV* cell are explained in Section 2.3. Section 2.4 concludes with broad categories of technology used for *PV* cells. *DC/DC* converters used for the *MPPT* system are explained in Section 2.5.

2.1 Operating Principle

Photovoltaic cells are the basic components of larger solar arrays. Ninety-nine percent of today's solar cells are made of silicon (*Si*)[26], the second most abundant material on earth. However, scarce indium and tellurium are used in some cells[16]. Energy is created when photons of light from the sun strike a solar cell and are absorbed within the semiconductor material. This excites the semiconductor's electrons, causing the electrons to flow, and creating a usable electric current. The current flows in one direction and thus the electricity generated is termed direct current (*DC*) as will be explained in brief below[28]. The photoelectric conversion in the *PN* junction. *PN* junction (diode) is a boundary between two differently doped semiconductor layers; one is a *P*-type layer (excess holes), and the second one is an *N*-type (excess electrons). At the boundary between the *P* and the *N* area, there is a spontaneous electric field, which affects the generated electrons and holes and determines the direction of the current. A diagram of the *PN* junction showing the effect of the mentioned electric field is illustrated in Fig. 2[27]. To obtain the energy by the photoelectric effect, there shall be a directed motion of photoelectrons, i.e. electricity. All charged particles, photoelectrons also, move in a directed motion under the influence of electric field. The electric field in the material itself is located in semiconductors, precisely in the impoverished area of *PN* junction (diode). It was pointed out for the semiconductors that, along with the free electrons in them, there are cavities as charge carriers, which are a sort of a byproduct in the emergence of free electrons. Cavities (holes) occurs whenever the valence electron turns into a free electron, and this process is called the generation, while the reverse process, when the free electron fills the holes, is called recombination. If the electron hole pairs occur away from the impoverished areas it is possible to recombine before they are

separated by the electric field. Photoelectrons and holes in semiconductors are accumulated at opposite ends, thereby creating an electromotive force. If a consuming device is connected to such a system, the current will flow and we will get electricity[27,29].

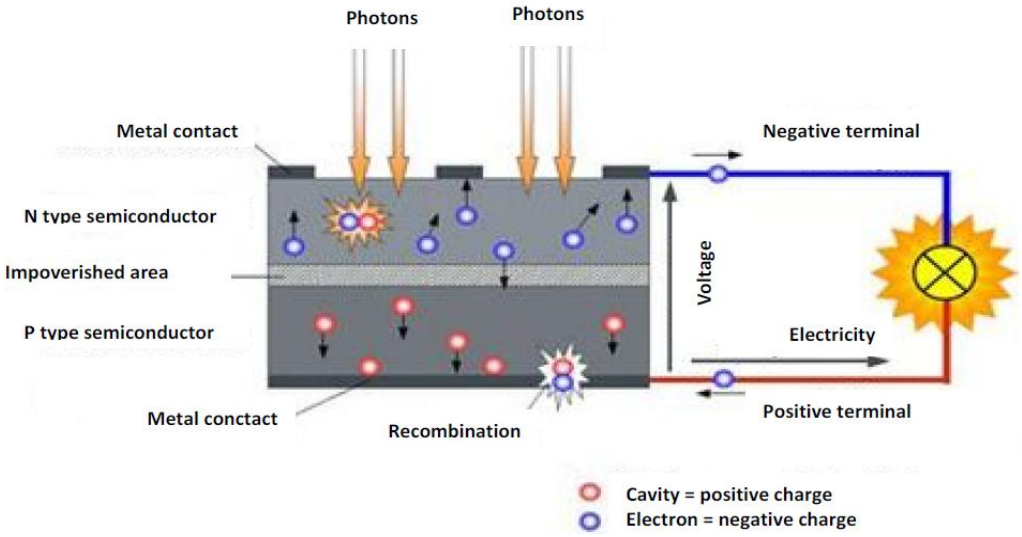

Fig. 2: *P-N* junction

2.2 Equivalent Circuit of a Solar Cell

The equivalent circuit of the general model consists of a photo current, a diode, a parallel resistor (R_{SH}) expressing a leakage current, and a series resistor (R_S) describing an internal resistance to the current flow, as shown in Fig. 3. The terminal current is given by equation (2.1)[24].

$$I = I_{PH} - I_S \left[exp\left(q \frac{(V + IR_S)}{KT_C A} \right) - 1 \right] - \frac{V + IR_S}{R_{SH}} \tag{2.1}$$

Where I_{PH} is a light-generated current or photocurrent, I_S is the cell saturation of dark current, $q = 1.6 \times 10^{-19} C$ is an electron charge, $k = 1.38 \times 10^{-23} J/K$ is Boltzmann's constant, T_C is the cell's working temperature, A is an ideal factor, R_{SH} is a shunt resistance, and R_S is a series resistance.

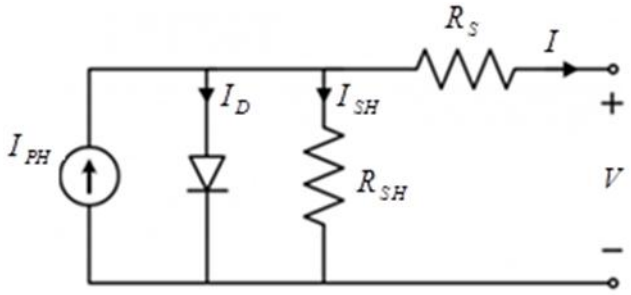

Fig. 3: Equivalent circuit models of PV cell.

Since a typical *PV* cell produces less than 2W at 0.5V approximately, the cells must be connected in series-parallel configuration on a module to produce enough high power. A *PV* array is a group of several *PV* modules which are electrically connected in series and parallel circuits to generate the required current and voltage. The equivalent circuit for the solar module arranged in N_P parallel and N_S series is shown in Fig. 4.

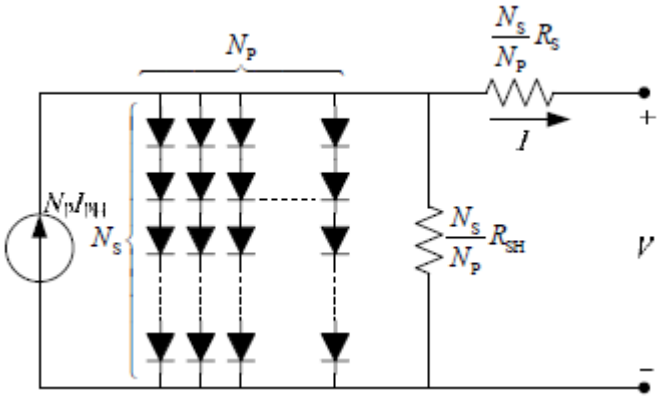

Fig. 4: Equivalent circuit models of generalized PV

The terminal equation for the current and voltage of the array is

$$I = N_P I_{PH} - N_P I_S \left[exp\left(q \frac{\left(\frac{V}{N_S} + \frac{IR_S}{N_P} \right)}{KT_C A} \right) - 1 \right] - \frac{\left(\frac{N_P V}{N_S} + IR_S \right)}{R_{SH}} \qquad (2.2)$$

$$V_{Th} = KT_C$$

For an ideal *PV* cell, there is no series loss and no leakage to ground, i.e., $R_S = 0$ and $R_{SH} = \infty$ [24]. However, this ideal case is not possible but scientists work to reduce the effect of both a series and a shunt resistance.

2.3 Basic Concepts of Solar *PV* Cell

Parameters such as the open-circuit voltage V_{OC}, short circuit current I_{SC} , fill factor *FF*, efficiency η, and the cell voltage, current and power at the maximum power point, $P = P_{MPP}$ V_{MPP}, I_{MPP}, and P_{MPP}, respectively. These parameters describe the operation of the *PV* cell appear in the generic *I-V* curve displayed in Fig. 5. The figure displays the power delivered by the module which equal the product of voltage and current[25].

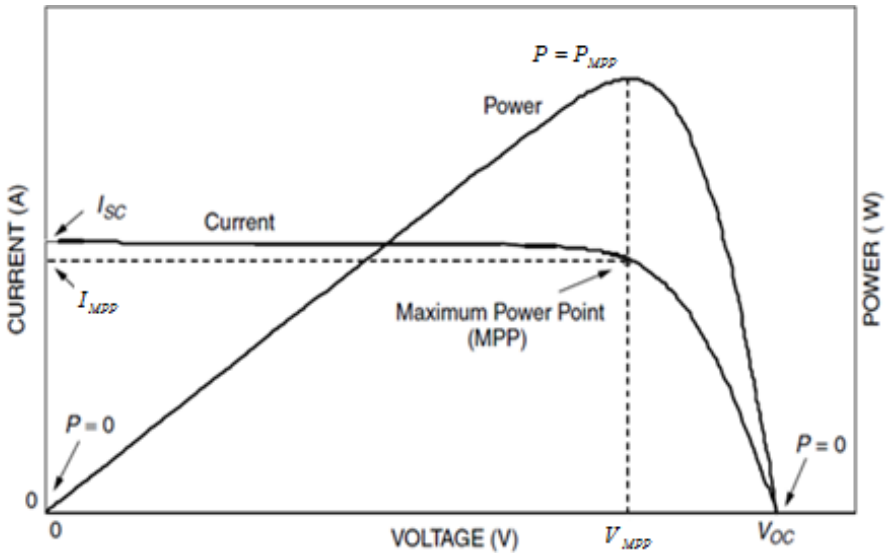

Fig.5: The *I-V* curve and power output for a *PV* module.

2.3.1 The Short-Circuit Current ISC and the Open-Circuit Voltage VOC

There are two conditions of particular interest for the actual *PV* cell and for its equivalent circuit. As shown in Fig. 6, they are the current that flows when the terminals are shorted together which called the short-circuit current, I_{SC} and the voltage across the terminals when the leads are left open which called the open circuit voltage, V_{OC} . When the leads of the equivalent circuit for the *PV* cell are shorted together, no current flows in the (real) diode since $V_d = 0$, so all of the current from the ideal source flows through the shorted leads. Since that short circuit current must equal I_{SC} , the magnitude of the ideal current

source itself must be equal to I_{SC}. And V_{OC} can be approximated from equation (2.1) when the output current of the cell is zero, i.e. *I=0* and the shunt resistance R_{SH} is neglected. It is represented by equation (2.3).

$$V_{OC} = \frac{KT_C A}{q} \ln(\frac{I_{PH}}{I_S} + 1) \tag{2.3}$$

In both cases, since power is the product of current and voltage, no power is delivered by the module and no power is received by the load[25].

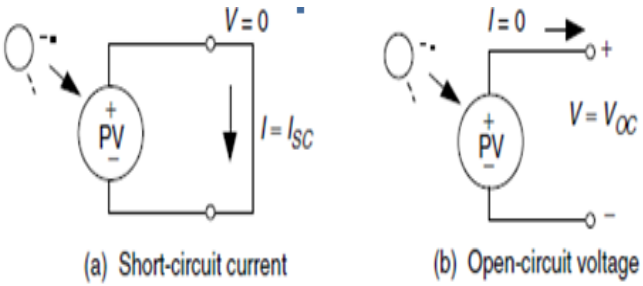

Fig.6: The short-circuit current I_{SC} and the open-circuit voltage V_{OC}

2.3.2 Fill Factor

The *PV* arrays are often characterized by a parameter known as fill factor (*FF*). *FF* actually measures the quality of the *PV* array. It is the ratio of the power at the maximum power point (actual) to the product of V_{OC} and I_{SC} (theoretical) , *FF* can be expressed as:

$$FF = \frac{P_{MAX}}{P_T} = \frac{I_{MP} V_{MP}}{I_{SC} V_{OC}} \tag{2.4}$$

And it can be interpreted graphically as the ratio of the rectangular areas defined by the *I-V* curve as illustrated in Fig. 7[25][27][35].

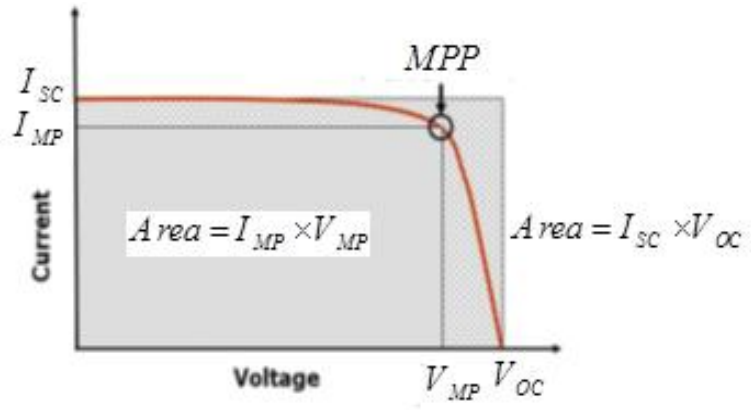

Fig. 7: Graphical interpretation of *FF*

High performance cell are designed with a low series resistance values and high parallel resistance values[35], to reach ideal situation where the current held right up to the short circuit value, then reduced suddenly to zero at the *MPP*, and have a *FF* of unity. Needless to say, practical cells do not achieve this value where they depend on *PV* arrays types [31]. The maximum value of the *FF* in Si is 0.88[33].

The importance of *FF* is to indicate the power achieved. The array with higher *FF* will produce more power; e.g., in case of two individual *PV* modules having the same values of I_{SC} and V_{OC}. Also, any impairment that reduces the *FF* will reduce the output power[35].

2.3.3 Efficiency

The efficiency of a solar cell is defined as the ratio of the output electric power over the input solar radiation power under standard illumination conditions at the maximum power point[35].

2.3.4 Electric Characteristics of *PV* Cell

Two factors must be taken into account are the sunlight intensity and *PV* cell temperature where the output power of *PV* module is dependent on these two parameters. Solar irradiance has direct relation and temperature has reverse relation with output power of *PV* module. It means increasing the sunlight intensity; the output power rises up. Increasing the temperature; the power comes down. Fig. 8 and Fig. 9, show the output characteristics of *PV* module under variable sunlight intensity and different temperatures[32].

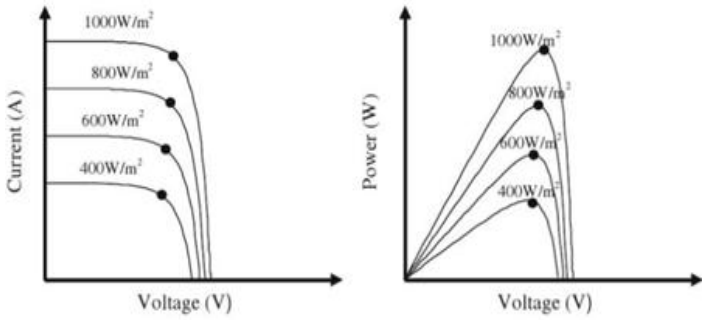

Fig. 8: Irradiance effect on electrical characteristic. a) *I-V*, b) *P-V*

From Fig. 8, we note that while sunlight intensity is increasing, the current I_{SC} increases quasi linearly, power increases and that the voltage V_{OC} increases slightly. Also from Fig. 9, we note that while temperature is increasing the short circuit current I_{SC} increases slightly, the power increases slightly, but the open circuit voltage V_{OC} strongly decreases.

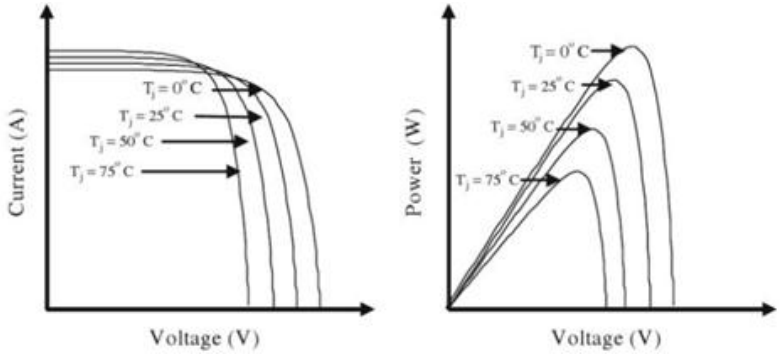

Fig. 9: Temperature effect on electrical characteristic. a) I-V, b) P-V

2.4 Solar *PV* Technology

There are two broad categories of technology used for *PV* cells, namely, crystalline silicon, and thin film, which is newer and growing in popularity[36]. The crystalline silicon solar cell was the first practical solar cell invented in 1954. The efficiency of such solar cells as mass produced is 14–20%, which is still the highest in single-junction solar cells. It also has a long life and a readiness for mass production. To date, it still accounts for more than 80% of the solar cell market. There are two versions of the crystalline silicon solar cell: mono crystalline and polycrystalline. Amorphous silicon thin-film silicon solar cells are much less expensive than the crystalline ones. But the efficiency is only 6–10%. In between are *CIGS* (copper indium gallium selenide) and *CdTe – CdS* thin film solar cells, with a typical efficiency of around 10% and account for about 15% of the

market. Because of the very high absorption coefficient, the amount of materials required is small, and the production process is simpler; thus the unit price per peak watt is lower than crystalline silicon solar cells. To date, organic solar cells still have low efficiency and a short lifetime, and the market share is insignificant, Table 1 summarizes several significant types of solar cells[38].

Type	Efficiency (%)	Cost ($/Wp)	Market share (%)
Monocrystalline Si	17–20	3.0	30
Polycrystalline Si	15–18	2.0	40
Amouphous Si	5–10	1.0	5
CIGS	11–13	1.5	5
CdTe-CdS	9–11	1.5	10

Table 1: Type of solar cell

2.5 *DC/DC* Converter Used for the *MPPT* System

A *MPPT* is used for extracting the maximum power from the solar *PV* module and transferring that power to the load. A *dc/dc* converter serves the purpose of transferring maximum power from the solar *PV* module to the load. Without *dc/dc* converter no *MPPT* system are designed, we can consider *dc/dc* converter acts as an interface between the load and the module as in Fig. 10.

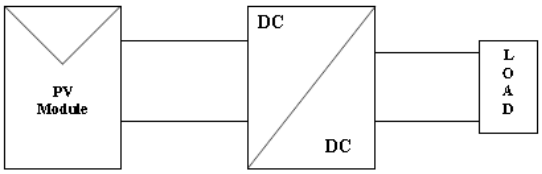

Fig. 10: Block diagram of Typical *MPPT* system

The type of the converter depends on the method we use *PV* panels. If system of *PV* panels and converter is not connected to power grid, we talk about off-grid system. At no-load, the energy obtained from *PV* panels is usually stored in batteries. If the consumption of energy begins, the converter starts to transfer the energy to the load through the inverter. If the level of power obtained from *PV* panels is higher than the system can offer, the converter starts to draw the energy from batteries[37,39].

There are many circuit configurations for switch converters. However, the most popular are: boost converter (step-up converter), buck converter (step-down converter), buck-boost converter (CUK).

2.5.1 Buck Converter

The buck converter is also known as the step down converter. It can be used in the cases where the output voltage (battery) required is less than or equal the input voltage (solar array voltage), and output current is larger than the input current, the power flow is controlled by adjusting the on/off duty cycle of the switching where the relation between input and output voltage are accounted by the conversion ratio $\mu = \frac{V_o}{V_i}$ which varies with the duty ratio D of the switch. Duty ratio depend on the ratio of the t_{on} to T so the relation becomes[36,37],

$$\mu = \frac{V_O}{V_i} = \frac{t_{on}}{T} = D \tag{2.5}$$

where t_{on} refer to the duration that the switch is active and T is the switching period where it's constant . In *PV* applications, the buck type converter is usually used for charging batteries, and for water pumping systems[40]. Ideal buck converter circuit is shown in Fig.11[36].

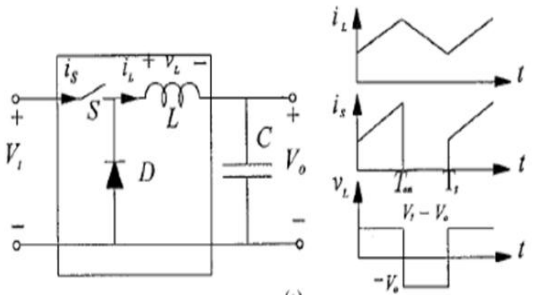

Fig. 11: Ideal buck converter circuit

2.5.2 Boost Converter

The boost converter is also known as the step-up converter. It can be used in the cases where the output voltage greater than the input voltage, essentially functioning like a reversed buck converter. The practical application which use a boost type converter

appear in grid systems. Fig. 12 shows the circuit of the boost converter where the (conversion ratio between input and output voltage) are[36,37].

$$\mu = \frac{V_O}{V_i} = \frac{T}{t_{off}} = \frac{1}{1-D} \tag{2.6}$$

Where t_{off} is the duration that the switch is not active.

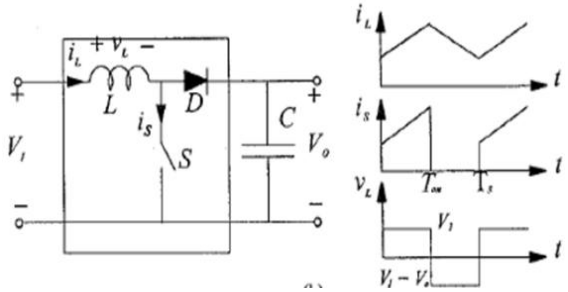

Fig. 12: Equivalent circuit of a boost converter

2.5.3 CUK Converter

The CUK converter uses capacitive energy transfer and analysis is based on current balance of the capacitor. But other types of converters use an inductor, CUK converter will be responsible to inverter the output signal from positive to negative or vise versa, that mean the output voltage magnitude is either greater than or less than the input voltage magnitude. The circuit of the cuk shows in Fig. 13. The conversion ratio is[36,37].

$$\mu = \frac{V_O}{V_i} = \frac{t_{on}}{t_{off}} = \frac{D}{1-D} \tag{2.7}$$

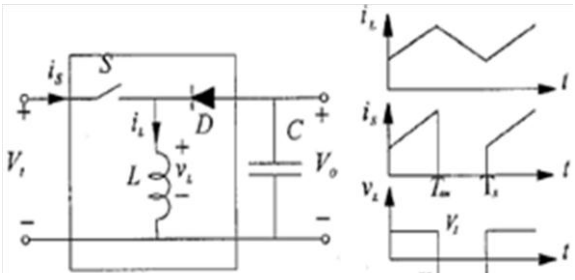

Fig.13: Equivalent circuit of CUK converter

CHAPTER 3 MAXIMUM POWER POINT TRACKING ALGORITHIMS

Obtaining the maximum power automatically from a solar modules or in other words making the system operates at maximum efficiency, depends on the used algorithm of *MPPT*. These algorithms take into account the varying of irradiation and temperature over time also the load impedance. These factors affects *MPP* thus reflected in the amount of electricity generated. The *MPPT* method vary in many aspects including complexity, cost, sensor dependence, convergence speed, implementation hardware, compensation for capacitance, range of effectiveness, popularity capability of escaping from local optima and their applications[54]. A complete review and compare of 57 *MPPT* methods for *PV* system can be found below.

There are different type of *MPPT* algorithm that used for the purpose of improving the efficiency of solar panel but the most commonly known are perturb and observe (*P&O*), incremental conductance (*IC*), open-circuit voltage (V_{OC}) control, neural network, fuzzy logic control and several other *MPPT* methods. In the next section some of the most popular *MPPT* techniques are discussed. Most popular algorithms is summarized in Section I. While Section II define the parameter which used to classification method. Characteristics of various *MPPT* algorithms are explained in Section III.

3.1 Most Popular Algorithms

3.1.1 Perturb and Observe (P&O)

The *P&O* algorithm also known "hill-climbing", is one of the most popular and commonly algorithm because of its low cost, ease of implantation, simple structure and the few measured parameters which are required. It only measures the voltage (V) and current (I) of the *PV* array. *PV* system controller changes *PV* array output with a smaller step in each control cycle. The step size is generally fixed while mode can also be increased or decreased. Both *PV* array output voltage and output current can be the control object, this process is called "perturbation". Then, by comparing *PV* array output power of the cycles before and after the perturbation. If the operating voltage of the *PV* array is perturbed in a given direction and $dP \succ 0$, it is known that the perturbation

moved the array's operating point toward the *MPP*. The *P&O* algorithm would then continue to perturb the *PV* array voltage in the same direction. If $dP \prec 0$, then the change in operating point moved the *PV* array away from the *MPP*, and the *P&O* algorithm reverses the direction of the perturbation. This process continues until it reaches the *MPP* point. It depends on the fact that the derivative of power with respect to voltage is zero at *MPP* point[41-44]. Although the advantage of this method, it fails under rapidly changed atmospheric conditioned. Also it has other limitation such as the slowly response speed oscillation around the *MPP*[41]. To reduce obstacles, a small sampling rate (step size) is required, finally to overcome disadvantages of this method, increment conductance is used.

3.1.2 Incremental Conductance Algorithm

The incremental conductance method is based on the fact that the sum of the instantaneous conductance (*I*/*V*) and the incremental conductance is zero at *MPP*. Because it is negative on the right side of *MPP* and positive on the left side of the *MPP*. This relationship is derived from the fact that the slope of the *PV* array power curve is zero at the *MPP*, positive on the left of the *MPP*, and negative on the right. Fig.14 shows the slope of the *P-V* array power curve. Thus, incremental conductance can determine that the *MPPT* has reached the *MPP* and stop perturbing the operating point of the *PV* array. If this condition is not met, the direction in which the *MPPT* operating point must be perturbed can be calculated using the above relationship.

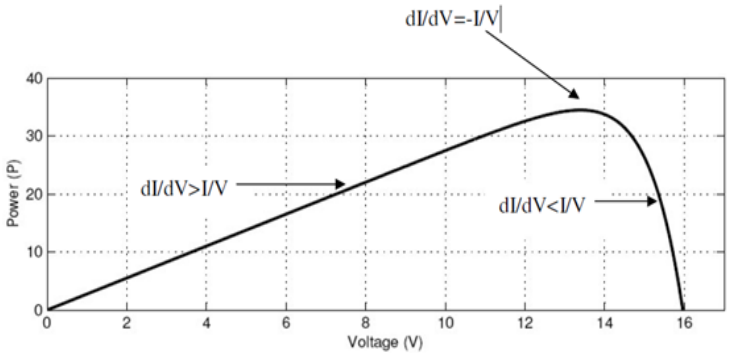

Fig.14: The slope of the *P-V* array power curve

Although incremental conductance is an improved version of *P&O*, it can track rapidly increasing and decreasing irradiance conditions with higher accuracy than *P&O*. However, this algorithm is increased complexity when compared to perturb and observe.

This increases computational time, slows down the sampling frequency of the array voltage and current[46-49].

3.1.3 Short Circuit Current Method

This technique is also known as constant current method. The principle of the constant electric current method is that the operating current of the solar cell has the approximate proportional relationship with the short circuit current at the *MPP*. This scale factor is invariant nearly when the sunshine and temperature outside changes. The operating current can be adjusted through the measure of the short circuit current of the battery board. Thus the maximum power point could be found from

$$I_{Max} = M_I \times I_{SC} \tag{3.1}$$

Where I_{Max} is the *MPP* current, I_{SC} is the short circuit current of the *PV* array and M_I is the current factor which approximately equals 90% of the short circuit current. The tracking accuracy is low because it needs to let the solar cell board short circuit for measuring the short circuit current. This has great effect on the life of the cell board. It holds the inferiority compared with the constant voltage method[50,51].

3.1.4 Open Circuit Voltage Method

This technique is also known as constant voltage method. Constant voltage method is based on the fact that the voltage of the solar cell has the approximate proportional relationship with the open circuit voltage. Open circuit voltage is a reference voltage at the *MPP* for different irradiation and temperature levels. Moreover, this scale factor is invariant nearly when the sunshine and temperature outside changes. The working voltage can be adjusted through the measure of the open circuit voltage of the battery board. Thus the *MPP* could be found from

$$V_{Max} = M_V \times V_{OC} \tag{3.2}$$

Where V_{Max} is the *MPP* voltage, V_O is the open circuit voltage of the *PV* array and M_V is the voltage factor which is always less than unity. Although this method is simple, it is difficult to determine the optimal value of constant M_V. In literature M_V varies from

0.71 to 0.8 depending upon the PV array characteristics. The common value used is 0.76; hence this algorithm is also called as 76% algorithm[50-51].

3.1.5 Parasitic Capacitances (Cp)

The algorithm of the parasitic capacitance is similar to that of the incremental conductance except that the effect of parasitic capacitance (Cp). Cp models the storage charges in the *P-N* solar cells junction and stray capacitance is included. Cp is added in parallel on the terminals of the previous models. It is added to the lighted diode equation (2.1). The observed current I_{obs} is expressed by

$$I_{obs} = I - I_{PC} \tag{3.3}$$

$$= I_{PH} - I_S \left[\exp\left(q \frac{(V + R_S I)}{A V_{Th}} - 1 \right) \right] - \left(\frac{V + R_S I}{R_{SH}} \right) - C_p \frac{dV}{dt} \tag{3.4}$$

$$= F(V) - C_p \frac{dV}{dt} \tag{3.5}$$

Where $C_p \frac{dV}{dt}$ is the current through C_p. From above equation, it shows that the first component I is function of the voltage $F(V)$ and the second one relates the current to the parasitic capacitance. The *MPP* is located at the point where $\frac{dP}{dV} = 0$. Multiplying the above result equation by the panel voltage V to obtain array power and differentiating the result. The equation of electric (array) power is obtained.

$$\frac{dF(V)}{dV} + \frac{F(V)}{V} = \frac{dI_{obs}}{dV} + \frac{I_{obs}}{V} + C_P \left(\frac{\dot{V}}{V} + \frac{\ddot{V}}{\dot{V}} \right) = 0 \tag{3.6}$$

Three terms in this expression represent observed incremental conductance, the observed instantaneous conductance, correction for parasitic capacities. First and second derivatives of array voltage take into account the ripple effect. The reader will note that if C_p is equal to zero, this equation simplifies to that used for the incremental conductance

algorithm. One disadvantage of this algorithm is that the parasitic capacitance in each module is very small, and will only come into play in large *PV* arrays where several module strings are connected in parallel to increase the effective capacitance seen by the *MPPT*. From this, the difference in *MPPT* efficiency between the parasitic capacitance and incremental conductance algorithms should be at a maximum in a high-power solar array with many parallel modules[32][38][52][64].

3.1.6 Fuzzy logic Controller *(FLC)*

FLC has wide range of applications in renewable energy. Its usage increased over the last decade due to its several advantages such as better performance, robust and simple design, deal with imprecise inputs. In addition, this technique does not require the knowledge of the exact model of system or an accurate mathematical model and can handle nonlinearity. It can also gets *MPPT* under changing weather conditions.

FLC consists of four categories as fuzzification, inference engine, rule base and defuzzification. Numerical input variables are converted into fuzzy variable known as linguistic variable based on a membership function similar to Fig.15. In this case, five fuzzy levels are used: *NB* (negative big), *NS* (negative small), *ZE* (zero), PS (positive small), and *PB* (positive big). For more accuracy seven fuzzy levels are used. In Fig. 15, *a* and *b* are based on the range of values of the numerical variable. Conventional fuzzy *MPPT* consists of two inputs and one output. The two input variables are the error (E) and the error change (ΔE), at sampled times *k* defined by:

$$E(K) = \frac{P_{PH}(K) - P_{PH}(K-1)}{V(K) - V(K-1)} \tag{3.7}$$

$$\Delta E(K) = E(K) - E(K-1) \tag{3.8}$$

where $P_{PH}(K)$ is the power of the photovoltaic generator, The input $E(k)$ shows if the load operation point at the instant k is located on the left or on the right of the maximum power point on the *PV* characteristic, while the input $\Delta E(k)$ expresses the moving direction of this point.

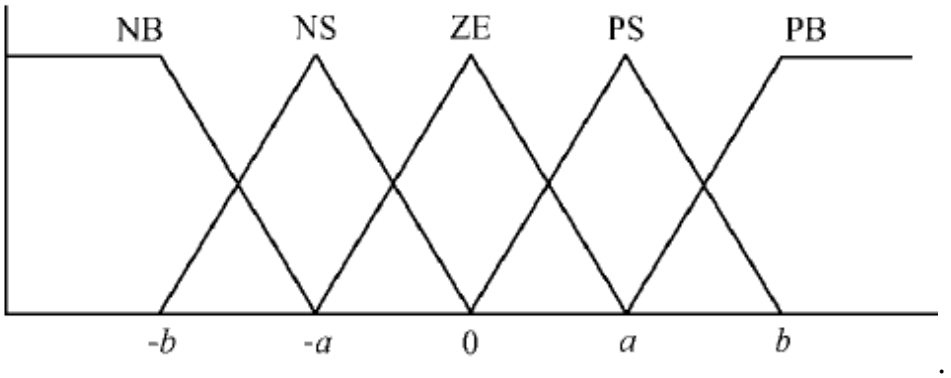

Fig.15: Membership function

Inference engine defines controller output in order to fuzzified input, rule base and fuzzy inference methods using Madani's method. Finally output linguistic terms are converted to numerical variable using one of the most commonly defuzzification techniques is called Center of Gravity *(COG)* to compute the output (duty ratio) of this fuzzy logic. However, the effectiveness of this method depends a lot on the knowledge of the user or control engineer in choosing the right error computation and coming up with the rule base table but this method provides faster results compared to other Artificial Intelligent control methods such as Genetic Algorithm and Neural Networks [34][47][53-55].

3.1.7 Temperature Method

Utilization a temperature method is a good option where the shortcomings of variations in temperature, which strictly changes the *MPP*, can be avoided. For this purpose, a low cost temperature sensor is adopted and modifies the *MPP* algorithm function, maintaining the right track of *MPP*. However, temperature sensing in practical implementations can be a problematic issue due to irregular distribution of *PV* array temperature, which can be avoided in small *PV* converters. Moreover, the sensor may be poorly calibrated or not correctly attached, providing wrong measurements of *PV* temperature. The equation that guides the temperature method is presented in

$$V_{MPP(t)} = V_{MPP(Tref)} + T_{KVOC}\left(T - T_{ref}\right) \qquad (3.9)$$

Where V_{MPP} is the *MPP* voltage, *T* is the panel temperature surface, T_{KVOC} is the temperature coefficient of V_{MPP}, and T_{ref} is the standard test conditions temperature [56-58].

3.1.8 Beta Method

This method differs from other methods in that it combines between fast and accurate tracking based on analysis of the *I-V* characteristics of a *PV* array, the approximation of the point of maximum power through the equation of an intermediate variable β, as given in the following.

$$\beta = \ln\left(\frac{I}{V}\right) - C \times V = \ln\left(I_S \times C\right) \tag{3.11}$$

where I_S is reverse saturation current and *C* is the diode constant equals $\frac{q}{AKTN_S}$ with *q, A, k, T* and N_S denoting the electronic charge, ideality factor, Boltzmann constant, temperature in Kelvin and the number of series connected cells, respectively. Moreover, as the operating conditions change, the value of β at the optimum point remains almost constant. Thus, β can be continuously calculated using the voltage and current of the panel and inserted on a conventional closed loop with a constant reference. However, for optimal performance, it is mandatory to know the *PV* electrical parameters, which can reduce the attractiveness of this method. Thus, β method approximates the *MPP* while conventional *MPPT* technique is used to track the exact *MPP*[56,58].

3.1.9 Neural Network

Neural networks commonly have three layers: input, hidden, and output layers as shown in Fig.16. The number of nodes in each layer varies and is user-dependent. The input variables can be *PV* array parameters like V_{OC} and I_{SC}, atmospheric data like irradiance and temperature or any combination of these. The output is usually one or several reference signal *(s)* like a duty cycle signal used to drive the power converter to operate at, or close to, the *MPP*, how close the operating point gets to the *MPP* depends on the algorithms used by the hidden layer and how well the neural network has been trained.

The links between the nodes are all weighted. The link between nodes *i* and *j* is labeled as having a weight of W_{ij} in Fig.16. To accurately identify the *MPP*, the W_{ij} *S* have to be carefully determined through a training process, whereby the *PV* array is tested over months or years and the patterns between the input *(s)* and output *(s)* of the neural network are recorded. Since most *PV* arrays have different characteristics, a neural network has to be specifically trained for the *PV* array with which it will be used. The characteristics of a *PV* array also change with time, implying that the neural network has to be periodically trained to guarantee accurate *MPPT*[56].

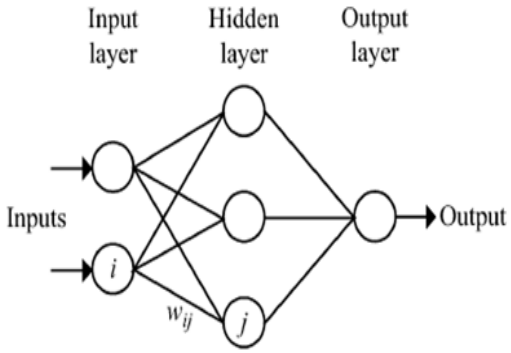

Fig.16: Example of neural network

3.1.10 Ripple Correlation Control *(RCC)*

When a *PV* array is connected to a power converter, the switching action of the power converter imposes voltage and current ripple on the *PV* array. As a consequence, the *PV* array power is also subject to ripple. *RCC* makes use of ripple to perform *MPPT*. *RCC* correlates the time derivative of the time-varying *PV* array power with the time derivative of the time-varying *PV* array current or voltage to drive the power gradient to zero, thus reaching the *MPP*. If the voltage or the current is increasing and the power is increasing, then the operating point is below (to the left of) the *MPP* ($V \prec V_{MPP}$ or $I \prec I_{MPP}$). On the other hand, if *V* or *I* is increasing and *p* is decreasing, then the operating point is above (to the right of) the *MPP* ($V \succ V_{MPP}$ or $I \succ I_{MPP}$). When the power converter is a boost converter, increasing the duty ratio increases the inductor current, which is the same as the *PV* array current, but decreases the *PV* array voltage. Therefore, the equation which controls the duty cycle can be written as[56]:

$$d(t) = -K_3 \int pv \cdot dt \tag{3.10}$$

$$d(t) = K_3 \int p \cdot i \cdot dt \tag{3.11}$$

Where k_3 is a positive constant.

3.1.11 Current Sweep

The current sweep method uses a sweep waveform for the *PV* array current such that the *I–V* characteristic of the *PV* array is obtained and updated at fixed time intervals. The V_{mpp} can then be computed from the characteristic curve at the same intervals to ensure that the sweep searches for the highest peak in case of multiple peaks. Current sweep method is implemented through analog computation. The current sweep takes about 50 ms, implying some loss of available power. It is pointed out that this *MPPT* technique is only feasible if the power consumption of the tracking unit is lower than the increase in power that it can bring to the entire *PV* system[56].

3.1.12 DC-Link Capacitor Droop Control

DC-link capacitor droop control is *MPPT* technique that is specifically designed to work with a *PV* system that is connected in cascade with an *AC* system line. The duty ratio *D*, of an ideal boost converter is given by

$$D = 1 - \frac{V}{V_{link}} \tag{3.12}$$

Where *V* is the voltage across the *PV* array and V_{link} is the voltage across the *DC* link. If V_{link} is kept constant, increasing the current going to the inverter increases the power coming out of the boost converter, and consequently increases the power coming out from the *PV* array. While the current is increasing, the voltage V_{link} can be kept constant as long as the power required by the inverter does not exceed the maximum power available from the *PV* array. If that is not the case, V_{link} starts drooping. Right before that point, the current control command I_{peak} of the inverter is at its maximum and the *PV* array operates at the *MPP*. The *AC* system line current is feedback to prevent V_{link} from drooping and *D* is optimized to achieve *MPPT*[56].

3.1.13 Load Current or Load Voltage Maximization

The purpose of *MPPT* techniques is to maximize the power coming out of a *PV* array. When the *PV* array is connected to a power converter, maximizing the *PV* array power also maximizes the output power at the load of the converter. Conversely, maximizing the output power of the converter should maximize the *PV* array power, assuming a lossless converter. It is pointed out that most loads can be of voltage source, current-source, resistive, or a combination of these types.

For almost all loads, it is adequate to maximize either the load current or the load voltage to maximize the load power. Consequently, only one sensor is needed. In most *PV* systems, a battery is used as the main load or as a backup, and a positive feedback is used to control the power converter such that the load current is maximized and the *PV* array operates close to the *MPP*. Operation exactly at the *MPP* is almost never achieved because this *MPPT* method is based on the assumption that the power converter is lossless[56].

3.1.14 $\frac{dP}{dV}$ or $\frac{dP}{dI}$ Feedback Control

This method is an obvious way of performing *MPPT* algorisms to compute the slope $\frac{dP}{dV}$ *or* $\frac{dP}{dI}$, of the *PV* power curve and feed it back to the power converter with some control to drive it to zero. The way the slope is computed and its sign is stored for the past few cycles. Based on these signs, the duty ratio of the power converter is either incremented or decremented to reach the *MPP*. A dynamic step size is used to improve the transient response of the system[56].

3.1.15 System Oscillation Method

This is a novel technique for efficiently extracting the maximum output power from a solar panel under varying conditions. The methodology is based on connecting cuk converter (power conversion stage) between a solar panel and a load, or battery bus. By injecting the switching frequency with a small-signal sinusoidal variation and comparing the maximum variation and the average value at the input voltage, the *MPP* can be located. This method is simple and ensures maximum power transfer under all conditions without using microprocessors for calculation[56].

3.1.16 Constant Voltage Method

Constant voltage method only a voltage sensor is necessary and the *DC-DC* converter duty cycle is changed in order to provide a constant *PV* output voltage. This method depends on the physical fact that the temperature characteristic of the *p-n* junction diode is very similar to that of the solar array. A solar-cell surface-temperature change by the environment is detected in the forward voltage drop of the *p-n* junction diode installed at the backside surface of the solar array, which is used as a reference voltage of the constant tracker. The main advantage of this algorithm are single sensor, ease of implementation, and tracking accuracy dependent on the *PV* surface temperature[56,78].

3.1.17 Look-up Table Method

Look up table is classified as an offline method of *MPP* tracking. In look- up table method, the prior knowledge of *PV* panel material, like technical data, panel characteristics at different environmental conditions, is required. In this method, the measured values of the *PV* generator's voltage and current are compared with those stored in the controlling system, which correspond to the operation at the maximum point, under predetermined climatologically conditions. These algorithms have the disadvantage that a large capacity of memory is required for storage of the data. Moreover, the implementation must be adjusted for a panel *PV* specific. In addition, it is difficult to record and store all possible system conditions. But it has also some advantages. It is simple and the system is able to perform fast tracking, as all the data regarding maximum point are available[56,79].

3.1.18 On-Line *MPP* Search Algorithm

In this algorithm, the main task is to determine the value of reference maximum power, and then, the current power is compared with it. This difference is called maximum power error. In order to have the *PV* array be operated at its *MPP* the maximum power error should be zero or near to zero. The operating power is the *PV* array output power to the load, and is given as; the multiplication of *PV* array output voltage by the current. Here, first reference maximum power *(RMP)* is to be required. Since *RMP* is changed with variation in temperature and solar irradiation level, it is not a constant reference and has a non-linear uncertainty that makes the tracking of *PV* array reference maximum power is difficult. If the reference *MPP* is changed due to change temperature or solar

irradiation level, the algorithm adjusts the array voltage and finds the new *MPP*. This algorithm will not be able to determine the *PV* array *MPP* if the load power or current is much smaller than the *PV* array *MPP* power and current. In this case, additional loads should be connected to increase the *PV* array current so that the *PV* array can be operated at the *MPP*. It is preferred that we can charge the battery as an additional load[56].

3.1.19 Array Reconfiguration Method

Array reconfiguration is one of the only ways to achieve the maximum output power of a photovoltaic array when an array is partially shaded, partially damaged, or has hot spots[80]. In this method the *PV* arrays are arranged in different series and parallel combinations such that the resulting *MPPs* meet a specific load requirement. This method is time consuming and tracking of the *MPP* in real time is not obvious. According to the technique suggested to optimize the operation of photovoltaic system; it is assumed that the solar array is going to be divided into two modules. The first one represents the basic module, and the second will be divided into sub modules. Three ways of arranging these modules together can be achieved, the parallel, series, and parallel-series arrangements[56]. The array reconfiguration method is only practical for large arrays where there would be slow moving clouds or in situations where arrays face different directions, like in some satellites[80].

3.1.20 Linear Current Control Method

The main idea of this method is based on the graphical interpretation of the solution of two algebraic equations as the intersecting point of two curves on the phase plane. In this method, a *MPPT* circuit not only can track the maximum power of the array instantaneously but also can be implemented easily[56].

3.1.21 *IMPP* and *VMPP* Computation Method

IMPP & *VMPP* computation is a technique in which the *MPP* is calculated based on the measurements of the irradiance and the temperature using a model of the *PV* module. The drawbacks are the extra measurements needed, which are sometimes difficult to obtain, and the necessity of an accurate model of the *PV* array. On the other hand, the *MPP* is correctly tracked even under changing atmospheric conditions. It can be used in large

plants, where the economic investment is huge and a perfect tracking is needed to obtain the maximum available power from the solar arrays[81].

3.1.22 State-Based *MPPT* Method

The *PV* system is represented by a state space model, and a nonlinear time varying dynamic feedback controller is used to track the *MPP*. Simulations confirm that this technique is robust and insensitive to changes in system parameters and that *MPPT* is achieved even with changing atmospheric conditions, and in the presence of multiple local maxima caused by partially shaded *PV* array or damaged cells. However, no experimental verification is given[56].

3.1.23 One-Cycle Control *(OCC)* Method

OCC involves the use of a single-stage inverter where the output current of the inverter can be adjusted according to the voltage of the *PV* array so as to extract the maximum power from it. *OCC* topology has two functions: automatically adjusting the output power according to sunlight level, and outputting a sinusoidal current to the grid. This method have some advantage as, high power factor, simple circuit, low cost and high efficiency[56].

3.1.24 The Best Fixed Voltage (*BFV*) Algorithm

Statistical data is collected about irradiance and temperature levels over a period of one year and the *BFV* representative of the *MPP* is found. The control sets either the operating point of the *PV* array to the *BFV*, or the output voltage to the nominal load voltage. The advantages of this algorithm are simplicity and ease of implementation. However, it has limitations in efficiency and depends on a good mathematical statistical research to find the *BFV* to extract more power from the *PV* array. But the operation is therefore never exactly at the *MPP* and different data has to be collected for different geographical regions[56].

3.1.25 Linear Reoriented Coordinates Method (*LRCM*)

This method solves the *PV* array characteristic equation iteratively for the *MPP*, where the equation is manipulated to find an approximate symbolic for the *MPP*. It requires the measurement of V_{OC} , I_{SC} and other constants representing the *PV* array characteristic curve, to find the solution the maximum error in using *LRCM* to approximate the *MPP* was found to be 0.3%, but this was based only on simulation results. The main idea for the *LRCM* is to find the *I-V* curve knee point, which is the optimal current and the optimal voltage that produces maximum power. Using the *I-V* curve, a linear current equation can be determined from the initial and final values. The slope of the *I-V* curve at the knee point is approximated by the slope of the linear current equation[56].

3.1.26 Slide Mode Control Method

It is based on *INC* method, *INC* method consists in using the slope of the derivative of the voltage with respect to the current in order to reach the maximum power point. Therefore، there is no need to use the current reference directly in the formulation. Also, the mathematical modeling is developed for different *DC-DC* converter topologies such as buck converter, boost converter and buck-boost converter to achieve the *MPPT*. The switching function, *u* of the converter is based on the fact that $\frac{dP}{dV} \succ 0$ on the left of the *MPP*, and $\frac{dP}{dV} \prec 0$ on the right; *u* is expressed as

$$\begin{cases} u = 0 & S \geq 0 \\ u = 1 & S \prec 0 \end{cases} \tag{3.13}$$

Where *u = 0* means that the switch is open and *u = 1* means that the switch close and S is given by

$$S = \frac{dP}{dV} = I + V\frac{dI}{dV} \tag{3.14}$$

This control is implemented using a microcontroller that senses the *PV* array voltage and current. Simulation and experimental results showed that operation converges to the *MPP* in several tens of milliseconds[56,89].

3.1.27 Three Point Method

A three-point weight comparison method that avoids the oscillation problem of the perturbation and observation algorithm which is often employed to track the maximum power point. The *P&O* algorithm compares only two points, which are the current operation point and the subsequent perturbation point, to observe their changes in power and thus decide whether increase or decrease the solar array voltage. The algorithm of the three-point method runs periodically by perturbing the solar array terminal voltage and comparing the *PV* output power. This method is proposed to avoid the necessity to move the operating point rapidly, when the solar radiation is varying quickly. The *MPPT* can be traced accurately when the solar irradiance is stable and power loss is low. It compares the output power on three points of the *V-P* curve. The three points are the current operating point A, a point B, perturbed from point A, and a point C, perturbed in the opposite direction from point A as shown in Fig.17[56][84][86].

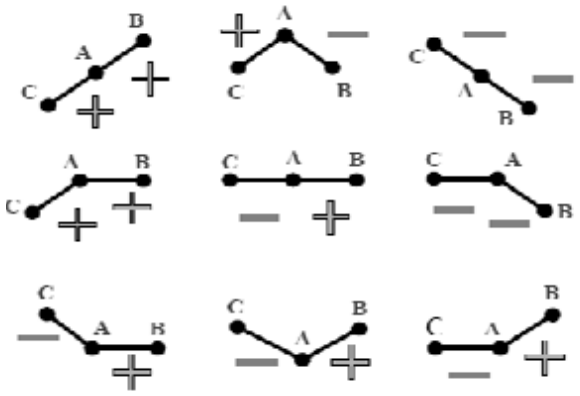

Fig. 17. Possible states of the three perturbation points.

3.1.28 *PV* Output Senseless *(POS)* Control Method

The main advantage of this method is that the current flowing into the load is the only one considerable factor. In case of a huge *PV* generation system, it can be operated much more safely than a conventional system. The load power is proportional to the source power of a *PV* array. A load power is equal to what multiplied the voltage with the current of a load terminal. So, if the load current increases when the load power increases, the load current will be proportional to the source power that is the output power of the solar cell. So, the *POS MPPT* can be applied to all *PV* generation systems with this simple algorithm. The power conversion system is controlled by *PWM* control. An increment of the duty ratio causes an increase in the output current of the power

converter which is the load current flowing into the load. The load current of *PV* generation system is the only significant component of the control method this makes the structure of the control circuit is simple, and the manufacturing cost of the control device is decreased. Especially in the case of a large *PV* generation system, the system can be operated effectively and much more safely, because the voltage and current feedback of *PV* modules are not needed[56] .

3.1.29 A Biological Swarm Chasing Algorithm

It is a novel photovoltaic *PV MPPT*, based on biological swarm chasing behavior, proposed to increase the *MPPT* performance for a module-integrated *PV* power system. Each *PV* module is viewed as a particle; as a result, the maximum power point is viewed as the moving target. Thus, every *PV* module can chase the *MPP* automatically. Theoretically experiments have proved that the *MPPT* performance in transient state is obviously improved. Comparing the proposed *Bio-MPPT* with a typical *P&O MPPT* method, the *MPPT* efficiency is improved about 12.1 in transient state. Experimental results have shown that the proposed *Bio-MPPT* algorithm can adapt well in changing environments, is flexible, and robust. A microcontroller is needed to implement this method[56].

3.1.30 Variable Inductor *MPPT* Method

This method presents a new topology of *MPPT* controller for solar power applications that incorporated a variable inductance versus current characteristic. Power transfer in solar photovoltaic applications is achieved by impedance matching with a *DC-DC* converter with *MPPT* by the incremental conductance method. Regulation and dynamic control is achieved by operating with continuous conduction. It has been shown that under stable operation, the required output inductor has an inductance versus current characteristic whereby the inductance falls off with increasing current corresponding to increasing incident solar radiation. This method shows how a variable sloped air-gap inductor, whereby the inductor core progressively saturates with increasing current, meets this requirement and has the advantage of reducing the overall size of the inductor by 60%, and increases the operating range of the overall tracker to recover solar energy at low solar levels. The variable inductor is based on a sloped air-gap *(SAG)* and the *L-i* characteristic of the inductor is controlled by the shape of the air-gap. The buck converter should work in the continuous current mode *(CCM)* to insure the stable operation of the

system during changing the duty cycle in *MPPT*. The role of the variable inductor in the stable operation of the buck converter is to keep the operation of the converter in the continuous conduction mode. This method gives very good results in the low level of solar intensity[56].

3.1.31 Variable Step-Size Incremental Resistance *(INR)* Method

The step-size for the incremental conductance *MPPT* determines how fast the *MPP* is tracked. Fast tracking can be achieved with bigger increments, but the system might not run exactly at the *MPP*, instead oscillates around it; thus, there is a comparatively low efficiency. This situation is inverted when the *MPPT* is operating with a smaller increment. Therefore, a satisfying trade off between the dynamics and oscillations has to be made for the fixed step-size *MPPT*. The variable step size iteration can solve the tough design problem. An improved variable step-size algorithm is proposed for the *INR MPPT* method and is devoted to obtain a simple and effective way to ameliorate both tracking dynamics and tracking accuracy. The primary difference between this algorithm and others is that the step-size modes of the *INRMPPT* can be switched by extreme values/points of a threshold function, which is the product *C* of exponential of a *PV* array output power P^n and the absolute value of the *PV* array power derivative $\left|\frac{dP}{dI}\right|$ as

$$C = P^n \times \left|\frac{dP}{dI}\right| \tag{3.15}$$

Where *n* is an index.

This method is also based on the fact that the slope of the *PV* array power curve is zero at the *MPP*, positive to the left of the *MPP*, and negative to the right. The *MPP* can thus be tracked by comparing the instantaneous resistance $\left(\frac{V}{I}\right)$ to the incremental resistance $\left(\frac{\Delta V}{\Delta I}\right)$. Once the *MPP* is reached, the operation of the *PV* array is maintained at this point unless a change in ΔV is noted, indicating a change in atmospheric conditions at the *MPP*. The algorithm decreases or increases reference current to track the new *MPP*[56].

3.1.32 *dP-P&O MPPT*

This method performs an additional measurement of power in the middle of the *MPPT* sampling period without any perturbation, as illustrated in the figure below.

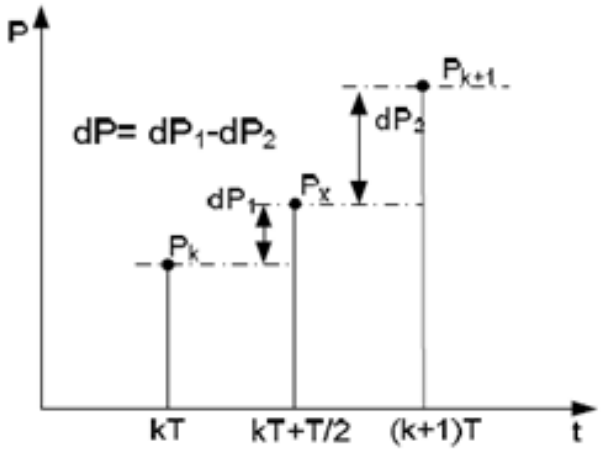

Fig. 18. Measurement of the power between two *MPPT* sampling

As it can be seen on the figure, the change in power between P_x and P_{k+1} reflects only the change in power due to the environmental changes, as no action has been made by the *MPPT*. The difference between P_x and P_k contains the change in power caused by the perturbation of the *MPPT* plus the irradiation change. Thereby, assuming that the rate of change in the irradiation is constant over one sampling period of the *MPPT*, the *dP* due to the *MPPT* action can be calculated as:

$$dP = dP_1 - dP_2 = (P_x - P_k) - (P_{k+1} - P_x) \tag{3.16}$$

$$= 2P_x - P_{k+1} - P_k \tag{3.17}$$

The resulting dP , reflects the changes due to the perturbation of the *MPPT* method[41,109].

3.1.33 Pilot cell

In the pilot cell *MPPT* algorithm, the constant voltage or current method is used, but the open-circuit voltage or short-circuit current measurements are made on a small solar cell, called a pilot cell, that has the same characteristics as the cells in the larger solar array. The pilot cell measurements can be used by the *MPPT* to operate the main solar array at

its *MPP*, eliminating the loss of *PV* power during the V_{OC} or I_{SC} measurement. However, the problem of a lack of a constant *K* value is still present. Also, this method has a logistical drawback in that the solar cell parameters of the pilot cell must be carefully matched to those of the *PV* array it represents. Thus, each pilot cell/solar array pair must be calibrated, increasing the energy cost of the system[60].

3.1.34 Modified Perturb and Observe *(MP&O)*

The *P&O* method implements a hill climbing technique, which works well in slow changing environment but has some limitations under rapidly changing atmospheric conditions. The methods may lead to incorrect or slow maximum power point tracking. To overcome such problems the *MP&O* method, isolates the fluctuations caused by the perturbation process from those caused by the irradiance or weather change. This method adds an irradiance-changing estimate process in every perturb process to measure the amount of power change caused by the change of atmospheric condition. Because the estimate process stops tracking maximum power point by keeping the *PV* voltage constant, the tracking speed of *MP&O* method is only half of the conventional *P&O* method[61].

3.1.35 Estimate, Perturb and Perturb *(EPP)*

The *EPP* technique is an extended *P&O* method, it improves the speed of the *MP&O* algorithm while keeping its main features. When compared with the *MP&O* algorithm, the *EPP* algorithm that uses one estimate mode for every two perturb modes increases significantly the tracking speed of the *MPPT* control, without reduction of the tracking accuracy. Comparing with the *MP&O* algorithm, the *EPP* algorithm has a tracking speed of 1.5 times faster but has the same delay time between the estimate process and the perturb process. Therefore, the *EPP* algorithm has obvious advantages over the *MP&O* algorithm, but it is a complex method[61,76].

3.1.36 Numerical Method - Quadratic Interpolation (*QI*)

A novel *MPPT* control algorithm based on numerical calculation for photovoltaic power generation systems is named quadratic interpolation *(QI)* method, makes a parabola model with the quadratic interpolation using the voltage and current parameters of three sampling points and calculates the location of the peak of the parabola to find the voltage

value of the *MPP*. The function values y_o, y_1 and y_2 corresponding to the voltage values represent the power values of the sampling points. Quadratic interpolation function is constructed by Basis Function Method as the following equation

$$L_2(X) = l_o(X) y_o + l_1(X) y_1 + l_2(X) y_2 \tag{3.18}$$

where $L_2(X)$ is the quadratic interpolation polynomial, $l_o(X), l_1(X), l_2(X)$ are quadratic interpolation basis functions. The *MPP* is obtained when the derivative of the eq. (3.18) is zero. The novel *MPPT* control algorithm can effectively improve the *MPPT* speed, stability and accuracy simultaneously, and it has a straightforward control policy with sample arithmetic so that it is easily implemented in hardware. Furthermore, the three sampling points design avoids misjudgments by the rapid environment change in a great degree[62].

3.1.37 *MPP* Locus Characterization

This method based on the offline characterization of the *MPP* locus of a *PV* module. The basic idea of this method is to find a linear relationship between voltage and current at the *MPP* (*MPP* locus). This relationship is the tangent line to the *MPP* locus curve for the *PV* current in which the minimum irradiation condition satisfies the sensitivity of the method. The equation that guides this method is given by (3.19). It is hard to obtain all the necessary parameters, and a linear approximation is made offline with the *PV* panel, translating it as an estimation method. As the *MPP* locus varies with temperature, the model needs to be updated. This is done by measuring the open-circuit voltage periodically, which means that the interface converter must open the *PV* circuit, resulting in loss of power in these instants. This *MPPT* method present better results in the high irradiation, high power conditions, with respect to the conventional solutions.

$$T_L = \left(\frac{A.V_T}{I_{MPP}} - N_S.R_S \right).I_{MPP} + \left\{ V_{OC} - A\left[VD_O + V_T \right] \right\} \tag{3.19}$$

where N_S is the number of cells, I_{MPP} is the current at *MPP*, V_T is the temperature voltage, A is an ideal factor, and VD_O is the differential voltage[58,77].

3.1.38 *CVT + INC-CON (P&O) + VSS* Method

The *INC-CON* method with variable step-size has good performance in tracking but makes the starting process more complex. The *CVT* method shows a better performance in the starting process. The control algorithm is simple, as it only needs to judge whether the output voltage of the *PV* array is bigger than the voltage instruction. The voltage is changed in only one direction, leading to an increasing power in one direction without oscillation[63].

3.1.39 Piecewise Linear Approximation With Temperature Compensated Method

This method can fast tracking photovoltaic panel maximum power point, and can also overcome the problem of the temperature drift. The simulation results indicate that, the maximum power point tracking efficiency of the proposed method is up to 90% - 99:9% under diffident irradiance, and the biggest change of the tracking efficiency is less than 1 percentage between the temperature of -5◦*C to* 55◦*C*.This method uses a fit line to present the *MPP* characteristic, and performs well in high irradiation, but gets low tracking efficient in low irradiation. Solar powered small electronic devices (such as wireless sensor networks node) needs to carry low complexity, high efficiency *MPPT* unit, which can quickly adapt to the changes of irradiance and temperature. It presents a technique models the nonlinear *V-I* characteristics of the solar panel using numerical approximations similar to that presented in Scarpa et al. to meet above requirement. To improve tracking efficiency, an additional approximation line is employed to model *MPP* locus under low irradiation[65].

3.1.40 Particle Swarm Optimization *(PSO)* Algorithm

PSO method is used to optimize complex problems with multivariable objective function. This method is effective in the case of the presence of multiple local maximum power points. *PSO* adapts the behavior and searches for the best solution-vector in the search space. A single solution is called particle. Each particle has a fitness/cost value that is evaluated by the function to be minimized, and each particle has a velocity that directs the flying of the particles. The particles fly through the search space by following the optimum particles. The algorithm is initialized with particles at random positions, and then it explores the search space to find better solutions. In every iteration, each particle

adjusts its velocity to follow two best solutions. The first is the cognitive part, where the particle follows its own best solution found so far. This is the solution that produces the lowest cost (has the highest fitness). This value is called p best (particle best). The other best value is the current best solution of the swarm. The *PSO* algorithm is based on the cooperation of multiple agents that exchange information obtained in their respective search process. Equation (3.20) and (3.21) represents the state of the algorithms. Since *MPPT* algorithms get stuck in local minima and maxima, *PSO* can help overcome the problem as well as decrease steady state error and increase the efficiency[66].

$$V_i^{K+1} = wV_i^k + c_1 r_1 \left(P_l^k - X_l^k\right) + c_2 r_2 \left(P_g^k - X_l^k\right) \tag{3.20}$$

$$X_i^{K+1} = X_i^k + X_i^{k+1} \tag{3.21}$$

Where

V_i^{K+1} : particle velocity

X_i^{K+1} :current Position of a particle

P_l^k :local best position

P_g^k :global best position

r_1, r_2 :random number between 0 & 1

c_1, c_2 :learning factors.

3.1.41 *PSO-INC* Structure

The *PSO-INC* algorithm uses the same block for the *PSO* section. In addition to this, a derivative block that takes the derivative of the output *PV* power is added to produce a pulse width modulation (*PWM*) signal. The later serves as a duty cycle tuner and one of the inputs to a *DC-DC* converter that generates the adequate input voltage to the *PV* module. To control the photovoltaic power system is necessary to use a *DC-DC* converter; the most adequate is the buck converter[66].

3.1.42 Dual Carrier Chaos Search Algorithm

The traditional chaos search has blindness, that is, determining the search times is difficult and related to the complexity of the objective function and the optimization space size. The single chaos iterative mechanism cannot ensure sufficiency of search to improve *MPPT* precision and speed in the *PV* system. In this method logistic mapping and $y_{n+1} = \mu(\pi y_n)$ mapping is adopted as the chaos generators to produce the carrier, taking the carrier as the stochastic searching step. After some steps from the two different chaoses are reordered together, they can be used to disturb the system for searching *MPP*. When the output power displays low-high-low (the second power point is higher than the first, and the third power point is lower than the second), the two low points are taken as the end points to make the searching zone smaller. The search is continued in the new narrower zone. When the distance between the output power and the last is less than a threshold simultaneously, the distance between the output power and the next is also less than the threshold. The system stops searching and obtains the *MPP*[67].

3.1.43 Algorithm for Stimulated Annealing*(SA)*

Annealing is actually a thermodynamics term. If a solid is heated past melting point and then cooled, the structural properties of the solid depend on the rate of cooling. If the liquid is cooled slowly enough large crystals will form. However, if the liquid is cooled quickly the crystals will contain imperfections Thus crystal formation using intense heating and slow cooling is termed as stimulated annealing. This phenomenon can be explained more precisely for semiconductor behavior by solid state device theory. Generally at high temperature, probability of finding electrons in the higher energy state is more. At sufficiently high temperature, almost all the electrons jump to energy states above Fermi energy. Electrons at such high energy state freely move as they are not tightly bound to nucleus. Now if the temperature is slowly reduced, electrons will return to lower energy state in such a way that total energy of the whole system is even lesser than it was before heating. The model can be best described by solid state physics theory. Thus overall stability of the system will increase even before heating. Energy can be compared to cost function of *MPPT* algorithm. It is the inverse of power output from the panel which is to be minimized. Duty cycle can be thought as analogous to electrons. At higher temperature, probability of finding duty cycle corresponding to garbage power output is more. But if temperature reduces, probability of selecting duty cycle

corresponding to higher power output increases. At sufficiently low temperature, probability of selecting duty cycle corresponding to maximum power is unity. Thus oscillation is damped totally at steady state operation. So, steady state error will be absolute zero without using closed loop control scheme. As open loop iterative control scheme is being employed, no stability problem will arise. Furthermore, this algorithm solves the problem of getting stuck in local, non-global minima, when searching for global minima. *SA* algorithm depends on continuous learning rate of the system at each iteration. Best result for suitable purpose can be obtained by proper selection of parameters such as temperature, tolerance error and temperature reduction factor[68,69].

3.1.44 Artificial Neural Network *(ANN)* Based *P&O MPPT*

It is *MP&O* which based on an adaptive algorithm which automatically adjusts the reference voltage step size to achieve dynamic response and search *MPP* under rapidly changing conditions by exploiting artificial neural networks capabilities, where it is known that any atmospheric condition variation induce a proportional *PV* array output power variation.

The *ANN* role consists in predicting the power value during the next cycle of perturbation, the difference between *ANN* output value and the measured one (the reel furnished power) gives us a precious information about the atmospheric conditions evolution. This information will be used to adjust the perturbation step value for the next cycle perturbation according to the following equation

$$\Delta V_{i+1} = k \frac{\Delta \mathrm{P_r}}{\Delta V_i} . f\left(\frac{I_r}{I_P}\right) \tag{3.21}$$

with V_i is the perturbation step during the cycle *i*, *k* : a constant, $\mathrm{P_r}$: the reel furnished power, f is a function with the input/output characteristic, I_r is the reel currant and I_P its predicted value[70].

3.1.45 *VH-P&O MPPT* Algorithm

This method mainly based on the conventional *P&O* algorithm. The idea originated by realizing that the cause of the wrong *MPP* tracking during irradiance changes due to the poor synchronization between the *MPPT* algorithm, the controller and the system response *(VCPV)*. For instance, during the irradiance changes the system is forced to follow the reference voltage of *MPP* algorithm. The reference voltage will never match the naturally established voltage across the *PV* capacitor (*CPV)* as the latter is related to the increased/decreased generated *PV* current (dependent on irradiance) and this causes a 'confused' tracking behavior. *VH-P&O* algorithm stops the conventional perturbation process during the irradiance changes but before exceeding the *MPP* voltage, and directly holds the reference voltage to the *PV* capacitor voltage which is the essential tracking parameter in this algorithm. As soon as the irradiation change stops and the final *MPP* is achieved, the tracking step size has to be decreased gradually down to zero. Afterwards, if any *PV* power change occurs, the tracking step size will be reset to the initial value and therefore fast tracking will be maintained. Through this algorithm, the *PV* response to a change of irradiance results in a straight-line tracking behavior which is finished with suppressed oscillation at the *MPP*[71].

3.1.46 Ant Colony Algorithm

It is a kind of parallel positive feedback emulation algorithm with strong robustness, with certain advantage in aspect of optimal problem of complex solution combination. The ant colony algorithm based on different starting points randomly caused by each ant, searches path information by use of pheromone density and formula constituted by idea function, renews pheromone continuously, and figures out the optimal answer according to the pheromone density. Because basic ant colony algorithm is built in disperse field, while output curve of photovoltaic model is a successive curve in practice, the ant colony algorithm is brought in continuous field, and introduce Gaussian Mutation to optimize its algorithm so as to realize tracking the maximum power point combined with practical situation of photovoltaic electricity generation[72].

3.1.47 Variable *DC*-Link Voltage Algorithm

A variable *DC-link* reference voltage algorithm is proposes for wide range of *MPPT* for two-string *PV* systems. A multi-string system, which is a kind of *PV* system, is widely used due to its many merits (such as the ability to use low rating devices, high *MPPT* efficiency, and so forth). *PV* systems can choose their input voltages on the basis of their *PV* cell connection structure. The *PV* cell connection structure can be restricted because the input voltage and current affect the *PV* system design. This reduces the *MPPT* range under some weather conditions. In the restricted *PV* connection structure, this algorithm enlarges the *MPPT* range and minimizes the increment of the total harmonic distortion *(THD)* by selecting the appropriate *DC-link* voltage reference which is changed by comparing the sorted input voltage. To verify the proposed algorithm, simulation and experiments are conducted to show the results of the performance for the proposed algorithm[73].

3.1.48 Extremum Seeking Control Method *(ESC)*

Recently, Krstic et al. presented a systematic *ECS* methodology supported by rigorous theories such as averaging and singular perturbation. This real-time optimization methodology involves a nonlinear dynamic system with adaptive feedback. This *ESC* method has been successfully applied in various systems such as traction maximization in antilock braking for a car, power reduction maximization of a flight, pressure rise maximization of an aero engine compressor, autonomous vehicle target tracking, and Proportional Integral Derivative(*PID)* tuning. This method has also been specifically adapted for *PV* systems in order to track *MPP*. The *ESC* approach has two main advantages. First, the optimization problem involving power maximization is explicitly solved by using the dynamic adaptation-based feedback control law for a sinusoidal perturbation. Attainment of *MPP* is, hence, guaranteed when the control algorithm is convergent. Second, this approach does not require any parameterization or structural formalization of the modeling uncertainty. The disadvantage of the *ESC* method lies in the complexity associated with its implementation as well as the necessity to evaluate signals of relatively low amplitude[74].

3.1.49 Gauss-Newton Method

The Gauss–Newton method is the fastest algorithm in comparison to the steepest descent and the hill climbing also this method called Newton–Raphson method, which uses a root-finding algorithm . The Gauss–Newton method uses a first and second derivative of the change with parameter value to estimate the direction and distance the program should to go to reach a better point. When it is used to track *MPPs*, the computation of operating point can be illustrated in equation (3.22)[82].

$$V_{K+1} = V_K - \frac{\left.\frac{dp}{dv}\right|_{V=Vk}}{\left.\frac{d^2p}{dv^2}\right|_{V=Vk}} \tag{3.22}$$

Where $\frac{dp}{dv}$ is the deviation in power.

3.1.50 Steepest-Descent Method

The method of steepest descent can be applied to find the nearest local *MPP* when the gradient of the function can be computed. Based on the method of steepest descent, the algorithm of *MPPT* can be demonstrated by equation (3.23), where K_ε is the step-size corrector, and $\frac{dP}{dV}$ is the derivation in power. The value of K_ε decides how steep each step takes in the gradient direction.

$$V_{K+1} = V_K - \frac{\left.\frac{dP}{dV}\right|_{V=Vk}}{K_\varepsilon} \tag{3.23}$$

The derivation in power can be calculated as

$$\frac{dP}{dV} = F(V, P) \tag{3.24}$$

$$F(V_K, P_K) = \frac{P_{K+1} - P_{K-1}}{2\Delta V} + O\left(\Delta V^3\right) \tag{3.25}$$

$O\left(\Delta V^{3}\right)$ is the local truncation error for the centered differentiation, which indicates a second-order accuracy. For *MPPT*, a controller needs to find the point where $F\left(V, P\right)=0$ [82].

3.1.51 Analytic Method

This technique is simple heuristic strategy provides an operating point close to the true value of the *MPP*. However, this result is based on observations and experimental results. This method present an analytic solution to the photovoltaic *MPP* problem. It is based on one of the most important theorems of real analysis, namely the mean value theorem. The exact expression of a point in the neighborhood of the *MPP* is obtained and proven to be inside a ball of small radius that also contains the *MPP*[83].

3.1.52 Polynomial Curve Fitting *(PCF)*

The curve-fitting techniques classified as an offline technique based on mathematical equations. *PCF* represent the electric characteristics of *PV* modules. To achieve an accurate *P-V* curve fitting, a third-order polynomial function as

$$p_{pv}=aV_{PV}^{3}+\beta V_{PV}^{2}+\gamma V_{PV}+\delta \tag{3.26}$$

Where the coefficients α, β, γ, and δ are determined by sampling of *PV* voltage and power in intervals. According to the power–voltage characteristics of the *PV* cell, the *MPPs* occur when $\frac{dP}{dV}=0$, where *P* is the *PV* module's output power and *V* is the *PV* voltage which can be calculated as

$$V_{MPP}=\frac{-\beta\pm\sqrt{\beta^{2}-3\alpha\gamma}}{3\alpha} \tag{3.27}$$

The advantage of curve fitting method is its simplicity , because no differentiations are to be calculated. The disadvantage of this method is that it needs prior knowledge of the *PV* model, the mathematical equations of method and parameter dependence on cell material and specifications. Also, it requires large memory because of the number of calculations

is large. Speed is less as large computation time is required to calculate α , β , γ , and δ for different environmental conditions[111].

3.1.53 Differentiation Method *(DM)*

These methods generally depend on numerical differentiation which is a process of finding a numerical value of a derivative of a given function at a given point[111].

3.1.54 Incremental Conductance *(IC)* Based on *PI*

To improve the *IC* method, by adding a simple *PI* controller to minimizing the error between the actual conductance and the incremental conductance, where the compensator can be adjusted and updated according to the system necessity. Moreover, *PI* controller can reduce the ripple oscillations in steady state, minimize the issues involving digital resolution implementation. This method can be seen as an adaptative solution once it presents large step sizes when the *PV* is far from the *MPP*; then, the step sizes are reduced according to the distance of *MPP*, and finally, when the *MPP* is achieved, the system operation point is not changed, unless the climate conditions are modified[58].

3.1.55 Azab Method

The method is considered as a modified perturb and observe method. However, the principle difference between Azab method and any other tracking method. Most *MPPT* techniques attempt to find (search) the *PV* voltage that results in the maximum power point V_{MPP} , or to find the *PV* current I_{MPP} corresponding to the maximum power point. This algorithm tracks neither the V_{MPP} nor the I_{MPP} . However, it tracks directly the maximum possible power P_{MPP} that can be extracted from the *PV* where it donate as a reference value (set point) of the control system. Therefore, a reduction (decreasing) in the computed P_{MPP} must be done until the error between P_{MPP} and P_{ACT} is limited between upper and lower limit[87].

3.1.56 Modified Incremental Conductance(*IC*)Algorithm

An alternative approach of the *IC* method focusses on modifying the *PV* array current instead of the array voltage . It derives from the consideration that on the right side of the *MPP* the panel voltage varies slowly and can be considered constant, so between two

sampling times the voltage variation can be neglected. In this hypothesis, $\frac{dP}{dV}$ against I gives almost a linear relation compared to the variation of $\frac{dP}{dV}$ against V . Hence, it can be seen that the reference current I_{ref} will be easy to compute considering the linear variation with the $\frac{dP}{dV_{pv}}$, while the computing V_{ref} is more difficult considering the nonlinear variation of V versus $\frac{dP}{dV}$. In this case, a slightly modified *IC* method will result, its output will not be the reference voltage, but the current. The operating point is adjusted by changing the current of the solar panel. When $dI \neq 0$ it means that the atmospheric conditions have varied. If $dI \prec 0$ then $\frac{dP}{dV} \prec 0$ and the reference current must be increased in order to move the operating point toward the *MPP*. The opposite operation is made, when $dI \succ 0$[88].

3.1.57 Newton-Like Extremum Seeking Control method

This technique uses the gradient and Hessian of the panel characteristic in order to approximate the operation point to the optimum, where it requires from a Hessian estimation of voltage power characteristic[90].

3.2 Parameters of *MPPT* Evaluation

Many *MPPT* techniques available to *PV* system users, The performance of the *MPPT* depends on some factors it might not be obvious for the latter to choose which one better suits their application needs. The main factors that emerge out of this comparative study are briefly discussed next with respect to various performance parameters.

3.2.1 Implementation (Types of Circuitry)

The ease of implementation is an important factor in deciding which *MPPT* technique to use. However, this greatly depends on the end-users' knowledge. Some users might be more familiar with analog circuitry. Others might be willing to work with digital circuitry, even if that may require the use of software and programming. Furthermore, a few of the *MPPT* techniques only apply to specific topologies. In one word *MPPT* techniques are classified based on type circuitry used (analog or digital)[47].

3.2.2 Sensors (Number of Variables)

The number of sensors required to implement *MPPT* also affects the decision process such as the accuracy and convergence speed. Often, for more precise *MPPT*, you may need to use more sensors. The number and type of sensors required depend largely on your *MPPT* technique[93]. With regard to the sensed variables, it is easier and more reliable to measure voltage than current whereas current sensors are usually expensive and bulky. In systems that consist of several *PV* arrays with separate *MPP* trackers, it is preferred to use *MPPT* methods that require only one sensor or that can estimate the current from the voltage[47]. The irradiance or temperature sensors are very expensive and uncommon[75].

3.2.3 Convergence Speed

Convergence speed is the time taken to reach the *MPP* [84]. For a high-performance *MPPT* system, the time taken to converge to the required operating voltage or current should be low. Depending on how fast you need to do this and your tracking system requirements, the system has to accordingly maintain the load at the *MPP*[93]. The lower time ad periodic tuning taken to reach the *MPP* minimize power losses and maximize efficiency.

3.2.4 Detect Multiple Local Maxima

It is common for the irradiance levels at different points on a solar panel’s surface to vary. This leads to multiple local maxima in one system, that's reduces the effectiveness of the *MPPT* methods. Actually, it is found that the power loss of commercial power conditioning system(*PCS*) can be as high as 70% under partial shading condition, if a local maximum is tracked instead of the real *MPP*. The efficiency and complexity of an algorithm determine if the true maximum power point or a local maximum power point is calculated. In the latter case, the maximum electrical power is not extracted from the solar panel[93,94]. As mentioned previously, the current sweep and the state-based methods should track the true *MPP* even in the presence of multiple local maxima. However, the other methods require an additional initial stage to bypass the unwanted local maxima and bring operation to close the real *MPP*[47].

3.2.5 Performance Cost

The type of algorithm you use largely determines the resources required to set up this application[93]. A satisfactory *MPPT* costs comparison can be carried out by knowing the technique (analogical or digital) adopted in the control device where analogical implementations are generally cheaper than digital , the number of sensors required to implement the *MPPT* technique also affects the final costs, and the use of additional power component, considering the other costs (power components, electronic components, boards, etc…) equal for all the devices[75].

2.2.6 Applications (Relationship between cost, time, efficiency)

Different *MPPT* techniques discussed above will suit different applications. For example, in space satellites and orbital stations applications that involve large amount of money, the costs and complexity of the *MPP* tracker are not as important as its performance and reliability. The tracker should be able to continuously track the true *MPP* in minimum amount of time and should not require periodic tuning. In this case, hill climbing / *P&O*, IncCond, and *RCC* are appropriate. Solar vehicles would mostly require fast convergence to the *MPP*. Fuzzy logic control, neural network, and *RCC* are good options in this case. To achieve goal of high performance and low cost as required in solar vehicles , the step varying *IC* algorithm along with *PID* is implemented[92]. Since the load in solar vehicles consists mainly of batteries, load current or voltage maximization should also be considered. The goal when using *PV* arrays in residential areas is to minimize the payback time and to do so, it is essential to constantly and quickly track the *MPP*. Since partial shading can be an issue, the *MPPT* should be capable of bypassing multiple local maxima. Therefore, the current sweep method are suitable. Since a residential system might also include an inverter, the *OCC* can also be used. *PV* systems used for street lighting only consist in charging up batteries during the day. They do not necessarily need tight constraints; easy and cheap implementation might be more important, making fractional V_{OC} or I_{SC} viable[47].

3.2.7. Dependency on Array Parameters:

MPPT methods can be divide into tow case, direct (independency) and indirect (dependency) methods. The direct methods include those methods that use *PV* voltage and/or current measurements. These direct methods have the advantage of being

independent from the priori knowledge of the *PV* array configuration and parameter values for their implementation. Thus, the operating point is independent of isolation, temperature or degradation levels. The indirect methods are based on the use of a database of parameters that include data of typical *P-V* curves of *PV* systems for different irradiances and temperatures, or on the use of mathematical functions obtained from empirical data to estimate the *MPP*. In most cases, a prior evaluation of the *PV* generator based on the mathematical relationship obtained from empirical data is required[59,91].

3.3 Defining Parameter

From above, we can summarize the most important use to characteristic *MPPT* algorithm as shown in Table 2.

parameter	**define**
PV array dependent?	Methods can be applied to any *PV* array with or without the knowledge of its configuration and parameter values.
True *MPPT*	The *MPPT* algorithm can operate at maxima peak or other. If the actual *MPPT* is not the true *MPPT* then the output power will be less than the expected actually.
Analog or digital?	Types of circuitry which used in method analog or digital.
Periodic tuning?	Is there an oscillation around the *MPP* or not?
Convergence speed	It is effected by the amount of time required to reach *MPP*.
Implementation complexity	This standard describes the method in general.
Sensors	It is depend on the Number of variables which we need.

Table 2: Defining parameter

3.4 Characteristics of Various *MPPT* Algorithms

MPPT technique	PV array dependent?	True MPPT?	Analog or digital?	Periodic tuning?	Convergence speed	Implementation complexity	Sensed parameters
Hill Climbing / *P&O*	No	Yes	Both	No	Varies	Low	Voltage, Current
Incremental Conductance	No	Yes	Digital	No	Varies	Medium	Voltage, Current
Fractional *Voc*	Yes	No	Both	Yes	Medium	Low	Voltage
Fractional *Isc*	Yes	No	Both	Yes	Medium	Medium	Current
Fuzzy Logic Control	Yes	Yes	Digital	Yes	Fast	High	Varies
Neural Network	Yes	Yes	Digital	Yes	Fast	High	Varies
RCC	No	Yes	Analog	No	Fast	Low	Voltage, Current
Current Sweep	Yes	Yes	Digital	Yes	Slow	High	Voltage, Current
DC Link Capacitor Droop Control	No	No	Both	No	Medium	Low	Voltage
Load I or V Maximization	No	No	Analog	No	Fast	Low	Voltage, Current
dP/dV or dP/dI Feedback Control	No	Yes	Digital	No	Fast	Medium	Voltage, Current
β Method	Yes	Yes	Digital	No	Fast	Medium	Voltage, Current
System Oscillation Method	Yes	No	Analog	No	N/A	Low	Voltage
Constant Voltage Tracker	Yes	No	Digital	Yes	Medium	Low	Voltage
Lookup Table Method	Yes	No	Digital	Yes	Fast	Medium	Voltage, Current,
Online MPP Search Algorithm	No	Yes	Digital	No	Fast	High	Voltage, Current
Array Reconfiguration	Yes	No	Digital	Yes	Slow	High	Voltage, Current
Linear Current Control	Yes	No	Digital	Yes	Fast	Medium	Irradiance
IMPP and VMPP Computation	Yes	Yes	Digital	Yes	N/A	Medium	Irradiance, Temperature
State Based MPPT	Yes	Yes	Both	Yes	Fast	High	Voltage, Current
OCC MPPT	Yes	No	Both	Yes	Fast	Medium	Current
BFV	Yes	No	Both	Yes	N/A	Low	None
LRCM	Yes	No	Digital	No	N/A	High	Voltage, Current
Slide Control	No	Yes	Digital	No	Fast	Medium	Voltage, Current
Temperature method	Yes	Yes	Digital	Yes	Medium	Low	Voltage, Temperature
Three Point Weight Comparison	No	Yes	Digital	No	low	Low	Voltage, Current
POS Control	No	Yes	Digital	No	N/A	Low	Current
Biological Swarm Chasing MPPT	No	Yes	Digital	No	Varies	High	Voltage, Current, Irradiance, Temperature
Variable Inductor MPPT	No	Yes	Digital	No	Varies	Medium	Voltage, Current
INR method	No	Yes	Digital	No	High	Medium	Voltage, Current
Parasitic capacitances	No	Yes	Analog	No	High	low	Voltage, Current
dP-P&O MPPT	No	Yes	Digital	No	High	Medium	Voltage, Current
Pilot cell	Yes	No	Both	Yes	Medium	Low	Voltage, Current
Modified Perturb and Observe	No	Yes	Digital	No	High	Medium	Voltage, Current
Estimate, Perturb and Perturb	No	Yes	Digital	No	High	Medium	Voltage, Current
numerical method - quadratic interpolation (QI)	No	Yes	Digital	No	High	Medium	Voltage, Current
MPP Locus Characterization	Yes	Yes	Digital	Yes	High	Low	Voltage, Current

MPPT technique	PV array dependent?	True MPPT?	Analog or digital?	Periodic tuning?	Convergence speed	Implementation complexity	Sensed parameters
CVT + INC-CON (P&O) + VSS Method	Yes	Yes	Both	No	High	Medium	Voltage
piecewise linear approximation with temperature compensated Method	Yes	Yes	Both	Yes	High	low	Voltage, Current, Irradiance, Temperature
Particle Swarm Optimization PSO algorithm	Yes	Yes	Digital	Yes	High	Medium	Voltage, Current
PSO-INC Structure	No	Yes	Digital	No	High	low	Voltage, Current
Dual carrier chaos search algorithm	No	Yes	Digital	No	High	Medium	Voltage, Current
Algorithm for Stimulated Annealing(SA)	Yes	Yes	Digital	No	High	High	Voltage, Current
Artificial neural network *(ANN).* based *P&O MPPT*	No	Yes	Both	No	High	Medium	Voltage, Current
VH-P&O MPPT Algorithm	No	Yes	Digital	No	Medium	Medium	Voltage
Ant Colony Algorithm	No	Yes	Digital	No	High	Medium	Voltage, Current
Variable DC-Link Voltage Algorithm	No	Yes	Digital	No	Medium	Medium	Voltage
Extremum seeking control method *(ES*C)	No	Yes	Both	No	Fast	Medium	Voltage, Current
Gauss-Newton method	No	Yes	Digital	No	Fast	low	Voltage, Current
Steepest-Descent method	No	Yes	Digital	No	Fast	Medium	Voltage, Current
Analytic-method	Yes	No	Both	yes	Medium	High	Voltage, Current
Polynomial Curve Fitting *(PCF)*	Yes	No	Digital	yes	Slow	low	Voltage
Differentiation Method *(DM)*	No	Yes	Digital	yes	Fast	High	Voltage, Current
IC Based On PI	No	Yes	Digital	No	Fast	Medium	Voltage, Current
Azab Method	Yes	Yes	Digital	yes	Medium	low	----
Modified INC Algorithm	No	Yes	Digital	No	Medium	High	Voltage, Current
Newton-Like Extremum Seeking Control method	No	Yes	Both	No	Fast	High	Voltage, Current

Table 3: Characteristics of Various MPPT Algorithms

CHAPTER 4 MODELING AND SIMULATION OF PHOTOVOLTAIC

In this chapter, a detailed mathematical method of modeling photovoltaic arrays, based on information from the datasheet discussed. The model is used as a source for the maximum power point tracker system. It is described through an equivalent circuit include a photocurrent source, a diode, a series resistor and a shunt resistor. Also, the analysis of a photovoltaic panel array characteristics taking into consideration the effect of partial shading is described in details. Literature reviews are explained in section 4.1. Section 4.2 summarizes photovoltaic Models. Simulation Methods are explained in section 4.3. While section 4.4 present the simulation and results.

4.1 literature reviews

Khamis et al. (2012) [97] built mathematical model of all system components to investigate the dynamic behavior of each system. Also, the proposed control technique of the system was presented. This includes On/Off switch control of the system modes of operation and inverter control. The proposed system components implemented in Matlab/Simulink environment and interface with SimPowerSystem toolbox. The dynamic behavior of each subsystem is investigated showing the interaction between different components of grid connected *PV* system. Renewable energy based power generation as *PV* with battery storage for microgrid system are simulated**.**

Mohammed (2011) [104] presented modeling of *PV* module using MATLAB/Simulink. The model is developed based on the mathematical model of the *PV* module. Two particular *PV* modules are selected for the analysis of developed model. The essential parameters required for modeling the system are taken from datasheets. *I-V* and *P-V* characteristics curves are obtained for the selected modules with the output power of 60W and 64W from simulation and compared with the curves provided by the datasheet. The results obtained from the simulation model are well matched with the datasheet information.

Wang and Hsu (2010)[100] presented an analytical modeling of *PV* power system for studying the effects of partial shading and different orientation of *PV* modules. The proposed analytical model, although limited to the case of series *PV* modules and

composed of complicated non-linear implicit functions, allows several important electrical characteristics of a *PV* system, such as *I–V* curve, open-circuit voltage, short-circuit current, maximum power and reverse voltage, to be investigated and presented in two- and three-dimensional graphs to provide in-depth physical interpretation of the issue.
In their work, they are content with mismatches in series cells and modules. Indeed, the proposed analytical model can also be extended to deal with mismatch problems in *PV* systems with more complicated circuit topologies. However, authors kept the system under study as simple as possible since an analytical method rapidly reaches its limit when the number of non-linear equations increases to a certain value.

Villalva et al. (2009)[96] presented an easy and accurate method of modeling photovoltaic arrays. The method is used to obtain the parameters of the array model using information from the datasheet. The *PV* array model can be simulated with any circuit simulator. The equations of the model are presented in details and the model is validated with experimental data. Finally, simulation examples are presented. Their work is useful for power electronics designers and researchers who need an effective and straightforward way to model and simulate *PV* arrays.

Patel and Agarwal (2008)[103] studied the effect of temperature, solar insolation, shading and configuration on the performance of *PV* array. Often, the *PV* arrays get shadowed, completely or partially, by the passing clouds, neighboring buildings and towers, trees, and utility and telephone poles. The situation is of particular interest in case of large *PV* installations such as those used in distributed power generation schemes. Under partially shaded conditions, the *PV* characteristics get more complex with multiple peaks. Yet, it is very important to understand and predict them in order to extract the maximum possible power. In their work, they present a MATLAB-based modeling and simulation scheme suitable for studying the *I–V* and *P–V* characteristics of a *PV* array under a uniform insolation due to partial shading. It can also be used for developing and evaluating new maximum power point tracking techniques, especially for partially shaded conditions. The proposed models conveniently interface with the models of power electronic converters, which is a very useful feature. It can also be used as a tool to study the effects of shading patterns on *PV* panels having different configurations. It is observed that, for a given number of *PV* modules, the array

configuration (how many modules in series and how many in parallel) significantly affects the maximum available power under partially shaded conditions. This is another aspect to which the developed tool can be applied. The model has been experimentally validated and the usefulness of this research is highlighted with the help of several illustrations.

4.2 Photovoltaic Models

There are five models representing *PV* cell. First model is a general model with equivalent circuit composed of photo current source, diode, parallel resistor expressing the leakage current, and series resistor describing the internal resistance to the current flow. This model is already discussed in Chapter 2. The second model is double exponential model (extra diode). It is more accurate model that describes the *PV* cell to represent the effect of the recombination of carriers. This model consists of a light generated current source, two diodes, a series resistance and a parallel resistance. However, because implicit and nonlinear nature of the model, it is difficult to develop expressions for the *I-V* curve parameters. Therefore, this model is not widely used in literature and is not taken into consideration for the generalized *PV* model. While the third model neglects the effect of the shunt resistance. This model is called approximated model. The forth model is simplified model (ideal cell). It doesn't include series loss and no leakage to ground, i.e., $R_S = 0$ and $R_{SH} = \infty$, respectively. The fifth model is a three-diode model which proposed to include the influence of effects which are not considered by the double exponential model and other models[95,96].

4.2.1 *PV* Module and Array Model

PV cell is a basic unit of *PV* system, but the power produced by a single *PV* cell is very low and not enough for general use. Therefore, the cells should be arranged in series-parallel configuration. Combination of *PV* cells is known as a module. The efficiency of a *PV* module is less than a *PV* cell due to some solar irradiation is reflected by the glass cover and frame shadowing. The power produced by a single module is rarely enough for commercial use, so modules are connected to form an array to supply the load. The connection of modules in an array is the same as that of cells in a module. Modules can also be connected in series to get an increased voltage or in parallel to get an increased current[95].

4.3 Simulation Methods

PV module model is simulated using two methods: The mathematical modeling using math function block and the physical modeling using Simulink Sim Power Systems toolbox. The mathematical model has more advantages than the physical model, because parallel and series *PV* cells combinations can be formed without the need for repeating the block diagrams. However, to make a parallel combination in the physical model, the block of the *PV* cell has to be duplicated, which add more complexity to the model[95].

4.4 Simulation and Results

4.4.1 Simulation

The general *PV* module is used to represent the *PV* modeling using Matlab/Simulink depending on equation (2.2) which represents the *I-V* characteristic of *PV* system. The main reason for choosing this model refers to the fact that it is more practical. An equivalent circuit model based on the *PV* model is given in Fig. 19[97].

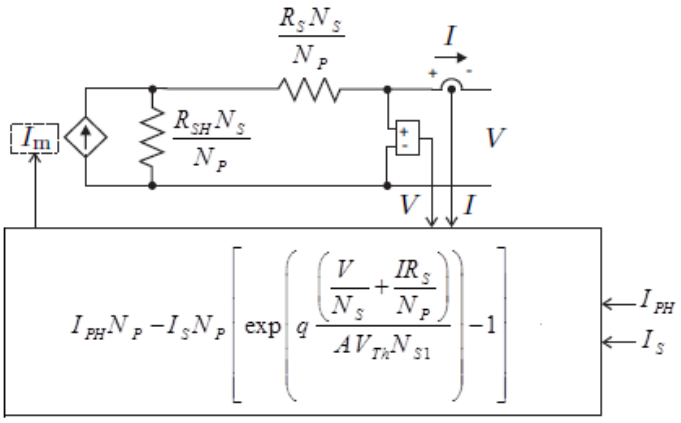

Fig. 19: *PV* system model circuit with a controlled current source, equivalent resistors, and the equation of the model current (I_m).

4.4.1.1 *PV* Array Circuit Model

The value of the model current I_m is calculated by the computational block that has *V*, *I*, I_S and I_{PH} as inputs. The input parameters developed by using mathematical function, we can built the *PV* circuit model as shown in Fig. 20[97].

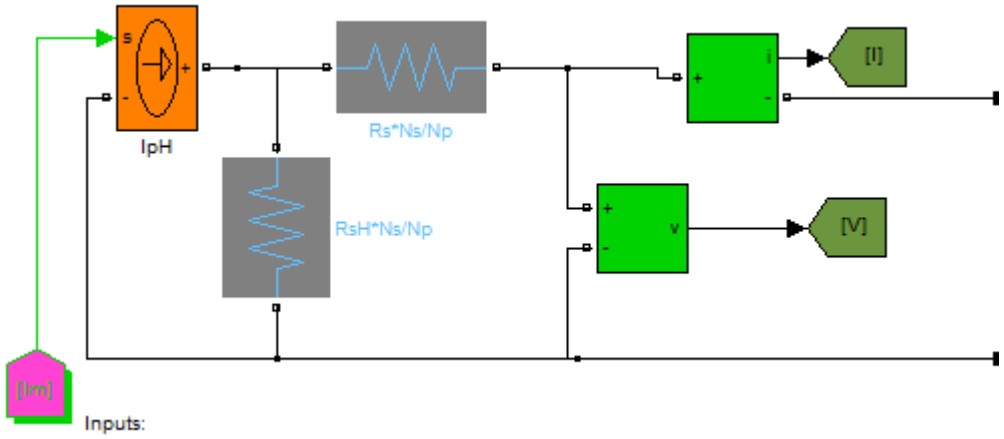

Fig. 20: Equivalent model of *PV* system in Matlab Simulink with input and output port that connect to outside of subsystem.

To create the model current I_m, of the equivalent circuit of *PV*, the saturation current I_S and the light generated current I_{PH} must be developed.

4.4.1.2 Saturation Current (I_S)

I_S is defined by equation (4.1). Then the mathematical model of (I_S) was developed in Matlab/Simulink as shown in Fig. 21[97][99].

$$I_S = \frac{I_{sc,n} + K_i \Delta T}{\exp\left(q \frac{V_{oc,n} + K_v \Delta T}{A V_{Th} N_{S1}} \right) - 1} \tag{4.1}$$

Where $I_{sc,n}$ is the short circuit current at the normal condition (usually 25 ^{0}C and 1000 W/m^2), $V_{oc,n}$ the open-circuit voltages at the nominal condition, K_v the open-circuit voltage/temperature coefficient, K_i the short circuit current/temperature coefficient, $\Delta T = T - T_n$ where T and T_n the actual and nominal temperatures [K], and N_{S1} number of cells in series. These values are listed in Table 4 and for more details see appendix A.

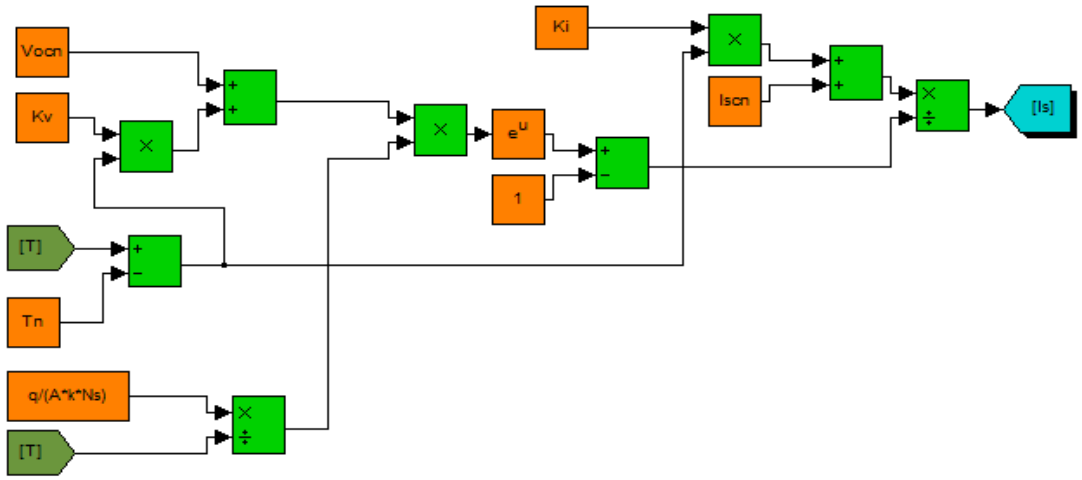

Fig. 21: Mathematical model of I_S

4.4.1.3 Light Generated Current

The light generated current I_{PH} is defined by equation (4.2). Then, the mathematical model of (I_{PH}) was developed in Matlab simulink as shown in Fig. 22[97,99].

$$I_{PH} = \left(I_{PH,n} + K_i \Delta T\right)\frac{G}{Gn} \tag{4.2}$$

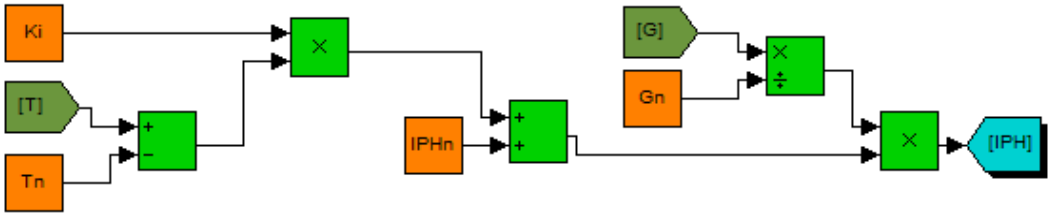

Fig. 22. Mathematical model of I_{PH} .

4.4.1.4 Calculate Model Current

I_S and I_{PH} with the selected parameters were inserted to get the model current I_m. Then, the mathematical model of I_m was developed in Matlab/Simulink as shown in Fig. 23[97,99].

$$I_m = I_{PH} N_P - I_S N_P \left[\exp\left(q \frac{V + R_S \left(\frac{N_S}{N_P} \right) I}{A V_{Th} N_S N_{S1}} \right) - 1 \right] \tag{4.4}$$

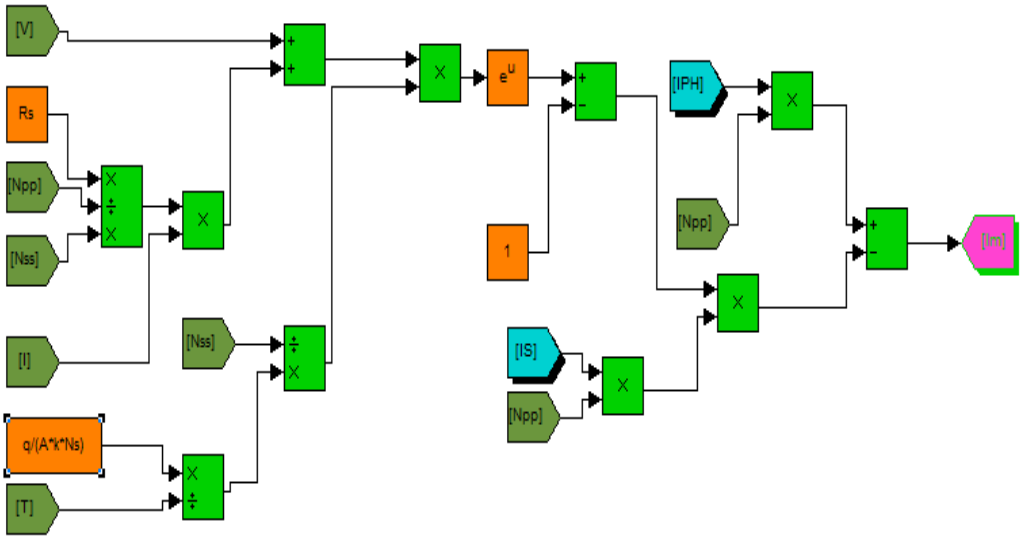

Fig. 23: Mathematical model of I_m.

4.4.2 Results

4.4.2.1 Parameters of *PV* Array

Kyocera offers a wide range of highly efficient and reliable crystalline silicon solar *PV* power modules, where the conversion efficiency of the Kyocera solar cell is over 16%, so we built our simulation based on KC200GT solar array datasheet. The inputs data which used for the simulations in this thesis using MATLAB/Simulink are shown in Table 4[98,108].

Parameters	Abbreviation	Values
Nominal short-circuit current [A]	$I_{sc,n}$	8.21
Nominal array open-circuit voltage [V]	$V_{oc,n}$	32.9
Parallel resistance [Ω]	R_P	415.405
Series resistance [Ω]	R_S	0.221
Nominal operating temperature [K]	T_n	25 + 273.15
Number of series cells	N_S	54
Nominal irradiance [W/m^2] at 25^{0}C	G_n	1000
Array current at maximum power point [A]	I_{MP}	7.61
Array voltage at maximum power point [V]	V_{MP}	26.3

Table 4: Parameters of *PV* Array (for more details see appendix A)

4.4.2.2 Simulink Model of the Solar *PV* Module

Fig. 24 shows the *PV* module implement using Matlab program, the model parameter are evaluated using equation(4.4), the *I-V* characteristics and *P-V* characteristics curves obtained from the simulation for KC200GT. The module *I-V*, *P-V* characteristics at different insulation and temperature levels are illustrated below with the point of *MPP* at each level.

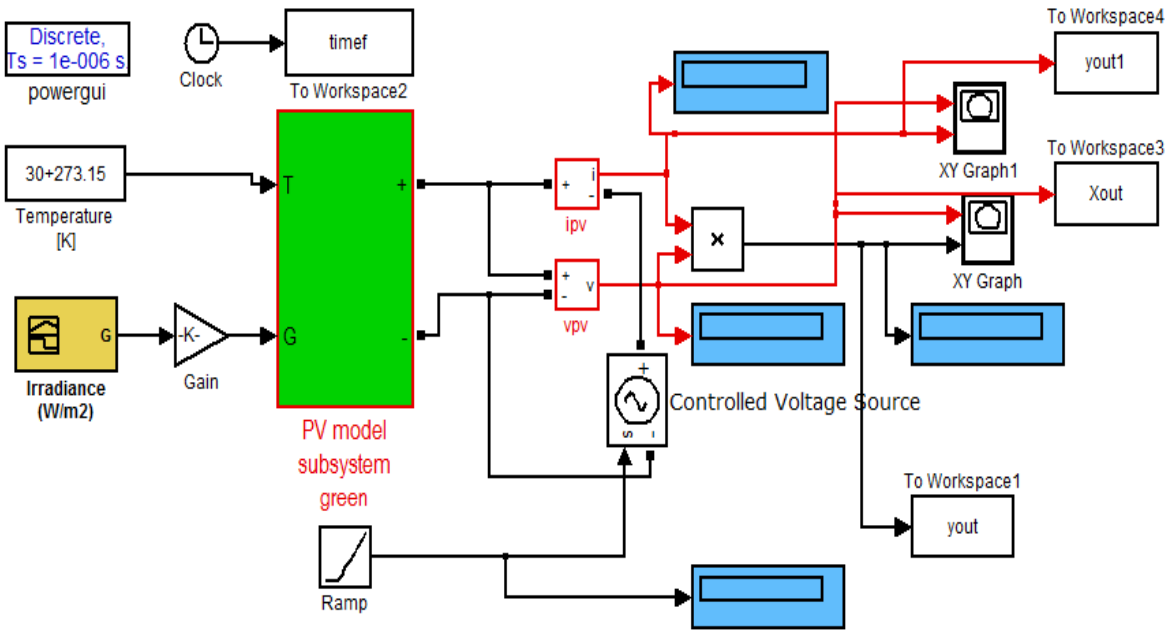

Fig. 24: Simulink model of the solar *PV* module

4.4.2.3 Effects of Solar Radiation Variation

For a given cell temperature, we can observe the effect of radiation variation as in Fig. 25 and Fig. 26. The irradiance was changed from 1000 W/m² down to 800 W/m² and finally to 600 W/m^2. Results are summarized in Table 5. From figures 48 and 49 and Table 5, we conclude that, the *PV* cell current is highly dependent on solar radiation. When the irradiance increases the output current increases, while the open-circuit voltage increases slightly and short circuit current increases. Also maximum output power increases but that *FF* decreases as irradiance increases.

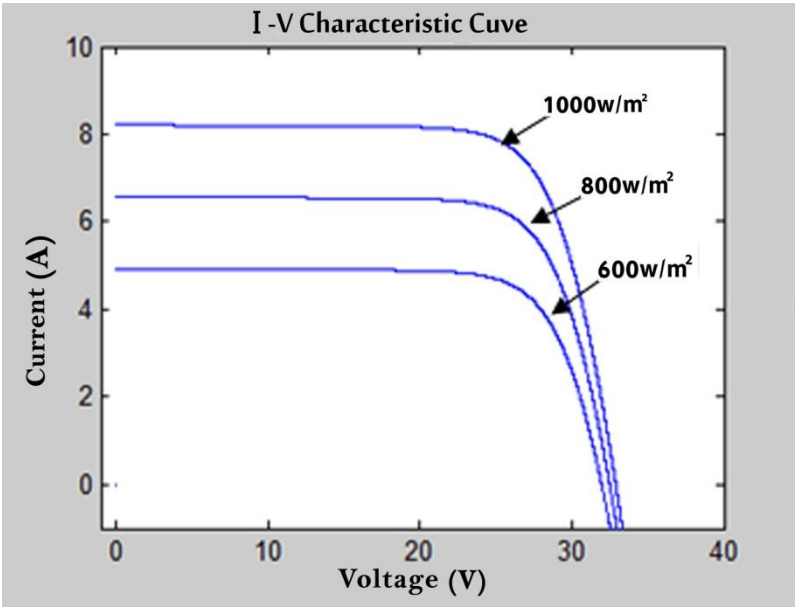

Fig. 25: I-V characteristic of a cell under varied irradiance

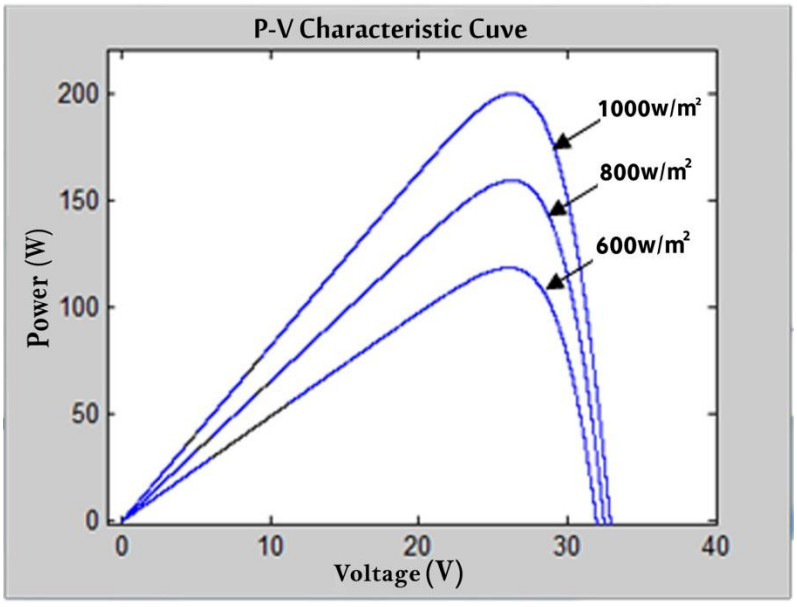

Fig. 26: P-V characteristic of a cell under varied irradiance

Irradiance [W/m^2]	*MPP* [W]	Voltage at *MPP* [V]	Current at MPP [A]	open-circuit voltage [V]	short-circuit current [A]	Fill factor [FF]
1000	200.1	26.3	7.61	32.8825	8.21	.741
800	159.4	26.3	6.061	32.4765	6.568	.747
600	118.7	26.3	4.512	31.9585	4.943	.751

Table 5: *MPP* at different irradiance

We also notice from Table 5 that the maximum output power at standard irradiance 1000 W/m² equals 200.1 W. The *PV* produce maximum output power at the output current = 7.61A and the output voltage = 26.3 V. When the irradiance level decreases to 600 W/m², the maximum output power decreases to 118.7 W. This result occurs at the output voltage of = 26.3 V and at output current of = 4.512 A. From these results, to keep the output power at maximum, the irradiance level should be maximized.

4.4.2.4 Effect of Varying Cell Temperature

For a given solar radiation, we can observe the effect of temperature variation on *I-V* characteristic of *PV* module as shown in Fig. 27 and Fig. 28. The temperature was changed from 30°C down to 25°C and finally to 20°C. Table 6 summarize the main results at different temperature. From figures 27 and 28 and considering the values of Table 6, we notice that the voltage is highly dependent on the temperature. When the cell temperature increases, the short circuit current increases slightly and the open circuit voltage V_{OC} decreases. So power output of the cell decreases with increasing temperature.

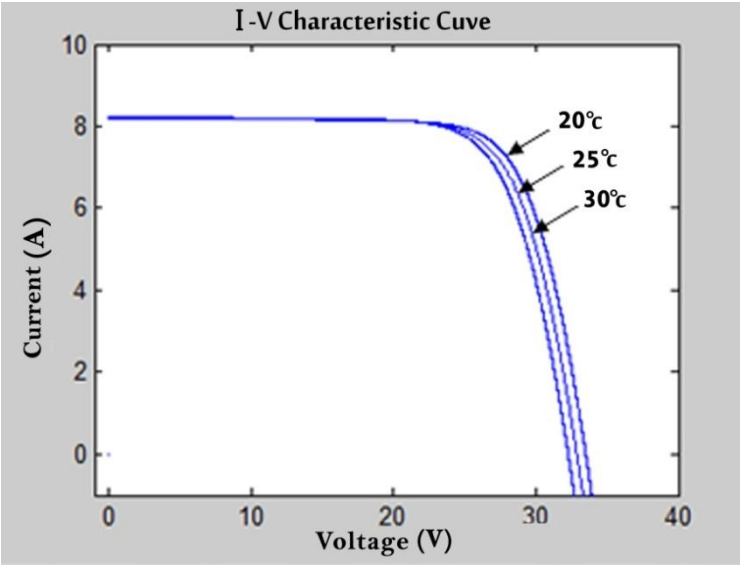

Fig. 27: I-V characteristic of a cell under varied temperature

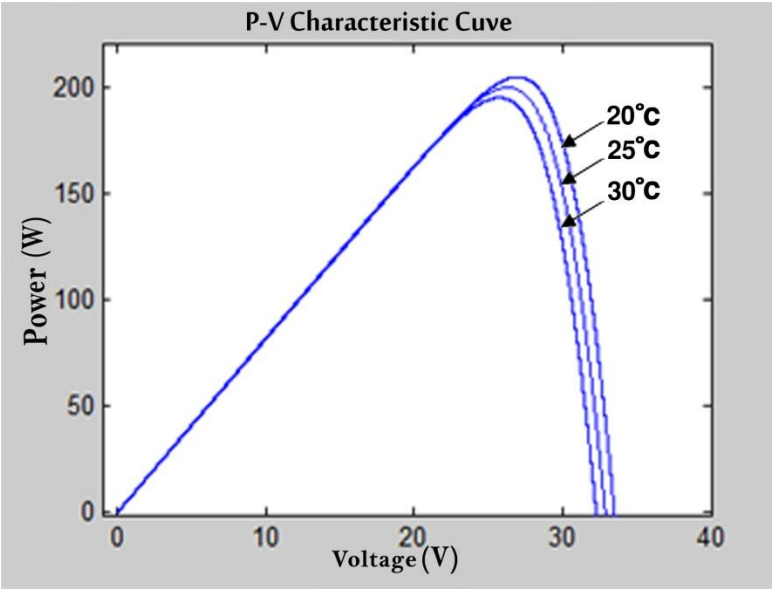

Fig. 28: P-V characteristic of a cell under varied temperature

Temperature [^{o}C]	*MPP* [W]	Voltage at *MPP*[V]	Current at MPP [A]	open-circuit voltage [V]	short-circuit current [A]	Fill factor [FF]
20	205	26.94	7.61	33.4985	8.194	.747
25	200.1	26.3	7.61	32.8825	8.21	.741
30	195.3	25.66	7.61	32.2700	8.226	.736

Table 6: *MPP* at different temperature

The maximum output power at the standard temperature 25^{0}C equal 200.1 W. The *PV* produce maximum output power at the output current 7.61 A and the output voltage 26.3 V. As temperature decreases to 20^{o}C, the maximum output power increases to 205 W. This result occurs at the output voltage = 26.94 V and output current = 7.61 A. While temperature increases to 30^{0}C, the maximum output power decreased to 195.3 W. This result happens at output voltage of = 25.66 V and output current = 7.61 A. We conclude temperature increases, the maximum output power of the cell decreases. Then to maximize the power output of the module, the temperature must be low.

4.4.2.5 Effect of Varying Shunt Resistance (R_{SH})

We can observe the effect of variation of shunt resistance on *I-V* characteristic of *PV* module as shown in Fig. 29 and Fig. 30. Shunt resistance was changed from 615.405 Ω down to 415.405 Ω and finally to 5 Ω. Table 7 summarizes the main results at different shunt resistance. From the figures and considering the values of Table 7, we notice that the small value of R_{sh} causes *PV* module current to fall more steeply indicating higher

power loss and low fill factor. Thus, shunt resistance must be large to increase output power and fill factor**.**

$R_{SH}[\Omega]$	*MPP* [*W*]	Voltage at *MPP*[V]	Current at *MPP* [*A*]	short-circuit current [*A*]	open-circuit voltage [*V*]	Fill factor [*FF*]
5	80.53	20.35	3.957	7.867	30.4605	.336
50	188	26.3	7.376	8.178	32.7495	.724
215.405	198.6	26.3	7.551	8.206	32.8685	.736
415.405	200.1	26.3	7.61	8.21	32.8825	.741
615.405	200.7	26.3	7.631	8.212	32.8895	.744
815.405	201	26.3	7.641	8.212	32.8930	.744
10000	201.7	26.3	7.671	8.214	32.9000	.747
20000	201.8	26.3	7.672	8.214	32.9	.747

Table 7: *MPP* at shunt resistance

From Table 7, the maximum output power at shunt resistance 5 Ω equal 80.53 W. The *PV* produce maximum output power at the output current 3.957 A and the output voltage 20.35V. As shunt resistance increases to 415.405 Ω, the maximum output power increases to 200.1W. This result occurs at the output voltage = 26.3 V and output current = 7.61. While shunt resistance increases to 10000Ω, the maximum output power increases to 201.7 W. This result happens at output voltage of = 26.3 V and output current = 7.671 A. We also observe the voltage at maximum output power doesn't affect with change values of shunt resistance while this values not very small. So, to maximize the power output of the module, the Shunt Resistance must be high**.**

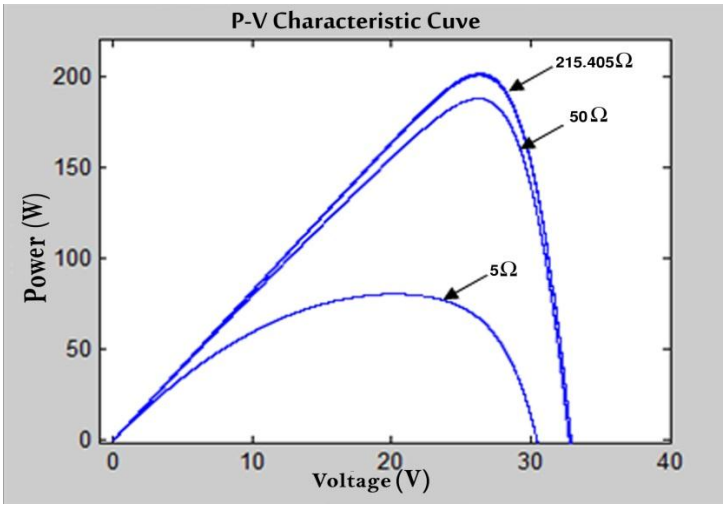

Fig. 29: P-V characteristic of a cell under varied Shunt Resistance

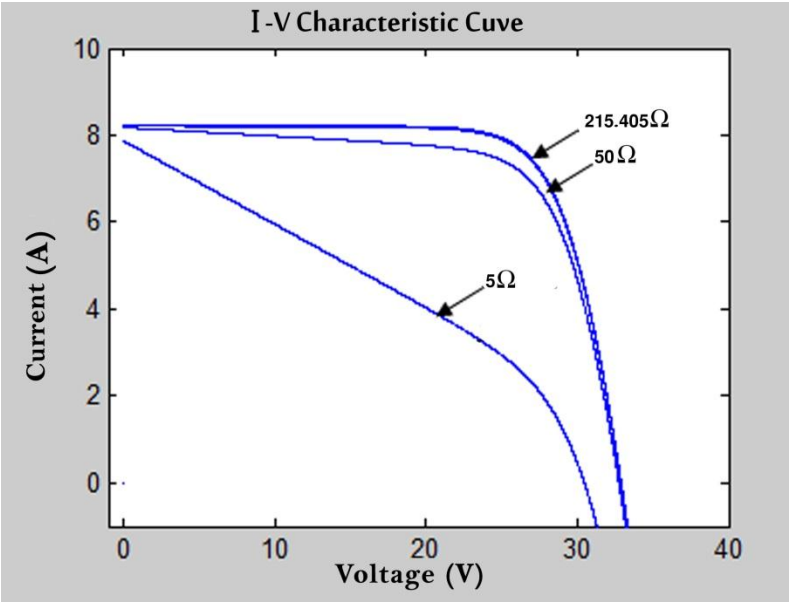

Fig. 30: I-V characteristic of a cell under varied shunt resistance

4.4.2.6 Effect of Varying Series Resistance (R_s)

We can observe the effect of variation of series resistance on *I-V* characteristic of *PV* module as shown in Fig. 31 and Fig. 32. Series resistance is changed from 1 Ω down to .221 Ω and finally to .121 Ω. Table 8 summarizes the main results at different series resistance. From the figures and considering the values of Table 8, we notice that the large value of R_s causes *PV* module current and voltage to fall more steeply indicating higher power loss and low fill factor. Series resistance must be low, if we take it into consideration.

Rs[Ω]	*MPP* (*W*)	Current at *MPP* [*A*]	Voltage at *MPP*[*V*]	short-circuit current [*A*]	open-circuit voltage [*V*]	Fill factor [*FF*]
.121	205.9	7.645	26.94	8.212	32.8825	.763
.221	200.1	7.61	26.3	8.21	32.8825	.741
.321	194.4	7.54	25.78	8.208	32.8825	.720
1	157	7.209	21.77	8.195	32.8825	.582

Table 8: MPP at different series resistance

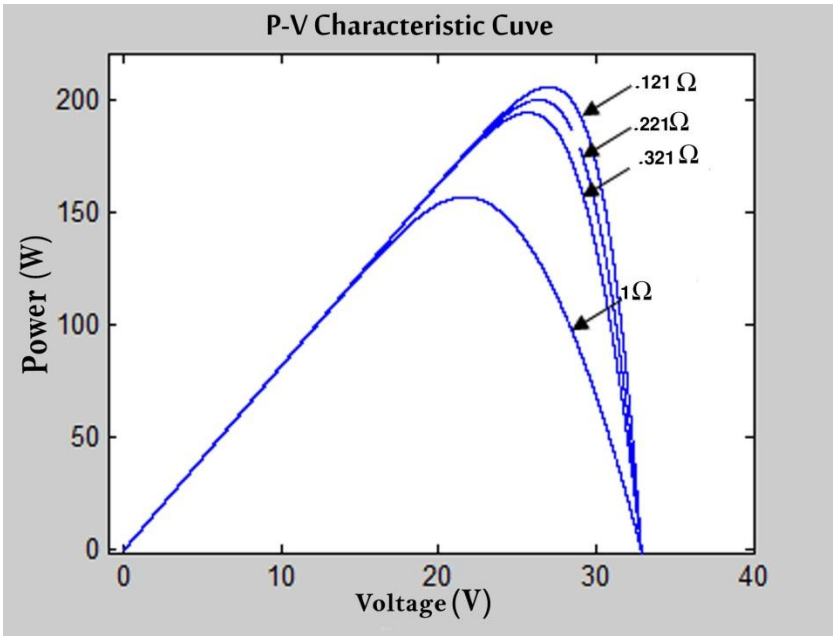

Fig. 31: P-V characteristic of a cell under varied series resistance

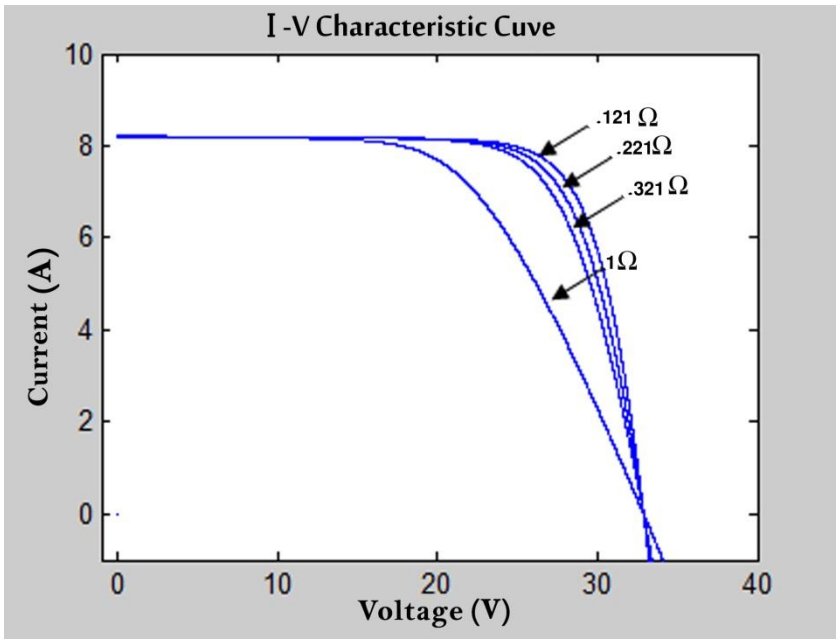

Fig. 32: I-V characteristic of a cell under varied series Resistance

From Table 8, the maximum output power at series resistance .121Ω equals 205.9 W. The *PV* produce maximum output power at the output current 7.645 A and the output voltage 26.94V. As series resistance increase to .221 Ω, the maximum output power decrease to 200.1 W. This result occurs at the output voltage = 26.3 V and output current = 7.61 A. While series resistance increases to 1 Ω, the maximum output power decreases

to 157 W. This result happens at output voltage equal to 21.77 V and output current equal to 7.209 A. To maximize the power output of the module, the series resistance must be low.

4.4.2.7 Effect of Varying Ideality Factor (*A*)

We can observe the effect of variation of ideality factor on *I-V* characteristic of *PV* module in Fig. 33 and Fig. 34. Ideality Factor was changed from 1.6 down to 1.3 and finally to 1. Table 9 summarizes the main results at different ideality factor. From the figures and considering the values of Table 9, we notice that as the value of ideality factor increase, maximum output power decrease also open circuit voltage decrease while short circuit current doesn't change.

Identity factor	*MPP* [*W*]	Voltage at *MPP*[*V*]	Current at *MPP*[*A*]	Short-circuit current [*A*]	Open-circuit voltage [*V*]	Fill factor [*FF*]
1	209.1	27.1	7.715	8.21	32.8860	.774
1.3	200.1	26.3	7.61	8.21	32.8825	.741
1.6	192.1	25.86	7.428	8.21	32.8790	.712

Table 9: MPP at different Ideality Factor

From Table 9 the maximum output power at ideality factor 1 equals 209.1 W. The *PV* produces maximum output power at the output current 7.715 A and the output voltage 27.1 V. As ideality factor increase to 1.3, the maximum output power decrease to 200.1 W. This result occurs at the output voltage = 26.3 V and output current = 7.61A. While ideality factor increases to 1.6, the maximum output power decreased to 192.1 W. This result happens at output voltage of = 25.86 V and output current = 7.428 A. To maximize the power output of the module, the ideality factor must be low.

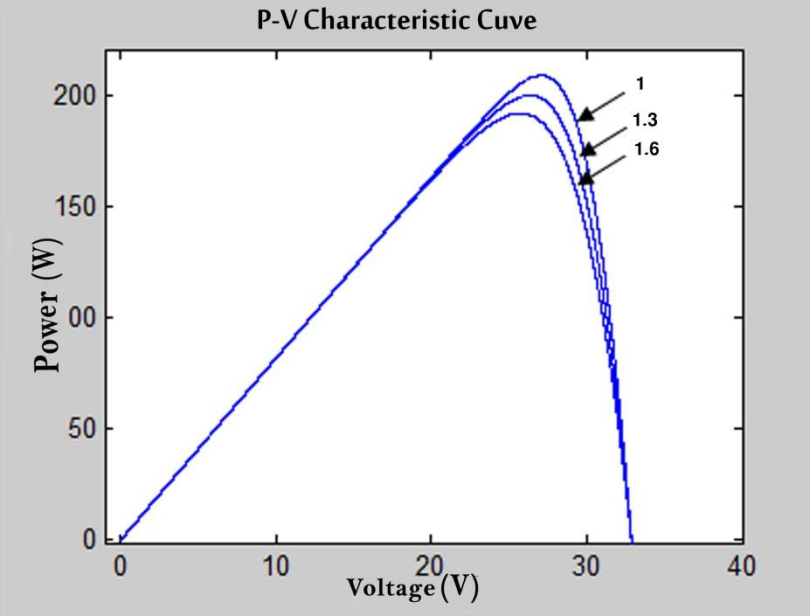

Fig. 33: P-V characteristic of a cell under varied Ideality Factor

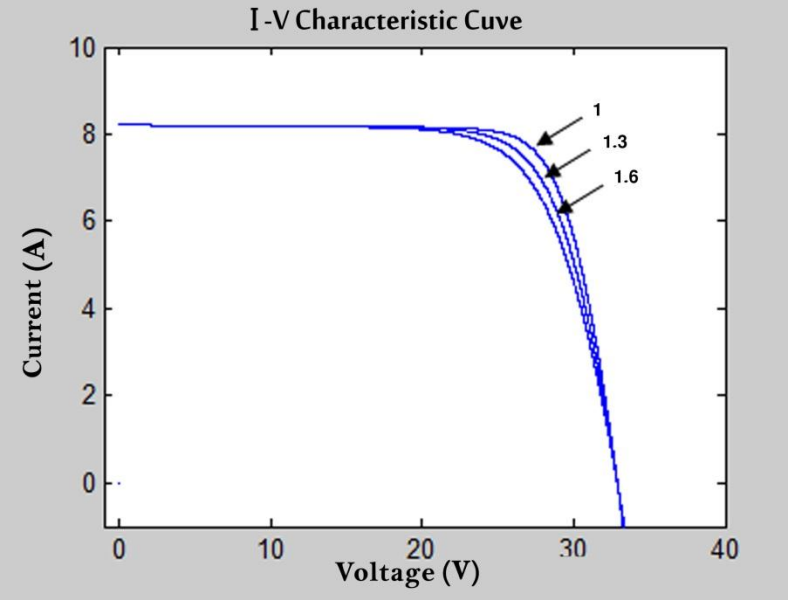

Fig. 34: I-V characteristic of a cell under varied Ideality Factor

4.4.2.8 Effect of Varying Saturation Current (I_s)

We can observe the effect of variation of I_s on *I-V* characteristic of *PV* module in Fig. 35 and Fig. 36. I_s is changed from 98.252*10^-8 A down to 9.8252*10^-8 A and finally to 0.98252*10^-8 A. Table 10 summarizes the main results at different *Is*. From the figures and Table 10, we realize that as the value of I_s increases, the maximum output power decreases, the open circuit voltage decreases, and the *Is* short circuit current doesn't change.

I_S [A]	MPP [W]	Voltage at MPP[V]	Current at MPP[A]	short-circuit current [A]	open-circuit voltage [V]	Fill factor [FF]
.98252*10^-8	231.6	30.2	7.667	8.21	35	.805
9.8252*10^-8	200.1	26.3	7.61	8.21	32.8825	.741
98.252*10^-8	169	22.63	7.466	8.21	28.7315	.716

Table 10: MPP at different I_S

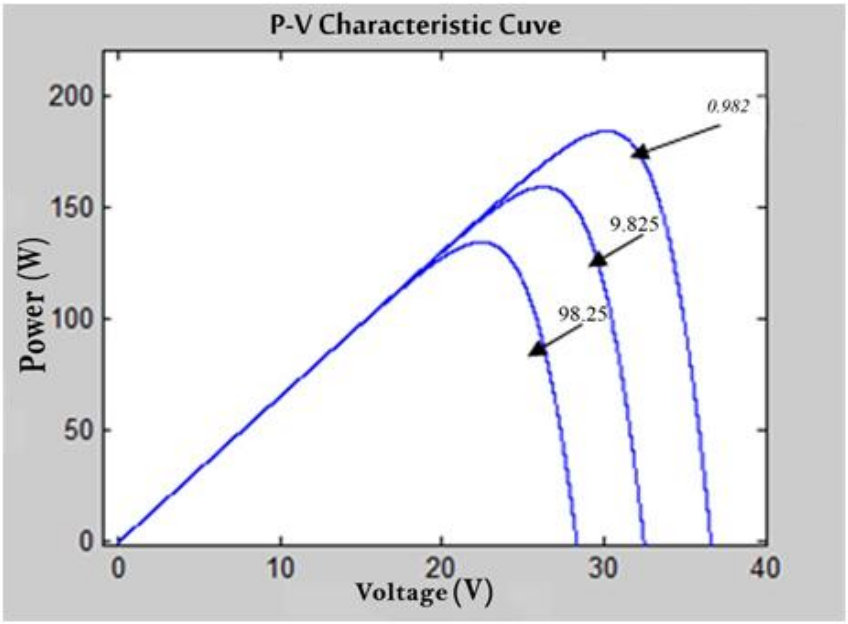

Fig. 35: P-V characteristic of a cell under varied saturation current

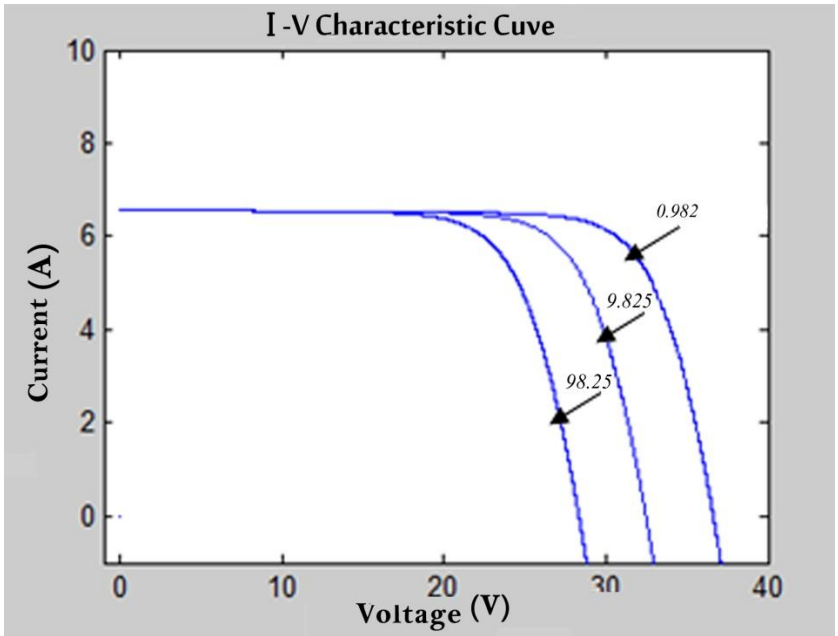

Fig. 36: I-V characteristic of a cell under varied saturation current

4.4.2.9 Effects of Partial Shading on *PV*

Partial shading of *PV* modules is the most commonly encountered mismatch phenomena in a *PV* power system[100]. *PV* power system is affected by temperature, solar insulation, shading, and array configuration. We have already discussed the effect of temperature and solar insulation. Here, we will discuss the effect of shading. *PV* system might be shaded fully or partially by trees, passing clouds, high building, etc., which result in non-uniform insolation conditions[101]. Although *PV* arrays under uniform illumination conditions has nonlinear characteristic with the occurrence of one *MPP* in the *P-V* curve, when the P*V* array is under partially shading conditions, the *P-V* characteristic becomes more complex[102]. During partial shading, part of the *PV* cells which receive uniform irradiance still operates at the optimum efficiency. Since current flow through every cell in a series configuration is naturally constant, the shaded cells need to operate with a reverse bias voltage to provide the same current. However; the resulting reverse power polarity leads to power consumption and a reduction in the maximum output power of the partially-shaded *PV* module. This problem solved by adding a bypass diode to a specific number of cells in the series circuit[101].

Here we presents a MATLAB based modeling for studying the *I–V* and *P–V* characteristics of a *PV* array under partial shading. It can also be used for developing and evaluating maximum power point tracking techniques. It can also be used as a tool to study the effects of shading patterns on *PV* panels having different configurations. It is observed that, for a given number of *PV* modules, the array configuration (depend on the number of series and parallel connections) significantly affects the maximum available power under partially shaded conditions[103].

4.4.2.9.1 Effect of Bypass and Blocking Diodes

It is important to note that the characteristics of an array with bypass diodes and blocking diodes differ from the one without these diodes. When the solar irradiance on *PV* array is in good order, only one *MPP* is founded on the *P-V* characteristic curve. likewise, because of the bypass diodes and the blocking diodes, many local maximum power points (multiple local maxima) can be existed under partially shaded condition. The presence of multiple peaks reduces the effectiveness of the existing *MPPT* schemes. The purpose of bypass diodes is to provide a low-resistance current path around the shaded cells, thereby minimizing module heating and array current losses, when cell expose to shade, the

current of the unshaded cells have a path through bypass diode and all the cells of the module become forward-biased [98][101][94][103].

In systems utilizing a battery, the blocking diodes connected in series with the string of series connected *PV* modules to avoid current imbalance caused by shading. Blocking diodes are typically placed between the battery and the solar module output to prevent battery discharge at night. It will prevent the reverse current through the series composition, which generate lower output voltage as compared to the others connected in parallel. This reverse current may cause excessive heat generation and thermal breakdown of *PV* modules[98,103].

It is important to know that the bypass diodes are connected in parallel with each *PV* module. And the blocking diode is connected in series with each string, which is a group of series connected *PV* module, to protect the modules from the effect of potential difference between series connected strings[94].

4.4.2.9.2 Simulation of *PV* Module with Partial Shading

A partially shaded module can be represented by two groups of *PV* cells in series. Both groups receive different levels of irradiance. Fig. 37 illustrates built diagram of *PV* array when one of the *PV* modules under shading condition equal to 50%. The output parameter for the solar panel with and without bypass diodes under different shading condition are summarized in Table 11.

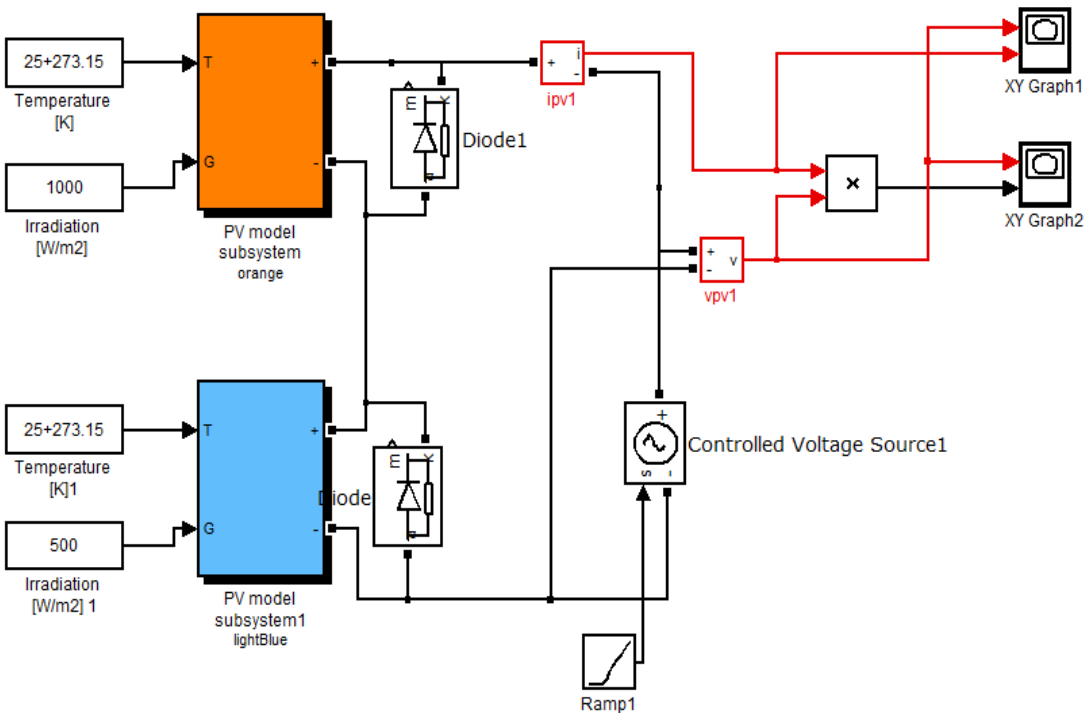

Fig. 37: Simulation of two modules in series

Case	Cell (1) irradiance [W/m²]	Cell (2) irradiance [W/m²]	*MPP* [*W*]	Voltage at *MPP*[*V*]	Current at *MPP*[*A*]
1. Full irradiance (Without shading) effect and with bypass diodes (full irradiance)	1000	1000	400.2	52.43	7.633
2. Full irradiance (Without shading) effect and without bypass diodes (full irradiance)	1000	1000	400.3	52.65	7.603
3. Partial irradiance (one cell with partial shading effect) and with bypass diode	1000	500	217.5	55.4	3.927
4. Partial irradiance (one cell with partial shading effect) and without bypass diode	1000	500	217.6	55.6	3.914
5. Partial irradiance (two cells with partial shading effect) and with bypass diode	500	500	196.2	51.61	3.801
6. Partial irradiance (two cells with partial shading effect) and without bypass diode	500	500	196.2	51.7	3.796
7. Partial irradiance (one cell with full shading effect and second with full irradiance) and with bypass diode	1000	0	193.9	25.47	7.614
8. Partial irradiance (one cell with full shading effect and second with full irradiance) and without bypass diode	1000	0	.4491	16.63	0.02
9. Partial irradiance (one cell with partial shading effect and second with full shading) and with bypass diode	500	0	94.88	24.77	3.83
10. Partial irradiance (one cell with partial shading effect and second with full shading) and without bypass diode	500	0	.4152	15.6	.02

Table 11: *MPP* under different partial shading condition with and without bypass diodes

We can observe the effect of bypass diode on *I-V* characteristic of *PV* module in Fig. 38. By reading the results and follow-up figures with and without bypass diodes we arrive nearly to the same value of *MPP* unless there are full shading. But in the presence of bypass diode many local maximum power points appear where one of them is the global maximum. The bypass diode is very important in the case when one module is under full shading. It is important because when we don't apply bypass diode on the module under full shading, we get almost zero output power as in cases 8 and 10. However, when we add the bypass diode, we still obtain output power from the other cell. As in cases 7 and 9. Shading causes a large reduction on total outcome power does not commensurate with the small amount of shading. We mean that the relation between shading and output power is not linear. To give more explanation, we take case 1 and case 2 as examples. In case 1we have full irradiance and thus we get output power equal to 400.2 W. When one module has partial shading, the output power decreases to 217.5 W. If the relation is linear, then we might expect to get 300 W [200 W from the module with full irradiance and 100 W from the module under partial shading]. We notice in cases like cases 7 and 9 that the output power is less than the expect value. The reason might be due to the fact that some amount of the output power is dissipated in the other circuit parts which has been deactivated by the bypass diode (it works like dissipated resistance). When modules are under same amount of radiations [both are under full irradiance or both are under same shading], we notice that the amount of output power commensurate with amount of irradiance as in case 1 and 5. When modules are under different irradiance conditions, we notice that we have great loss in the output power. For example if we take case 3, we notice that when cell1 is under full irradiance and cell 2 is under partial shading, the output powers equal to 217.5 W. If we consider the output of cell 1 equal to 200 W (under full irradiance) and cell 2 output powers equal to 100 W (under partial shading), then output power that we expect at least 300 W. Again we many explain this by the fact that output power is not linear with shading effect. We can conclude that if we want to get maximum output power from our system, we must add bypass diodes to each cell. However this will be very expensive.

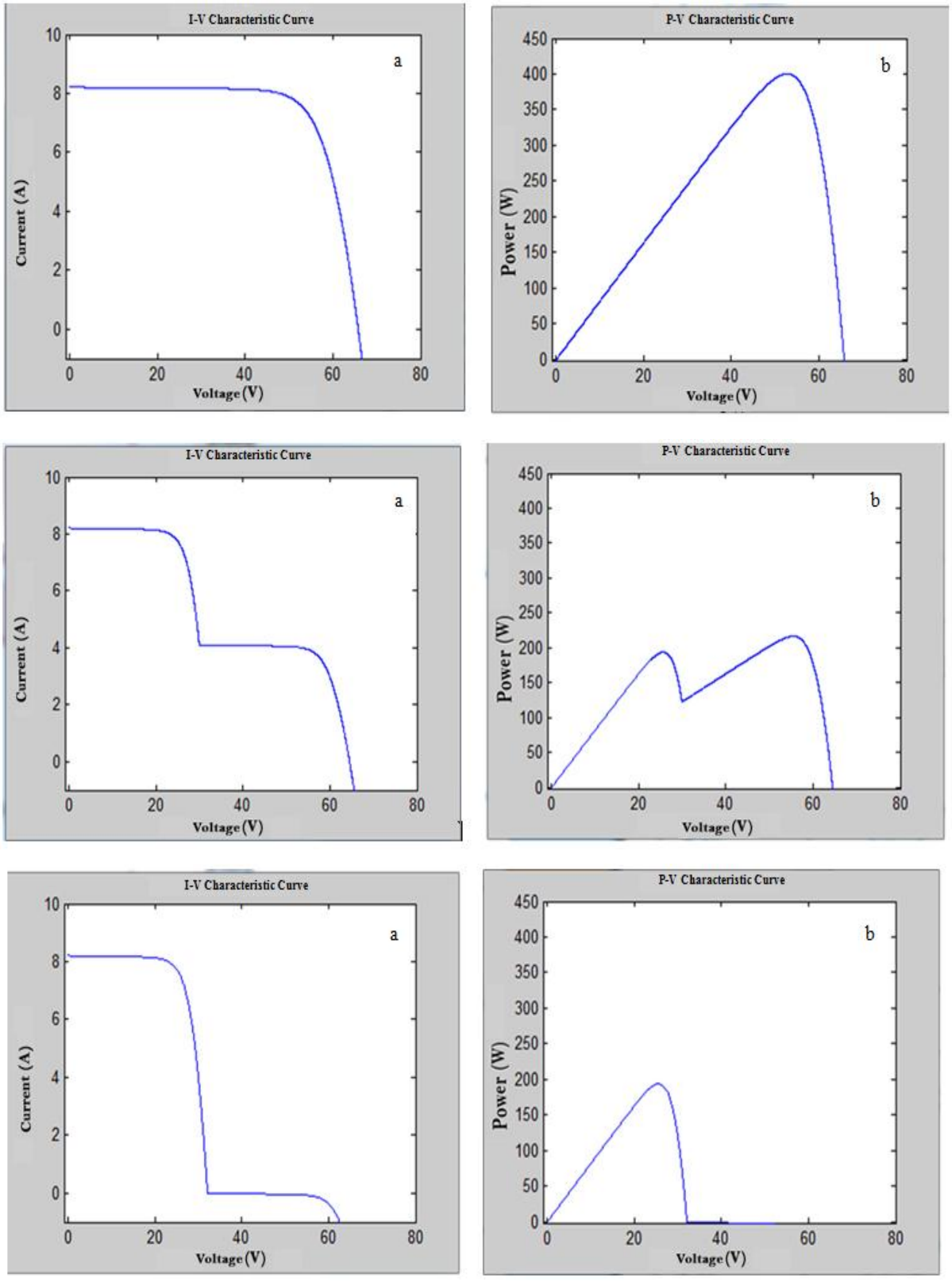

Fig. 38: a) I-V characteristic of a cell under different partial shading condition with and without bypass diodes
b) P-V characteristic of a cell under different partial shading condition with and without bypass diodes

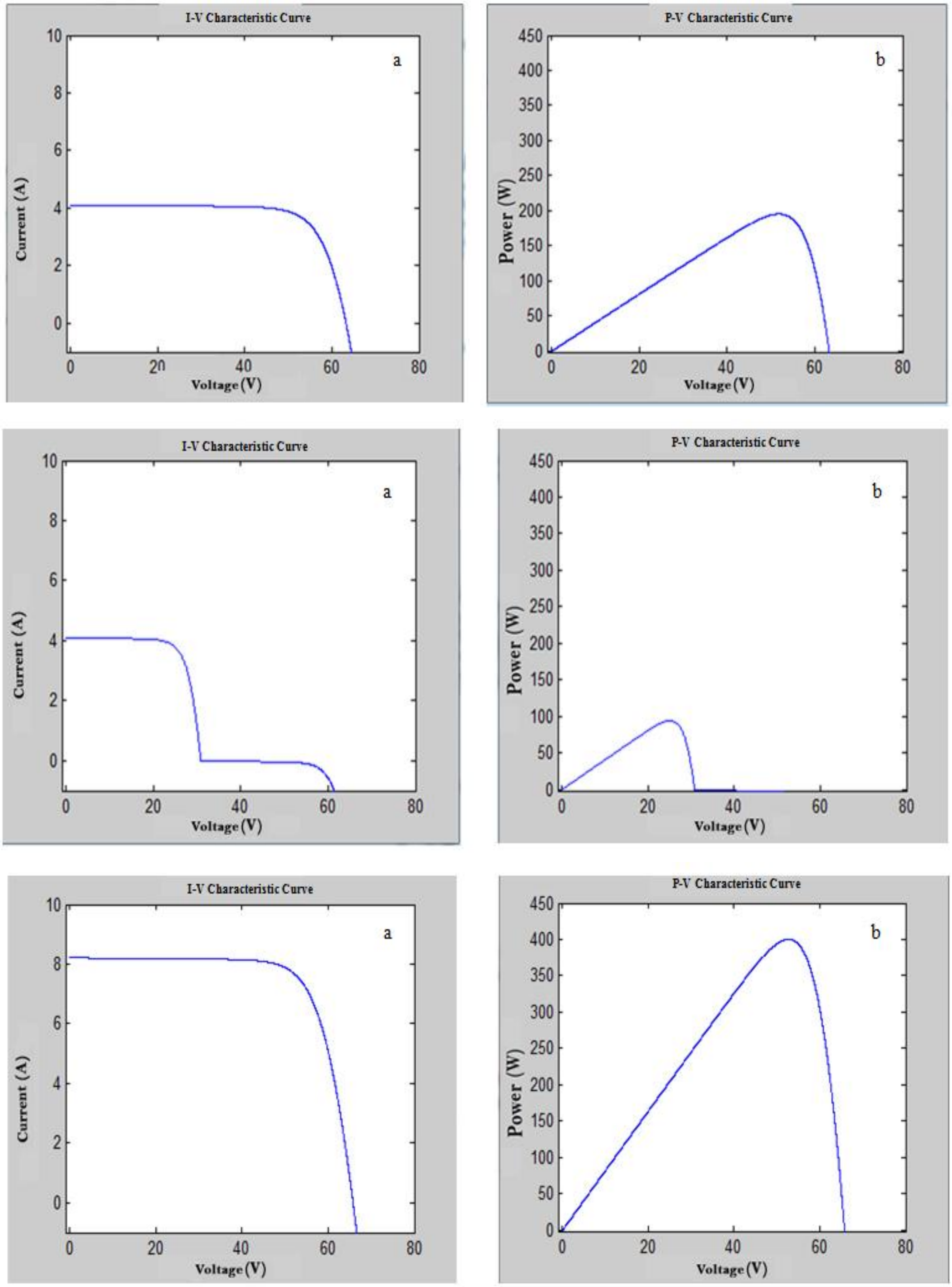

Fig. 38: Continued .

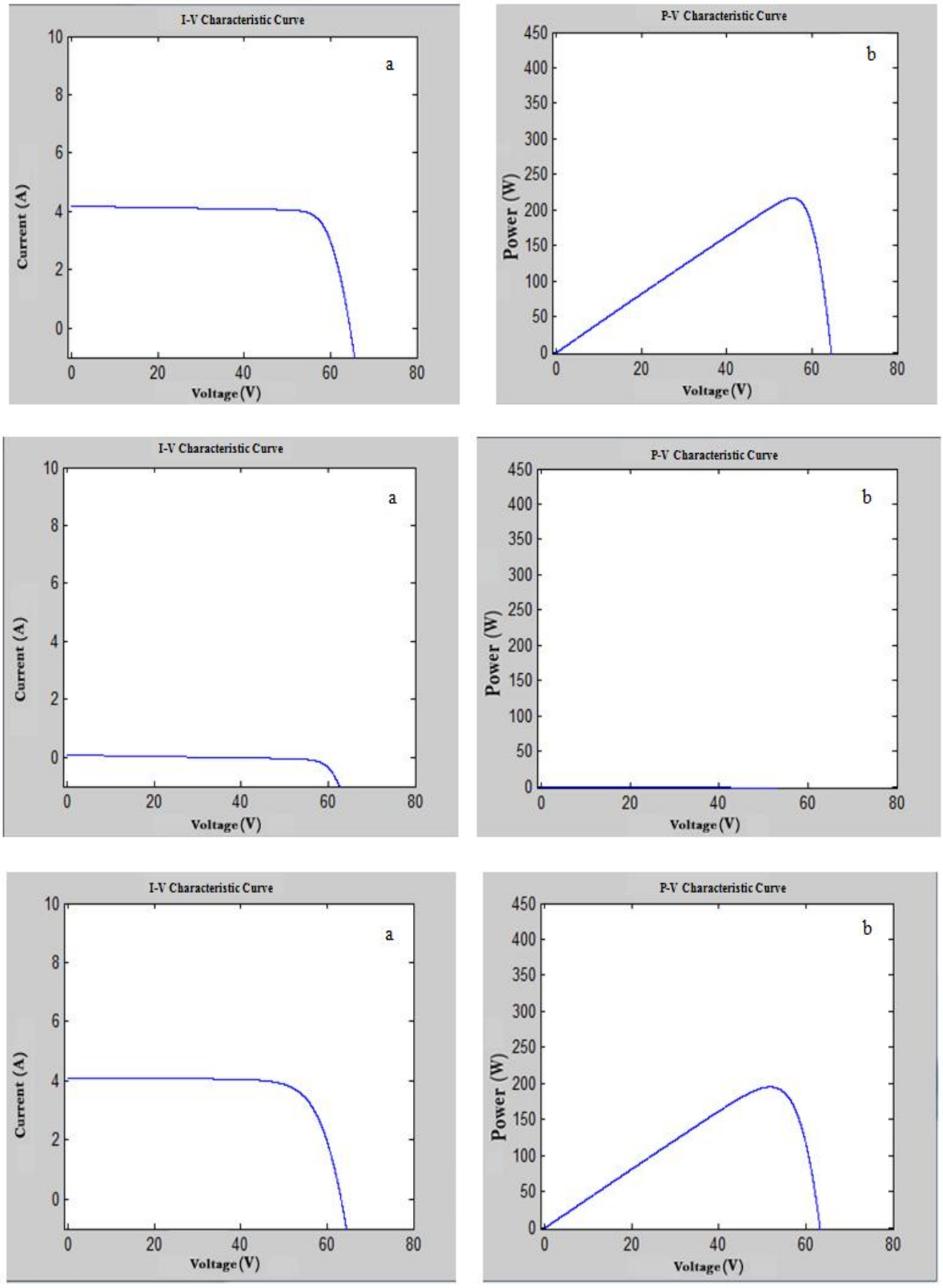

Fig. 38: Continued .

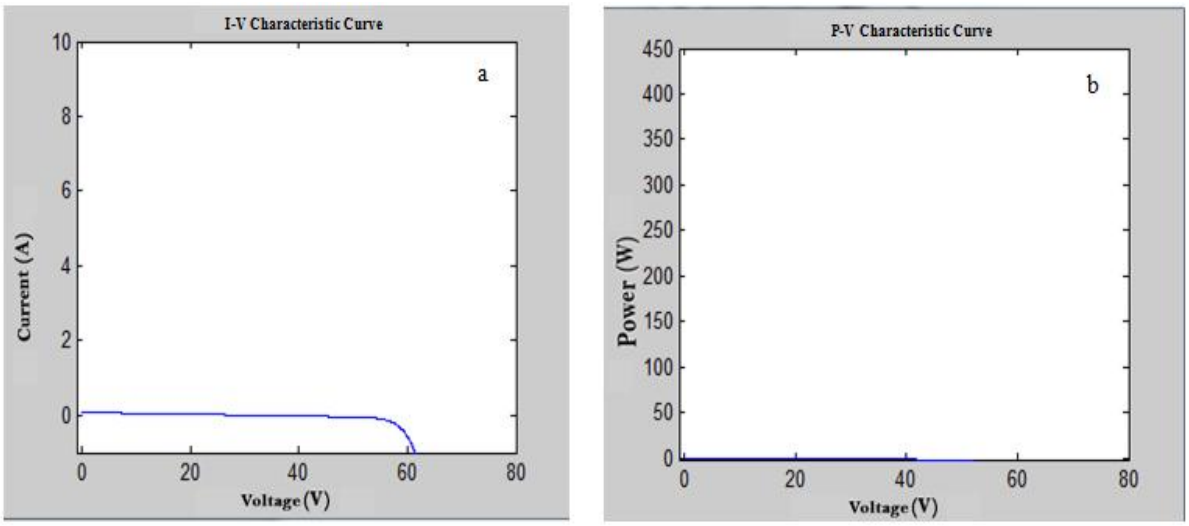

Fig. 38: Continued .

4.4.2.10 How Minimizing Temperature and Maximizing Irradiance

We can encounter the irradiance problems by sun tracking systems. The reason of irradiance problems is the rotation of the earth around its axis, the orbital motion of earth around the sun and the apparent position of the sun in the sky changes over time. Thus, to utilize the solar energy efficiently, we must understand the apparent motion of the Sun[39]. Based on solar tracking, we can improve tracking to the best direction and position to get maximum irradiance. However, using solar tracking system increases the cost. Also, we can encounter the temperature problem by building the field in the coolest places or where there is air current and wind.

CHAPTER 5 SIMULATION AND IMPLEMENTATION OF INCREMENTAL CONDUCTANCE MPPT

Solar panel converts 30-40% of energy incident on it to electrical energy. *MPPT* algorithm is necessary to increase the efficiency of the solar Panel. As noted earlier *MPPT* technology can be done using different techniques such as *P&O* (hill climbing method), Incremental conductance, Fractional Short Circuit Current, Fractional Open Circuit Voltage, Fuzzy Control, Neural Network Control etc. Among all the methods *P&O* and Incremental conductance are most commonly used because of their simple implementation, lesser time to track the *MPP* and several other economic reasons. In this chapter, we will discuss simulation and implementation of Incremental Conductance method. Though this method has high efficiency, its complexity is not low, hence the cost of implementation increases. So we trade off between complexity and efficiency. Also the efficiency of the system depends upon the converter.

MPPT is a fully electronic system that varies the electrical operating point of the modules so that the modules are able to deliver maximum available power. The *MPPT* varies the ratio between the voltage and current delivered to the battery, in order to deliver maximum power. If there is excess voltage available from the *PV*, then it converts that to additional current to the battery. As the voltage of the *PV* array varies with temperature and other conditions, it "tracks" this variance and adjusts the ratio accordingly[105].

Modeling of *PV* system are explained in Section 5.1. Section 5.2 summarizes Boost converter. *MPPT* Controller is explained in Section 5.3. While Section 5.4 present the simulation and results.

5.1 Modeling of *PV* System

The block diagram of the solar *PV* panel is shown in Fig. 39 below. This system has been modeled on MATLAB 2011 and Simulink. Where the parameter on our simulation based on KC200GT solar array datasheet. The inputs to the solar *PV* panel are temperature (*Ta*), solar irradiation (*G*). Simulation circuit diagram contain block of the Incremental Conductance method.

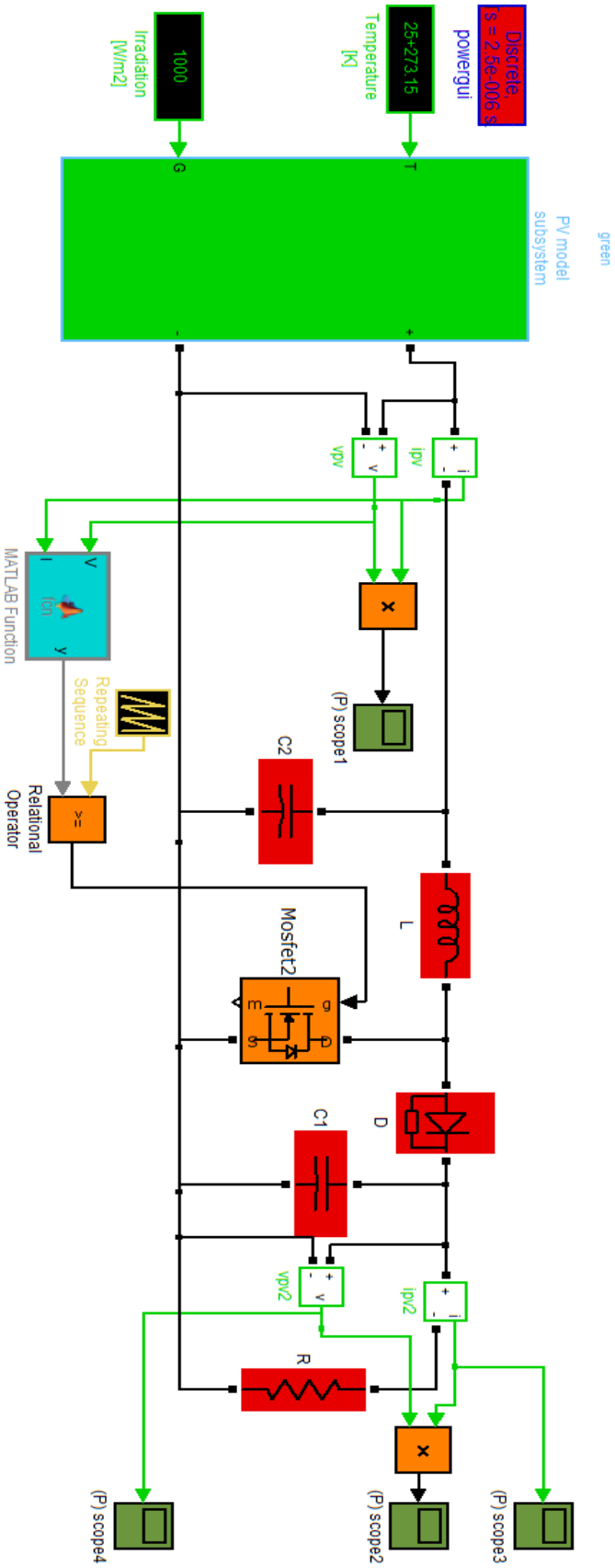

Fig. 39: Circuit diagram of the Incremental Conductance method

5.2 Boost Converter

The boost converter is nothing but a *DC/DC* converter which has boosting the voltage to maintain the maximum output power constant for all the conditions of temperature and solar irradiance variations. Shown in figures 40 and 41 when the switch *S* is on, the current builds up in the inductor *L* due to the positive inductor voltage is equal to the input voltage. The switch is then opened after some small period of time. When *S* is off, the voltage across *L* reverses and adds to the input voltage, thus makes the output voltage greater than the input voltage. For steady state operation, the average voltage across the inductor over a full period is zero[105,112]. The maximum power point tracker uses the *DC/DC* converter to adjust the *PV* voltage at the maximum power point. A boost converter select to implement *MPPT* because of their simplicity and its common use in practical applications.

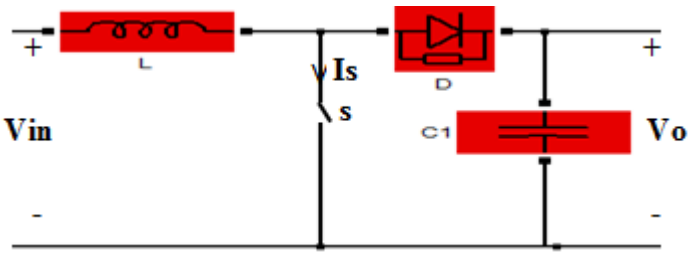

Fig. 40: Boost converter

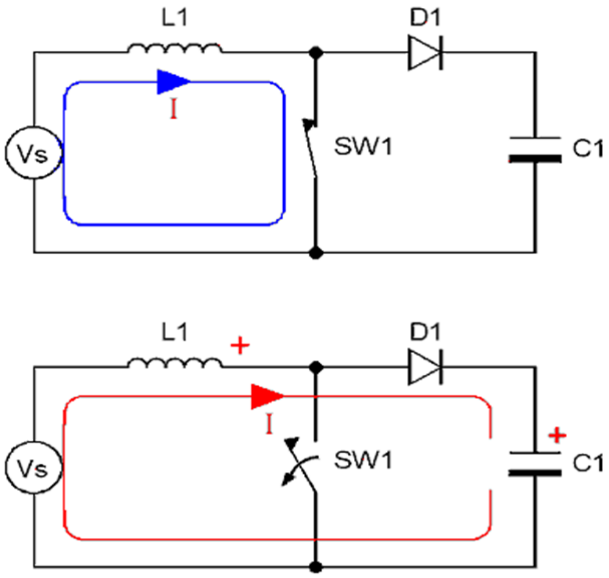

.;

Fig. 41:Operation boost converter

5.3 Pulse Width Modulation Generation(*PWM*)

The percentage of time the switch is ‘on’ for a set switching speed is duty cycle (*D*). Fig .42 illustrate the comparison of *D* (modulating signal) with a triangle wave (carrier signal) that ranges from zero to one. When the value of the triangle waveform is higher than *D*, the *MOSFET* (switch) is ‘off’. Similarly, when the value of the triangle waveform is lower than *D*, the *MOSFET* (switch) is ‘on. This means output stays high as long as the modulating signal is greater than the carrier as shown in Fig. 43, the *MPPT* adjusts the pulse width of the *DC/DC* converter to obtain the *MPP* for the *PV* system[107,110].

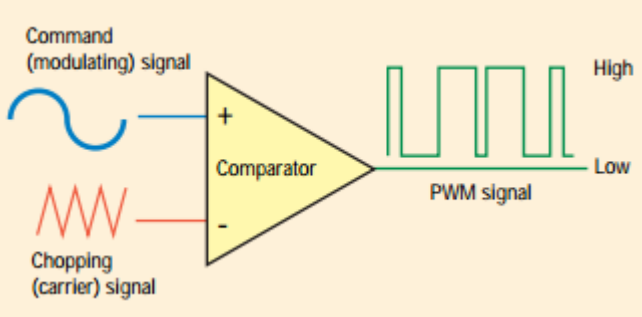

Fig. 42 : PWM signal

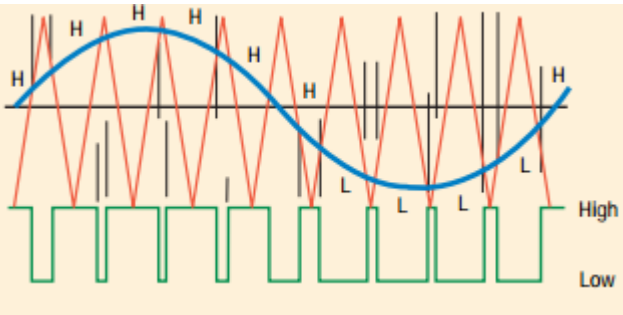

Fig. 43: Operation PWM signal

5.4 *MPPT* Controller

The flowchart shown in Fig. 44 explain the operation of this algorithm where the *MPP* can be tracked by comparing the instantaneous conductance *(I/V)* to the incremental conductance *(ΔI/ΔV)*. It starts with measuring the present values of *PV* module voltage and current. Then, using the present values and previous values of voltage and current. The incremental changes, *dI* and *dV* can be calculated. The track depend on below relationships.

$$\frac{\Delta I}{\Delta V} = \frac{-I}{V} \quad \text{at } MPPT \tag{4.1}$$

$$\frac{\Delta I}{\Delta V} \succ \frac{-I}{V} \quad \text{at left of } MPPT \tag{4.2}$$

$$\frac{\Delta I}{\Delta V} \prec \frac{-I}{V} \quad \text{at right of } MPPT \tag{4.3}$$

If equation (4.1) is not satisfied, then as we start from zero point it is assumed that the operating point is at the left side of the *MPP*. Thus the tracker must be moved to the right by increasing the module voltage. Similarly, if the condition satisfies the inequality equation (4.3), it is assumed that the operating point is at the right side of the *MPP*, thus the tracker must be moved to the left by decreasing the module voltage. When the operating point reaches at the *MPP*, the condition satisfies the equation (4.1). At the end of cycle, it updates the history by storing the voltage and current data that will be used as previous values in the next cycle[47,106].

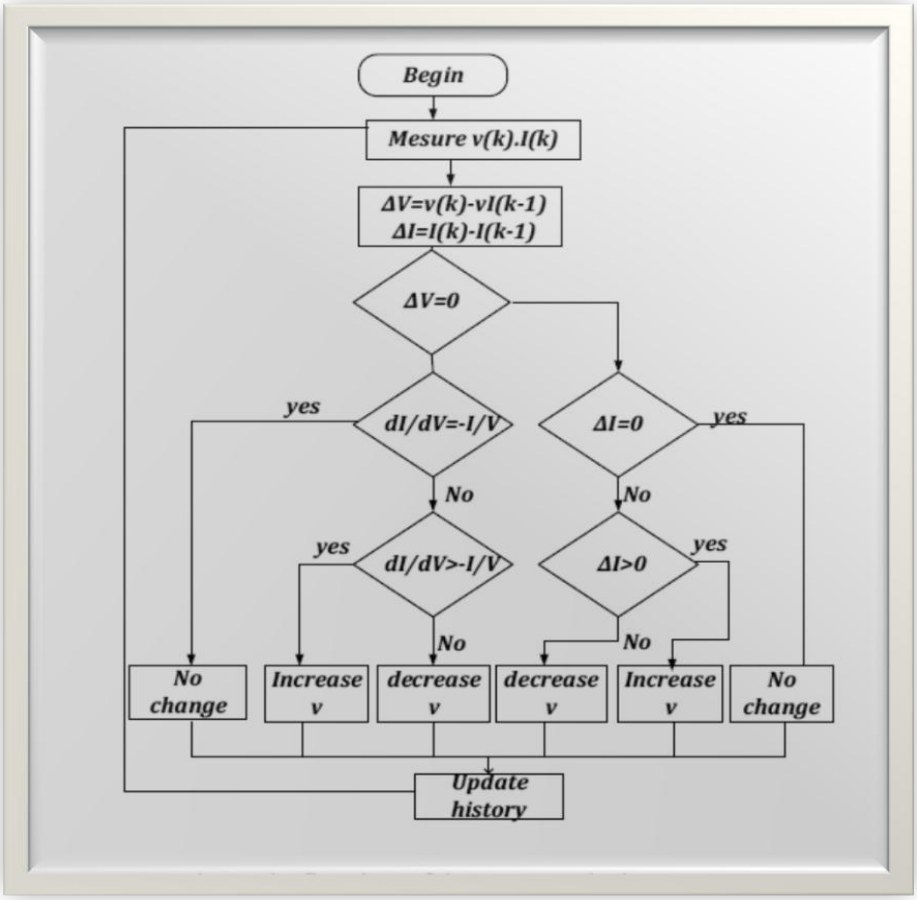

Fig. 44: Flowchart of algorithm

5.5 Results

After running the system the result appear in the scope shown in below figures. Fig. 45 shown output voltage, Fig. 46 shows output current, Fig. 47 shows output power.

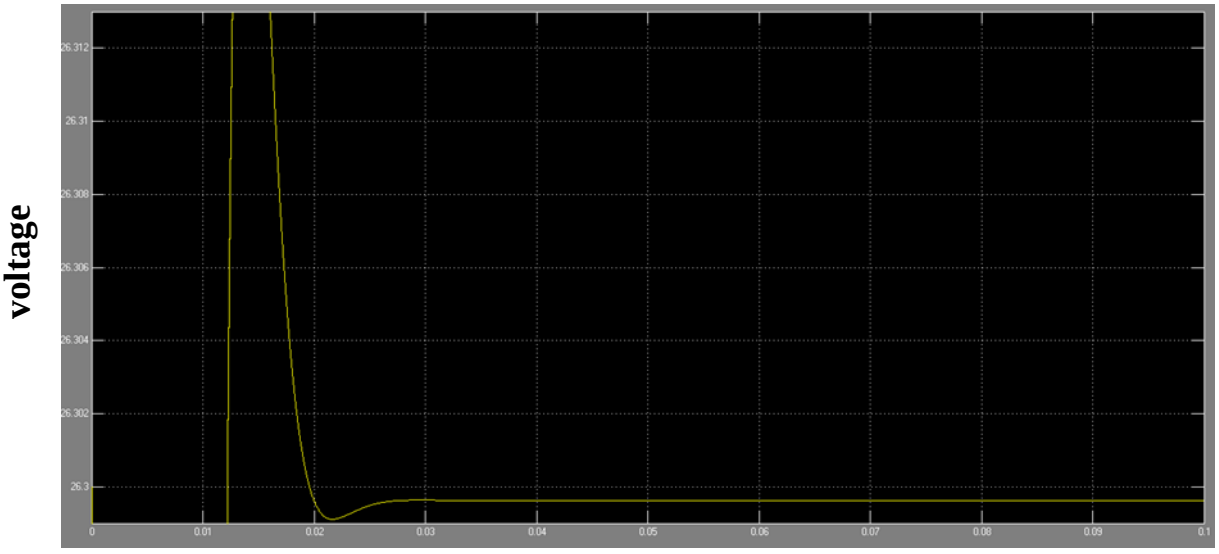

Fig. 45: Output voltage

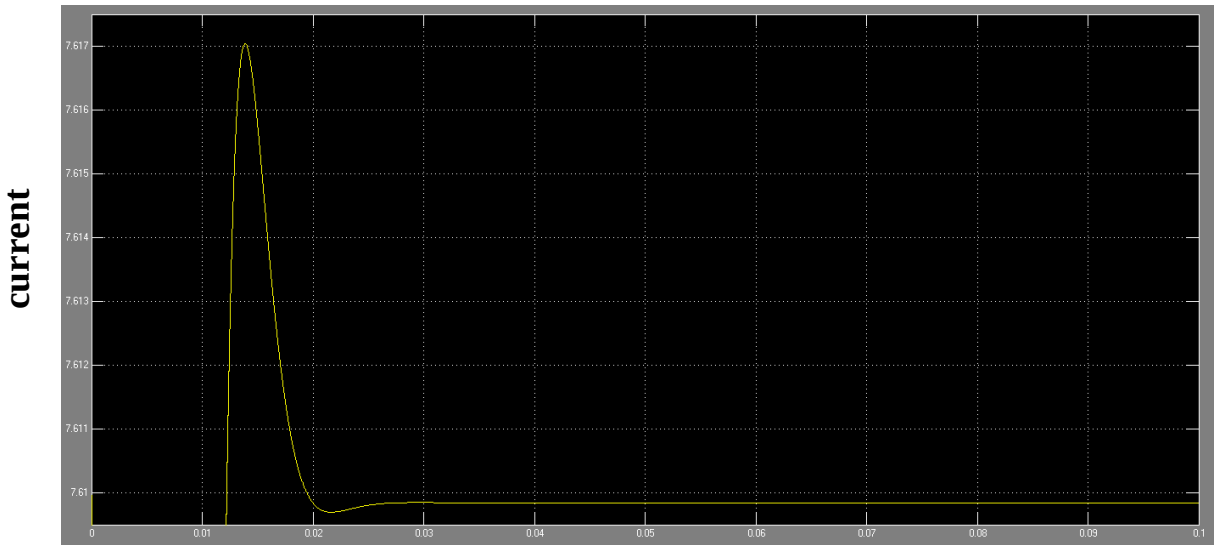

Fig. 46: Output current

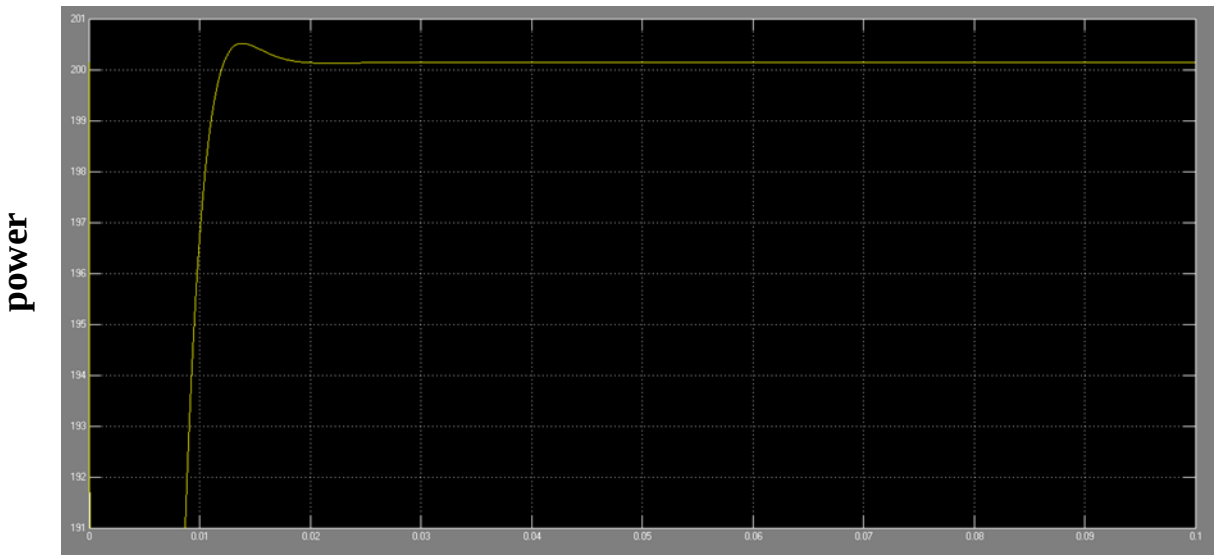

Fig. 47: Output power

Incremental conductance algorithm of *MPPT* is implemented using Boost converter. The model is simulated with MATLAB/SIMULINK. It is shown that *PV* system output power 200.13 W. We expected 200.143 W. We explain the small loss due the experimented error. The Incremental conductance gives the duty cycle to extract the maximum power from *PV* system where we get to maximum power point without oscillating around final value.

CHAPTER 6 CONCLUSION AND FUTUER WORK

6.1 Conclusion

Pollution resulting from the use of conventional energy leads to environmental health hazards and economic threats; therefore, the use of alternative energy will reduce these effects. Recently using renewable energy technology increased globally and developed rapidly where it plays an important role in clean application especially in electric power generation. By using solar energy, we can get electric energy directly by using photovoltaic module then using *MPPT* to maximize the photovoltaic output power.

Obtaining the maximum power automatically from a solar modules or in other words making the system operates at maximum efficiency, depends on the used algorithm of *MPPT*. There are different type of *MPPT* algorithm that used for the purpose of improving the efficiency of solar panel but not all method gives the same efficiency . The *MPPT* method vary in many aspects including complexity, cost, sensor dependence, convergence speed, implementation hardware, compensation for capacitance, range of effectiveness, popularity capability of escaping from local optima and their applications.In this thesis, we dealt with a range of methods used to get the maximum power and compared them with each other to determine the merits of each method and location for the other way. So it's easy for the researcher to choose the best way for practical applications in accordance with the limitations and the possibilities available to him.

MPPT algorithms take into account the effect of some factor which is reflected in the amount of electricity generated, in this thesis we have detailed study for all the factors affecting the properties of the cell and the impact of the change on the resulting energy, factors have been split between internal such as the impact of change in resistors and external such as the impact of the change in temperature, radiation and shade. By tracking the changes in parameters, we can reach to the mechanism that we can follow to get high *FF*.

In the end, we have implemented a simple practice demonstrates the use of one of the *MPPT* methods to get the maximum power. This method called Incremental Conductance

Algorithm. Incremental conductance algorithm is implemented using Boost converter. The model is simulated with MATLAB/SIMULINK. From results, we reach to fact that we get more efficiency by using *MPPT* method.

6.2 Future Work

An increase in the accuracy of the results and organization of the comparison. Re comparison between the method after harnessing the same data, variables and circuit. Also another future work is implementation of a *PV* system using a fast dSPACE DSP controller for some methods.

REFERENCES

1. Reported issued by IEA," Renewable Energy into Mainstream," SITTARD: The Netherlands, Oct. 2002.
2. G. Jones and L. Bouamane," “Power from Sunshine”: A Business History of Solar Energy," Working paper, Harvard Business School, May. 2012 .
3. J. Twedell and T. weir," Renewable energy Resources," 2nd edition, Taylors & Francis: London, 2006.
4. "Clean Energy, Air, Health, and Related Economic Impacts: Assessing the Many Benefits of State and Local Clean Energy Initiatives," http://www.epa.gov/statelocalclimate/documents/pdf/background_paper_06-14-2011.pdf , related on 21-4-2014
5. Reported issued by National Renewable Energy Laboratory," Dollars from Sense: the Economic Benefits of Renewable Energy," Printed in the United States of America, Sept. 1997 .
6. "Renewable Energies- a Success Story Germany’s Energiewende in Practice," http://www.london.diplo.de/contentblob/3665084/Daten/2690318/EnergiewendeFlyer.pdf, related on 21-4-2014.
7. World Health Organization," Health Indicators of sustainable energy," presented at the Context of the Rio+20 UN Conference on Sustainable Development, New York, May 2012.
8. Reported issued by Sierra Club," Health and Environmental Benefits of Renewable Energy," Denver, Sept. 2003.
9. F. Armstrong, E. Haworth, P. Tait, H. Barker, " Health and Energy Policy," Briefing Paper, Feb. 2013.
10. M. H. Panjeshahi, L. Ahmadi, S. Perry," Renewable Energies and Utility Systems," presented at Proceedings of the World Congress on Engineering and Computer Science (WCECS) 2008, San Francisco, USA, 2008.
11. A.K. Akella, R.P. Saini, M.P. Sharma," Social, economical and environmental impacts of renewable energy systems," Renewable Energy, pp. 390–396, 2009.
12. Reported issued by Department of Minerals and Energy Republic of South Africa "White Paper on Renewable Energy," Nov. 2003 .

13. A. V. Herzog, T. E. Lipman, D. M. Kammen," Renewable Energy Sources," Universityof California, Berkeley, USA, 2001. http://rael.berkeley.edu/sites/default/files/old-site-files/2001/Herzog-Lipman-Kammen-RenewableEnergy-2001.pdf.
14. Reported issued by Sustainable Energy Ireland," Wind Energy-General information," http://www.seai.ie/Publications/Renewables_Publications/Wind_Power/Archived_Wind_Publications/Wind_Energy_Factsheet.pdf.
15. A. Ashwinkumar," A study on Renewable Energy Resources in India," presented at International Conference on Environmental Engineering and Applications (ICEEA), pp. 49-53, Sept. 2010.
16. D.Holm, D.Arch," Renewable Energy Future for the Developing World," White Paper, Germany,2005.
17. j. sawin and w. r. moomaw," Renewable Revolution: Low-Carbon Energy by 2030," Worldwatch Institute, 2009` .
18. A. C. Jimenez, K. Olson," Renewable Energy for Rural Health Clinics," Produced for the U.S. Department of Energy, National Renewable Energy Laboratory: Golden, Sept. 1998.
19. A. C. Jimenez, K.Olson," Renewable Energy for Rural Health Clinics," National Renewable Energy Laboratory: USA, Sept. 1998.
20. B. T. Q. Yaseen," Renewable Energy Applications in Palestine," Palestinian Energy and Environment Research Center (PEC) – Energy Authority, Technical Department Director (PEC), Palestine.
21. Reported issued by Portland Trust," The Renewable Energy Sector in the Palestinian Territory," SITTARD: Al Nasher Advertising, July 2010.
22. Reported issued by European Commission "A 2030 framework for climate and energy policies," Green Paper, 2013.
23. Reported issued by MAS," Renewable Energy in the Palestinian Territory: Opportunities and Challenges," Round Table Discussion (4), 2012.
24. H. Tsai, Ci. Tu, Yi. Su," Development of Generalized Photovoltaic Model Using MATLAB/SIMULINK," presented at Proceedings of the World Congress on Engineering and Computer Science (WCECS), San Francisco, USA, Oct. 2008.
25. G. M. Masters," Renewable and Efficient Electric Power Systems," John Wiley & Sons: New Jersey, 2004.
26. Ch. Greacen," How Photovoltaic Cells Work," pp. 37-39, 1991. http://arizonaenergy.org/AltEnergyClub/HowSolarPVCellsWork.pdf.

27. Reported issued by Solmetric," Guide To Interpreting I-V Curve Measurements of PV Arrays," March, 2011.
28. "How Solar Cells Work-Converting sunlight to electricity," http://www.solarbc.ca/sites/default/files/pdf/how_a_solar_cell_works__dec_9.pdf, related on 21-4-2014.
29. P.Hersch and K. Zweibel" Basic Photovoltaic Principles and Methods," Technical Information Office: USA, 1982.
30. N. A. Azli, Z. Salam, A. Jusoh, M. Facta, B. C. Lim, S. Hossain," Effect of Fill Factor on the MPPT Performance of a Grid-connected Inverter under Malaysian Conditions," presented at 2nd IEEE International Conference on Power and Energy (PECon 08), Malaysia, pp. 460-462,2008.
31. P. A. Lynn," Electricity from Sunlight: An Introduction to Photovoltaics," SITTARD: John Wiley & Sons: Chichester,2010.
32. D. Rekioua, E.Matagne,"Optimization of Photovoltic Power Systems Modelization, Simulation and Control," Springer: London, 2012.
33. G. N. Tiwari and S. Dubey," Fundamentals of Photovoltaic Modules and their Applications," RSC: Cambridge, 2010.
34. A. Rezaei and S. A. Gholamian," Optimization of New Fuzzy Logic Controller by Genetic Algorithm for Maximum Power Point Tracking in Photovoltaic System," presented at ISESCO Journal of Science and Technology, vol. 9, no. 1, May 2013 .
35. C. J. Chen," Physics of Solar Energy," John Wiley & Sons: New Jersey, 2011.
36. Reported issued by Solmetric," Guide To Interpreting I-V Curve Measurements of PV Arrays," March 2011.
37. Ch. Hua and Ch. Shen, "Study of maximum power tracking techniques and control of DC/DC converters for photovoltaic power system," presented at Power Electronics Specialists Conference, 1998. PESC 98 Record. 29th Annual IEEE, vol.1, pp.86-93, May 1998.
38. H. N. Zainudin and S. Mekhilef," Comparison Study of Maximum Power Point Tracker Techniques for *PV* Systems," presented at 14th International Middle East Power Systems Conference (MEPCON'10), Cairo University, Egypt, Dec. 2010.
39. E. Eötvös, J. Dudrik, T. Béreš," Resonant *DC-DC* Converter for Photovoltaic Systems," Transactions on Electrical Engineering, vol. 1, no. 1, 2012.
40. A. Oi," Design and Simulation of Photovoltaic Water Pumping System," A Thesis Presented to the Faculty of California Polytechnic State University, San Luis Obispo, Sept. 2005.

41. D. Sera, T. Kerekes, R. Teodorescu, Frede Blaabjerg, "Improved MPPT Algorithms for Rapidly Changing Environmental Conditions," presented at Power Electronics and Motion Control Conference, 2006. EPE-PEMC 2006. pp.1614-1619, 2006 .
42. V. Busa, K. K. Narsingoju, G.V. Kumar," Simulation Analyis of Maximum Power Control of Photo Voltaic Power System," International Journal on Advanced Electrical and Electronics Engineering (IJAEEE), vol. 1, Issue.1, 2012.
43. J. S.Kumari, Ch. S. Babu, A. K. Babu," Design and Analysis of P&O and IP&O MPPT Techniques for Photovoltaic System," International Journal of Modern Engineering Research (IJMER), vol. 2, Issue. 4, pp. 2174-2180, 2012.
44. Ch.Seet Chin, P. Neelakantan, S. Siang Yang, B. Lii Chua, K. Kin Teo,"Effect of Partially Shaded Conditions on Photovoltaic Array's Maximum Power Point Tracking," Modelling, Simulation and Computing Laboratory, School of Engineering and Information Technology, vol. 12, no. 3, pp. 52-59, http://ijssst.info/Vol-12/No-3/paper8.pdf , 20-4-2014.
45. A. K. Mukerjee and N. Thakur," Photovoltaic Systems- Analysis and Design," A. K. Ghosh & PHI Learning Private Limited: New Delhi, 2011.
46. A. Yadav, S. Thirumaliah, G. Haritha, " Comparison of *MPPT* Algorithms for *DC-DC* Converters Based *PV* Systems," International Journal of Advanced Research in Electrical, Electronics and Instrumentation Engineering, vol. 1, pp. 18-23, July 2012
47. T. Esram and P. Chapman, "Comparison of Photovoltaic Array Maximum Power Point Tracking Techniques," IEEE Transactions on Energy Conversion, vol. 22, no. 2, pp. 439-449, June 2007.
48. M. H. Rashid," Power Electronic Handbook," 3th edition, printed in the USA, 2011 .
49. H. Zainudin and S. Mekhilef, "Comparison Study of Maximum Power Point Tracker Techniques for PV Systems," presented at International Middle East Power Systems Conference (MEPCON'10), Cairo University, Egypt, pp. 750-755, Dec. 2010.
50. J. Kumari, Ch. Babu," Comparison of Maximum Power Point Tracking Algorithms for Photovoltaic System, "International Journal of Advances in Engineering & Technology, Vol. 1, pp. 133-148, Nov. 2011.
51. J. Lee," Advanced Electrical and Electronic Engineering," Springer: Berlin, 2011.
52. D. P. Hohm and M. E. Ropp," Comparative Study of Maximum Power Point Tracking Algorithms," Progress in Photovoltaic: Research and Application, pp. 47-62, 2003.

53. P. Takun, S. Kaitwanidvilai, C. Jettanasen, "Maximum Power Point Tracking using Fuzzy Logic Control for Photovoltaic Systems," presented at International Multi Conference of Engineers and Computer Scientists, vol. 2, March 2011.
54. R. Rahmani, M. Seyedmahmoudian, S. Mekhilef , R.Yusof, " Implementation of Fuzzy Logic Maximum Power Point Tracking Controller for Photovoltaic System," American Journal of Applied Sciences, vol.10, pp. 209-218, 2013.
55. M.S. Cheikh, C. Larbes, G.F. Kebir , A. Zerguerras," Maximum power point tracking using a fuzzy logic control scheme," Revue des Energies Renouvelables, vol. 10, n.3 , pp. 387 – 395, 2007.
56. A. Ali, M. Saied, M. Mostafa, T. Moneim," A Survey of Maximum *PPT* techniques of PV Systems," *Energytech, 2012* IEEE , May 2012.
57. R. Faranda, S. Leva, " Energy comparison of *MPPT* techniques for *PV* Systems," Wseas Transaction on Power Systems, vol. 3, pp. 446-455, June 2008.
58. M. Brito, L. Galotto, L. Sampaio, G. Melo C. Canesin," Evaluation of the Main MPPT Techniques for Photovoltaic Applications," IEEE Transactions on Industrial Electronics, vol. 60, no. 3, pp. 1156-1167, March 2013.
59. S. Jain and V. Agarwa," Comparison of the performance of maximum power point tracking schemes applied to single-stage grid-connected photovoltaic systems," The Institution of Engineering and Technology, pp. 753-762, 2007.
60. Ch. Kumar, T. Dinesh, S. Babu," Design and Modelling of *PV* System and Different *MPPT* Algorithms," International Journal of Engineering Trends and Technology (IJETT), vol. 4, pp. 4104-4112, Sep. 2013.
61. A. Yafaoui, B. Wu, R. Cheung," Improvement of Maximum Power Point Tracking Algorithm for Residental Photooltic Systems," presented at 2nd Canadian Solar Buildings Conference, Calgary, June 2007.
62. J. Hu, J. Zhang, H. Wu," Novel *MPPT* Control Algorithm Based on Numerical Calculation for *PV* Generation Systems," presented at Power Electronics and Motion Control Conference, Baoding, China, pp. 2103-2107, May 2009.
63. S. Go, S. Ahn, J. Choi, W. Jung, S. Yun Yun, Il. Song," Simulation and Analysis of Existing MPPT Control Methods in a PV Generation System," Journal of International Council on Electrical Engineering, vol. 1, no. 4, pp. 446-451, 2011.
64. D. P. Hohm and M. E. Ropp," Comparative Study of Maximum Power Point Tracking Algorithms," Progress in Photovoltaic: Research and Application, pp. 47-62,2003.

65. Y. Yang, Z. Yan," A *MPPT* Method using Piecewise Linear Approximation and Temperature Compensation," Journal of Computational Information Systems, pp. 8639-8647, 2013.
66. R. Mandour and I. Elamvazuthi," Optimization of Maximum Power Point Tracking (*MPPT*) of Photovoltaic System using Artificial Intelligence (*AI*) Algorithms," Journal of Emerging Trends in Computing and Information Sciences, vol. 4, no. 8, Aug. 2013.
67. L. Zhou, Y.Chen, Q. Liu, J. Wu," Maximum power point tracking (*MPPT*) control of a photovoltaic system based on dual carrier chaotic search," J Control Theory Appl, pp. 244–250, 2012.
68. Md. Rahman, S. Poddar, M. Mamun, S. Mahmud, Md. Yeasin," Efficiency Comparison Between Different Algorithms for Maximum Power Point Tracker of A solar System," International Journal of Scientific Research and Management (IJSRM), vol. 1, pp. 157-167, 2013.
69. D. Bertsimas, J.Tsitsiklis," Simulated Annealing," Statistical Science, vol. 8, no. 1, pp. 10-15, 1993.
70. B. Amrouche, M. Belhamel, A. Guessoum," Artificial intelligence based *P&O MPPT* method for photovoltaic systems," Revue des Energies Renouvelables ICRESD, pp. 11-16, 2007.
71. I. Abdalla, L. Zhang, J. Corda," Voltage-Hold Perturbation & Observation Maximum Power Point Tracking Algorithm (*VH-P&O MPPT*) for Improved Tracking over the Transient Atmospheric Changes," presented at Power Electronics and Applications (EPE 2011) of the 2011-14th European Conference on , pp.1-10, 2011.
72. F. Qiang, T. Nan," A Strategy Research on *MPPT* Technique in Photovoltaic Power Generation System," TELKOMNIKA, vol. 11, no. 12, pp. 7627-7633 Dec. 2013.
73. J. S. Lee and K. B. Lee," Variable DC-Link Voltage Algorithm with a Wide Range of Maximum Power Point Tracking for a Two-String *PV* System," Energies 2013, vol.6, pp. 58-78, 2013.
74. A. Reisi, M. Moradi, Sh.Jamasb," Classification and comparison of maximum power point tracking techniques for photovoltaic system: A review," Renewable and Sustainable Energy Reviews, pp. 433-443, 2013.
75. R. Faranda, S. Leva, V. Maugeri," *MPPT* techniques for *PV* Systems: energetic and cost comparison," IEEE, 2008.

76. C. Liu, B. Wu, R. Cheung," Advanced Algorithm for *MPPT* Control of Photovoltaic System," presented at Canadian Solar Buildings Conference, Montreal, Aug. 2004.
77. Vladimir V. R. Scarpa, S. Buso, G. Spiazzi, " Low-Complexity *MPPT* Technique Exploiting the PV Module MPP Locus Characterization," IEEE Transactions on Industrial Electronics, vol. 56, no. 5, May 2009.
78. R. Coelho, F. Concer, D. Martins," A *MPPT* Approach Based on Temperature Measurements Applied in PV Systems," IEEE/IAS International Conference on Industry Applications, 2010.
79. Q. Abdulmajeed, H. Kazem, H. Mazin, M. Abd Malek, D. Maizana1, A. Alwaeli, M. Albadi, K. Sopian, A. Al Busaidi," Photovoltaic Maximum Tracking Power Point System: Review and Research Challenges," International Journal of Advanced Trends in Computer Science and Engineering (IJATCSE), vol. 2, no. 5, pp. 16-21, 2013.
80. J. Israel," Summary of Maximum Power Point Tracking Methods for Photovoltaic Cells," electronic matter.
81. D. S. Morales," Maximum Power Point Tracking Algorithms for Photovoltaic Applications,"A Thesis Presented to the Faculty of Electronics, Communications and Automation, Aalto University, 2010.
82. W. Xiao, W. Dunford, P. Palmer, A. Capel," Application of Centered Differentiation and Steepest Descent to Maximum Power Point Tracking," IEEE Transactions on Industrial Electronics, vol. 54, no. 5,pp. 2539-2549, Oct. 2007.
83. C. Rodriguez and G. Amaratunga," Analytic Solution to the Photovoltaic Maximum Power Point Problem," IEEE Transactions on Circuits and System—I: Regular Papers, vol. 54, no. 9, Sep. 200794 .
84. S. Walker, N. Sooriyaarachchi, N. Liyanage, P. Abeynayake, S. Abeyratne," Comparative Analysis of Speed of Convergence of MPPT Techniques," presented at 6th International Conference on Industrial and Information Systems, Sri Lanka, pp. 522-526, 2011.
85. M. Calavia1, J.M. Perié1, J.F. Sanz, J. Sallán," Comparison of *MPPT* strategies for solar modules," presented at International Conference on Renewable Energies and Power Quality (ICREPQ'10) Granada (Spain), March 2010.
86. J. Jiang, T. Huang, Y. Hsiao, Ch. Chen," Maximum Power Tracking for Photovoltaic Power Systems," Tamkang Journal of Science and Engineering, vol. 8, no 2, pp. 147-153,2005.

87. M. Azab," A New Maximum Power Point Tracking for Photovoltaic Systems," World Academy of Science, Engineering and Technology, pp. 571-574, 2008.
88. R. Mastromauro, M. Liserre, A. Aquila," Control Issues in Single-Stage Photovoltaic Systems: MPPT, Current and Voltage Control, IEEE Transactions on Industrial Informatics, vol. 8, no. 2, pp. 241-254, May 2012.
89. J. Ghazanfari and M. Farsangi," Maximum Power Point Tracking using Sliding Mode Control for Photovoltaic Array," Iranian Journal of Electrical & Electronic Engineering, vol. 9, no. 3, pp. 189-196, Sep. 2013.
90. H. Zazo, R. Leyva, E. Castillo," Analysis of Newton-Like Extremum Seeking Control in Photovoltaic Panels," presented at International Conference on Renewable Energies and Power Quality (ICREPQ'12), Santiago de Compostela, Spain, March 2012.
91. T. T. N. Khatib, A. Mohamed, N. Amim," An Improved Indirect Maximum Power Point Tracking Method for Standalone Photovoltaic Systems," presented at Proceedings of the 9th WSEAS International Conference on Applications of Electrical Engineering, Selangor, Malaysia, pp. 56- 62, 2010.
92. Sh. Gupta, A. Aneja, H. Mittal, J. Chaudhary," Performance and Cost Optimised *MPPT* for Solar Powered Vehicle," International Journal of Advanced Research in Computer Engineering & Technology (IJARCET),vol. 2, Issue 12, pp. 3091- 3096, Dec. 2013.
93. Reported issued by National Instruments," Maximum Power Point Tracking," 2009. http://www.ni.com/white-paper/8106/en /
94. Y. Hyok Ji, D. Yong Jung, Ch. Yuen Won, B. Kuk Lee, J. Wook Kim," Maximum Power Point Tracking Method for PV Array under Partially Shaded Condition," Energy Conversion Congress and Exposition, 2009. ECCE 2009. IEEE, pp. 307-312, Sept. 2009 .
95. S. Said, A.Massoud, M. Benammar, Sh. Ahmed," A Matlab/Simulink-Based Photovoltaic Array Model Employing SimPowerSystems Toolbox," Journal of Energy and Power Engineering, pp. 1965-19756, 2012.
96. M. G. Villalva, J. R. Gazoli, E. R. Filho," Modeling and circuit-based simulation of photovoltaic arrays," presented at power Electronics Conference, 2009. COBEP '09. Brazilian, pp.1244-1254, 2009.

97. A.Khamis, Mohamed, H. Shareef, A. Ayob," Modeling and Simulation of A microgrid Testbed Using Photovoltaic and Battery Based Power Generation, Journal of Asian Scientific Research,vol. 2, no. 11, pp. 658-666, 2011.
98. Datasheet for KC200GT, http://www.kyocerasolar.com/assets/001/5183.pdf.
99. J.A. Hernanz , J.J. Campayo, J. Larranaga, E. Zulueta, O. Barambones, J. Motrico, U. F. Gamiz, I. Zamora," Two Photovoltaic Cell Simulation Models in MATLAB/ SIMULINK," International Journal on Technical and Physical Problems of Engineering (IJTPE), Vol. 4, no. 1, Issue 10, pp. 45-51, March 2012.
100. Y. J. Wang and P. C. Hsu," Analytical modelling of partial shading and different orientation of photovoltaic modules," IET Renewable Power Generation, Vol. 4, Iss. 3, pp. 272–282, 2009 .
101. M. Seyedmahmoudian, S. Mekhilef, R. Rahmani, R. Yusof , E. T. Renani ," Analytical Modeling of Partially Shaded Photovoltaic Systems," Energies 2013, vol. 6, pp. 128-144,2013, doi:10.3390/en6010128.
102. Ch. Seet Chin, P. Neelakantan, S. Siang Yang, B. Lii Chua, K. Kin Teo,"Effect of Partially Shaded Conditions on Photovoltaic Array's Maximum Power Point Tracking," Chia Seet Chin et al: Effect of Partially Shaded Conditions on Photovoltaic…, vol. 12, no. 3, pp. 52-59،
103. H. Patel and V. Agarwal," MATLAB-Based Modeling to Study the Effects of Partial Shading on PV Array Characteristics," IEEE Transactions on Energy Conversion, vol. 23, no. 1, pp. 302- 310, March 2008.
104. S. Sh. Mohammed," Modeling and Simulation of Photovoltaic module using MATLAB/Simulink," International Journal of Chemical and Environmental Engineering, vol. 2, no. 5, Oct. 2011.
105. V. Ramesh, P. Anjappa, P. Dhanamjaya," Simulation and Implementation of Incremental Conductance *MPPT* with Direct Control Method Using Boost Converter," International Journal of Engineering Science and Innovative Technology (IJESIT), vol. 2, Issue. 6, Nov. 2013.
106. Sh. Rahman, N. S. Oni,Q. A. Masud," Design of a Charge Controller Circuit with Maximum Power Point Tracker (*MPPT*) for Photovoltaic System," A Thesis submitted to the Dept. of Electrical & Electronic Engineering, BRAC University in partial fulfillment of the requirements for the Bachelor of Science degree in Electrical & Electronic Engineering, Dec. 2012.

107. J. Wurz," Design of A maximum Power Point Tracker with Simulation, Analysis and Comparison of Algorithms," A Thesis submitted to NAVAL Postgraduate School, California, Dec. 2012.

108. A. A. El Tayyan," PV system behavior based on datasheet," Journal of Electron Devices, vol. 9, pp. 335-341, 2011.

109. D. Sera, S. Member, J. Hantschel, M. Knoll," Optimized Maximum Power Point Tracker for Fast-Changing Environmental Conditions," IEEE Transactions on Industrial Electronics, vol. 55, no. 7, pp. 2629-2637, July 2008.

110. " Pulse-width modulation," http://fab.cba.mit.edu/classes/MIT/961.04/topics/pwm.pdf , related on 21-4-2014.

111. Q. M Abdulmajeed, H. A Kazem, H. Mazin, M. F Abd Malek, D. Maizana, A. H A Alwaeli, M. H. Albadi, K. Sopian, A. Said Al Busaidi," Photovoltaic Maximum Tracking Power Point System: Review and Research Challenges," International Journal of Advanced Trends in Computer Science and Engineering (IJATCSE), vol. 2 , no. 5, pp.16-21, 2013.

112. "Electromagnetic Pistol: CS-P01A ," http://www.coilgun.eclipse.co.uk/electromagnetic_pistol_voltage_converter_design.html, related on 21-4-2014.

APPENDIX A

Kyocera KC Series Module Specification

Electrical Characteristics:@ STC							
Model Number	KC125GT	KC130GT	KC167GT	KC170GT	KC175GT	KC190GT	KC200GT
Rated Power, Watts (Pmax)	125	130	167	170	175	190	200
Open Circuit Voltage (Voc)	21.7	21.9	28.9	29.0	29.2	32.5	32.9
Short Circuit Current (Isc)	8.00	8.02	8.00	8.03	8.09	8.08	8.21
Voltage at Load (Vpm)	17.4	17.6	23.2	23.4	23.6	26.1	26.3
Current at Load (Ipm)	7.20	7.39	7.20	7.27	7.42	7.28	7.61
Maximum System Voc	600	600	600	600	600	600	600
Factory Installed Bypass Diode (Qty)	Yes (2)	Yes (2)	Yes (3)	Yes (3)	Yes (3)	Yes (3)	Yes (3)
Series Fuse Rating (Amps)	15	15	15	15	15	15	15
Thermal Characteristics:							
Temp. coefficient of Voc (V/•)	-8.21• 10^{-2}	-8.21• 10^{-2}	-1.09• 10^{-1}	-1.09• 10^{-1}	-1.09• 10^{-1}	-1.23• 10^{-1}	-1.23• 10^{-1}
Temp. coefficient of Isc (A/•)	3.18• 10^{-3}	3.18• 10^{-3}	3.18• 10^{-3}	3.18• 10^{-3}	3.18• 10^{-3}	3.18• 10^{-3}	3.18• 10^{-3}
Temp. coefficient of Vpm (V/•)	-9.31• 10^{-2}	-9.31• 10^{-2}	-1.24• 10^{-1}	-1.24• 10^{-1}	-1.24• 10^{-1}	-1.40• 10^{-1}	-1.40• 10^{-1}
Physical Characteristics:							
Model Number	KC125GT	KC130GT	KC167GT	KC170GT	KC175GT	KC190GT	KC200GT
Length, Inches (mm)	56.1(1425)	56.1(1425)	50.8 (1290)	50.8 (1290)	50.8 (1290)	56.1(1425)	56.1(1425)
Width, Inches (mm)	25.7(652)	25.7(652)	39.0 (990)	39.0 (990)	39.0 (990)	39.0(990)	39.0 (990)
Depth, Inches (mm)	1.42(36)	1.42(36)	1.42 (36)	1.42 (36)	1.42 (36)	1.42 (36)	1.42 (36)
Weight, Pounds (kg)	26.9(12.2)	26.9(12.2)	35.3 (16)	35.3 (16)	35.3 (16)	40.8 (18.5)	40.8 (18.5)
Mounting Hole Diameter inches (mm)	0.28"(7) Qty – 8	0.28"(7) Qty – 8	0.28" (7) Qty – 4	0.28" (7) Qty – 4	0.28" (7) Qty – 4	0.28"(7) Qty – 4	0.28"(7) Qty – 4
Grounding Hole Diameter inches (mm)	0.28"(7) Qty – 2	0.28"(7) Qty – 2	0.28" (7) Qty – 2	0.28" (7) Qty – 2	0.28" (7) Qty – 2	0.28"(7) Qty – 2	0.28"(7) Qty – 2

APPENDIX B

```
function y = fcn(V,I)
%#codegen
P=V.*I;
y=0;
db=zeros(1,length(P));
%%
for k=1:length(P)-1
    db(k)=P(k+1)-P(k);
end
r=1;
for k=1:length(P)-1
    if(db(k)==0)
        return,
    else
        if (db(k)>0)
%             if(V(k+1)-V(k)>0)
%                 r=r+.01;
%             else
%                 r=r-.01;
%             end
              r=k+1;
        else
%             if(V(k+1)-V(k)>0)
%                 r=r-.01;
%             else
%                 r=r+.01;
%             end

        end
    end
end
%%
y = V(r);
end
```

APPENDIX C

```
plot(Xout,yout,'b');
 figure
plot(Xout,yout1,'b');
 [C,I] = min(abs(yout1));
Xout(I)
```